University of Southampton

Calculation of fully non-adiabatic properties of the hydrogen molecular cation and its isotopomers

by

Loredana Valenzano

A dissertation submitted in partial fulfilment of the requirements for the degree of Doctor of Philosophy at the University of Southampton

Department of Chemistry

February 2003

UNIVERSITY OF SOUTHAMPTON

ABSTRACT

FACULTY OF SCIENCE

CHEMISTRY

Doctor of Philosophy

CALCULATION OF FULLY NON-ADIABATIC PROPERTIES OF THE HYDROGEN MOLECULAR CATION AND ITS ISOTOPOMERS

by Loredana Valenzano

By using a scattering approach combined with a transformed Hamiltonian theory, fully non-adiabatic properties of the vibration-rotational levels of the ground electronic state of the hydrogen molecular cation H_2^+ and its isotopomers, D_2^+ and HD^+, are studied. For low vibrational levels a variational method is also used, providing a check on the methods. The properties considered include the dissociation energies, the bond lengths and the dipole polarizabilities for all the three cations. Relativistic corrections are studied just for H_2^+.

While properties such as bond lengths and dipole polarizabilities are studied through analytic integration, a numerical integration approach is developed to study the relativistic corrections, since singular integrands are involved. In addition, a new calculation method is developed so that the scattering method may be used.

Non-adiabatic dissociation energies and bond lengths are also studied for the tritium heteronuclear isotopomers HT^+ and DT^+.

Few are those who see with their own eyes

and feel with their own hearts.

Albert Einstein

Acknowledgments

At the end of these three years I especially wish to thank my supervisor Dr. R.E. Moss for his help, support and trust and for making me feel at home from the first day.

I thank all the people I have met during this period; some of them are special for me and they already know who they are! Thanks for the laughs, the jokes, the company... and the nachos ;)
A big thank to my friend Umberto, always close to me from Italy.

I thank my parents and my grandmother Rina for loving me so proudly... even too much sometimes!
Last of this list but always first in my thoughts, my biggest thank goes to Maurizio for loving me so much.

I wish to thank the Engineering and Physical Science Research Council for funding the project.

Contents

Chapter 1

Overall aim of the project

The hydrogen molecular cation H_2^+ and its isotopomers, D_2^+ and HD^+, comprising of two nuclei and one electron, are the simplest molecules; for this reason they represent a good test to calculate theoretically and in an accurate way some properties and to compare them with experimental results.

Because of the absence of interelectron interactions, H_2^+ has been used as a model system to test many different approximations and methods. Even though for H_2^+ and D_2^+ the Born-Oppenheimer approximation allows the exact solution of the Schrödinger equation, further calculations (adiabatic and non-adiabatic) are needed to describe the coupling between electronic and nuclear motions [1]. For HD^+, the lack of a centre of symmetry due to the different nuclear masses, creates difficulties in the theory, as is explained in this work.

Theoretical studies on these small molecules are now so accurate that disagreements with experiments may be attribuited to the breakdown of the Born-Oppenheimer approximation while relativistic and radiative corrections have also to be accounted for. Allowance for the breakdown involves two types of correction: the adiabatic, which is diagonal in the electronic state and allows for the response of the nuclei to the instantaneous position of the electron, so that the uniformity of the motion of the centre of mass of the system is maintained; the non-adiabatic, which is off-diagonal in the electronic state and allows for the lag of the electron in its attempt to follow the nuclei during vibration and rotation. While the accurate dissociation energies of many bound and quasibound vibration-rotational levels have been calculated for H_2^+ [2], D_2^+ [3] and HD^+ [4] few fully non-adiabatic values of molecular properties of the hydrogen molecular cation have been calculated.

Extension of the calculation of the non-adiabatic correction to properties such as the bond lengths, the dipole polarizabilities and the relativistic corrections is the aim of this work. This is of fundamental academic interest, since the hydrogen molecular cation is the simplest molecule, for which non-adiabatic effects are supposed to be greatest and since electron correlation does not confuse the issue. There are, however, other reasons for which it is desirable to have extremely accurate property values for these ions.

The recent interest in exceedingly accurate non-adiabatic energies, has been prompted by the possibility of metrologists using very high resolution spectra of H_2^+ in ion traps to determine the ratio of the proton to the electron mass [5]. Although relatively low vibration-rotational levels are involved, some of them are difficult to study using a variational method. In addition, extremely accurate relativistic and radiative effects need to be calculated for each level and the only feasible way, at present, is to evaluate expectation values of the relevant operators. Although this has been done [2–4] using Born-Oppenheimer electronic wavefunctions as a function of internuclear separation and averaging over bond length for each vibration-rotational level, these estimates are good to no better than $1 \times 10^{-9} E_\mathrm{h}$ (0.0002 cm^{-1}) while at least an improvement to 0.000001 cm^{-1} is needed to be of use to metrologists.

In addition, the hydrogen molecular cation H_2^+ is supposed to be intimately involved in the initiation of astrochemistry in the interstellar medium but it has yet to be observed extraterrestrially, unlike H_3^+.

In this work, all the theoretical aspects involved in the study of the properties of the hydrogen molecular cation and its isotopomers are considered; all the levels of approximation are described accurately with a particular attention to the transformed Hamiltonian theory which allows for all the couplings between nuclear and electronic motions. Besides, a detailed explanation of the calculation methods used and developed is reported.

The non-adiabatic corrections to the dissociation energies and to the bond lengths and the non-adiabatic dipole polarizabilities for the ground electronic states of the three cations are discussed. In addition the relativistic correction for H_2^+ is considered. A short chapter is dedicated to the non-adiabatic dissociation energies and bond lengths for the tritium

cations HT^+ and DT^+.

While most of the integrals needed may be evaluated analytically, the study of the relativistic correction requires numerical integration to evaluate matrix elements with singular integrands.

The programs used are based on those of Kennedy and Sadler [6] and Leroy [7]; the original scattering program was written by Balint-Kurti [8].

Chapter 2

Theory

2.1 The full non-relativistic Hamiltonian and levels of approximation

The Schrödinger equation for the hydrogen molecular ion may be solved at different levels of approximation. The simplest and most common is the Born-Oppenheimer approximation, which is defined as the solution for the motion of the electron in the field of the fixed nuclei. A more accurate approximation is the adiabatic one, which includes only terms of the coupling between nuclear and electronic motions which are diagonal in the electronic state. But the complete solution is the one that includes also the off-diagonal terms of the coupling between the elctronic states: the non-adiabatic solution.

Because electronic energies are determined at fixed nuclear separation, both Born-Oppenheimer and adiabatic approaches separate nuclear and electronic motions, leading to the concept of electronic potential energy curves. This idea has to be abandoned in searching for the non-adiabatic solutions to allow for the electron following the nuclei during vibration and rotation of the molecule.

A system of point charges interacting electrostatically and moving through field-free space is studied. For such a system the complete non-relativistic Hamiltonian can be written as

$$H = -\hbar^2 \sum_i \frac{\nabla_i^2}{2m_i} + \frac{e^2}{4\pi\epsilon_0} \sum_i \sum_{j>i} \frac{Z_i Z_j}{r_{ij}} \tag{2.1}$$

where all the symbols have their usual meaning and the coordinates refer to the laboratory frame.

In order to obtain a convenient form of this Hamiltonian for the hydrogen molecular cation, a change is made from the laboratory frame to one centred on the geometric centre of the nuclei, applying the transformation

$$\begin{pmatrix} \boldsymbol{r}_{\mathrm{g}} \\ \boldsymbol{R} \\ \boldsymbol{R}_{\mathrm{CM}} \end{pmatrix} = \begin{pmatrix} -\frac{1}{2} & -\frac{1}{2} & 1 \\ -1 & 1 & 0 \\ \frac{m_1}{M} & \frac{m_2}{M} & \frac{m_{\mathrm{e}}}{M} \end{pmatrix} \begin{pmatrix} \boldsymbol{r}_1 \\ \boldsymbol{r}_2 \\ \boldsymbol{r}_{\mathrm{e}} \end{pmatrix} \tag{2.2}$$

which has as its inverse

$$\begin{pmatrix} \boldsymbol{r}_1 \\ \boldsymbol{r}_2 \\ \boldsymbol{r}_{\mathrm{e}} \end{pmatrix} = \begin{pmatrix} -\frac{m_{\mathrm{e}}}{M} & -\frac{(m_2+\frac{1}{2}m_{\mathrm{e}})}{M} & 1 \\ -\frac{m_{\mathrm{e}}}{M} & \frac{(m_1+\frac{1}{2}m_{\mathrm{e}})}{M} & 1 \\ \frac{M_{\mathrm{n}}}{M} & \frac{m_1-m_2}{2M} & 1 \end{pmatrix} \begin{pmatrix} \boldsymbol{r}_{\mathrm{g}} \\ \boldsymbol{R} \\ \boldsymbol{R}_{\mathrm{CM}} \end{pmatrix} \tag{2.3}$$

where $M = m_1 + m_2 + m_{\mathrm{e}}$ and $M_{\mathrm{n}} = m_1 + m_2$. The coordinate vectors are illustrated in figure 2.1: $\boldsymbol{r}_1$, $\boldsymbol{r}_2$, $\boldsymbol{r}_{\mathrm{e}}$ are the position vectors of the three particles relative to the arbitrary space-fixed origin O. The new basis vectors are the internuclear vector $\boldsymbol{R} = \boldsymbol{r}_2 - \boldsymbol{r}_1$, the position of the centre of mass relative to the space-fixed origin $\boldsymbol{R}_{\mathrm{CM}}$ and the position of the electron relative to the geometric centre of the nuclei $\boldsymbol{r}_{\mathrm{g}}$. Applying the transformation (2.2) to the kinetic energy operators in the Hamiltonian (2.1) leads to

$$-\hbar^2 \sum_i \frac{\nabla_i^2}{2m_i} = -\hbar^2 \Big(\frac{\nabla_{\mathrm{g}}^2}{2m_{\mathrm{e}}} + \frac{\nabla_{\mathrm{R}}^2}{2\mu} + \frac{\nabla_{\mathrm{g}}^2}{8\mu} + \frac{\nabla_{\mathrm{g}} \cdot \nabla_{\mathrm{R}}}{2\mu_{\mathrm{a}}} + \frac{\nabla_{\mathrm{CM}}^2}{2M} \Big) \tag{2.4}$$

where $\frac{1}{\mu} = \frac{1}{m_1} + \frac{1}{m_2}$ and $\frac{1}{\mu_{\mathrm{a}}} = \frac{1}{m_1} - \frac{1}{m_2}$. The convention to set m_1 as the mass of the proton and m_2 as the mass of the deuteron is chosen in order to have, for HD^+, a positive value for μ_{a}.

On the other hand, the electrostatic potential energy between the particles

$$V = \frac{e^2}{4\pi\epsilon_0} \Big[\frac{1}{R} - \frac{1}{r_{1\mathrm{e}}} - \frac{1}{r_{2\mathrm{e}}} \Big] \tag{2.5}$$

is unchanged by transformation (2.2), because it depends only upon the relative positions of the particles.

The complete Schrödinger equation for the system is then

$$\Big\{ -\hbar^2 \Big[\frac{\nabla_{\mathrm{g}}^2}{2m_{\mathrm{e}}} + \frac{\nabla_{\mathrm{R}}^2}{2\mu} + \frac{\nabla_{\mathrm{g}}^2}{8\mu} + \frac{\nabla_{\mathrm{g}} \cdot \nabla_{\mathrm{R}}}{2\mu_{\mathrm{a}}} + \frac{\nabla_{\mathrm{CM}}^2}{2M} \Big] + V \Big\} \Psi_{\mathrm{tot}} = E_{\mathrm{tot}} \Psi_{\mathrm{tot}}. \tag{2.6}$$

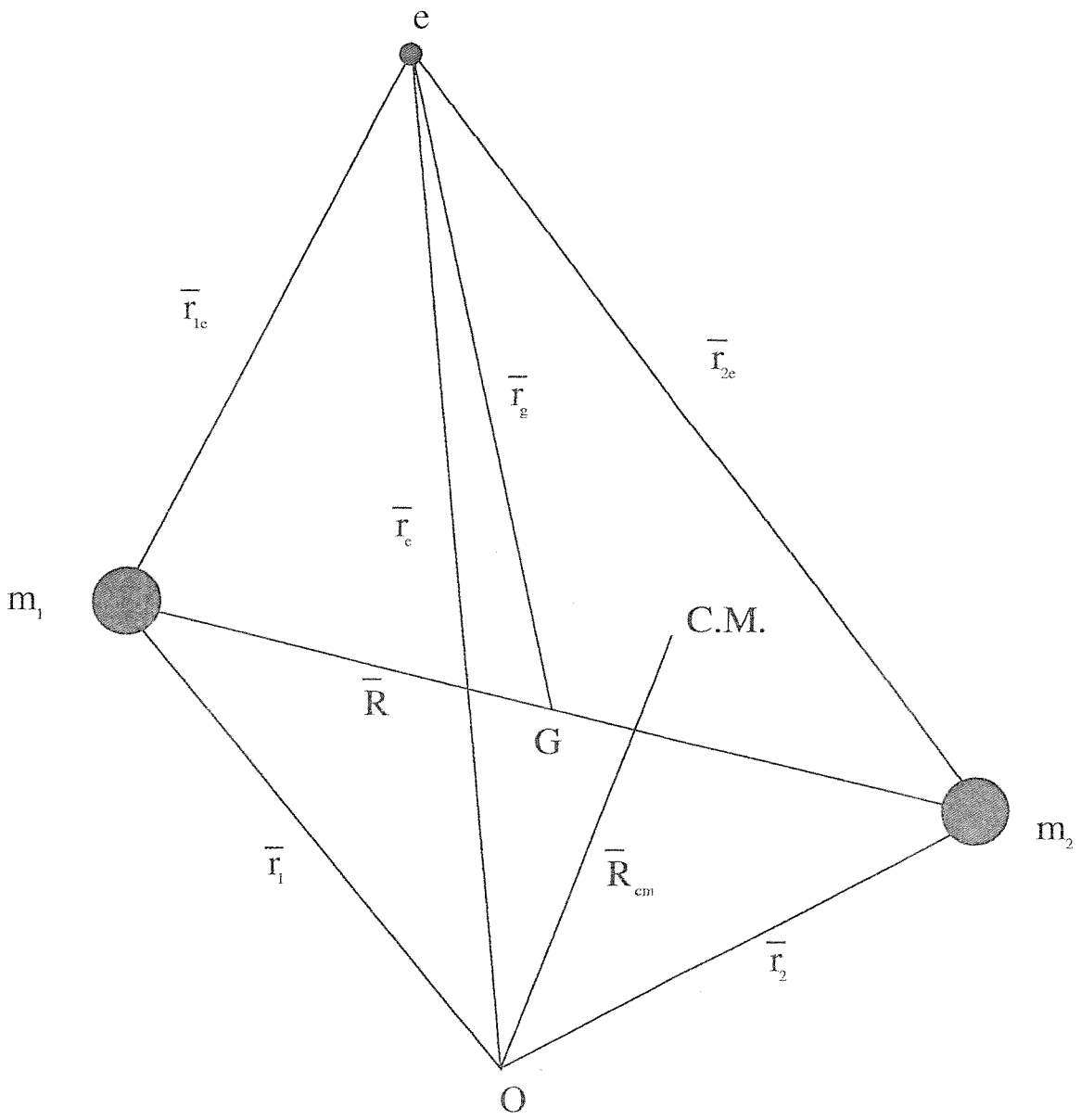

Figure 2.1: Coordinate system for the hydrogen molecular ion: O is the arbitrary space-fixed origin, C.M. is the centre of mass of the system and G is the geometric centre of the nuclei.

Because the motion of the centre of mass is contained in the $\nabla^2_{\rm CM}$ term, it can be separated out to write a solution of the form

$$\Psi_{\rm tot}(\boldsymbol{R}_{\rm CM}, \boldsymbol{R}, \boldsymbol{r}_{\rm g}) = A_{\rm CM}(\boldsymbol{R}_{\rm CM})\psi_{\rm mol}(\boldsymbol{R}, \boldsymbol{r}_{\rm g}) \tag{2.7}$$

that allows the separation of the total Schrödinger equation (2.6) into

$$\Big\{ -\hbar^2\Big[\frac{\nabla^2_{\rm g}}{2m_{\rm e}} + \frac{\nabla^2_{\rm R}}{2\mu} + \frac{\nabla^2_{\rm g}}{8\mu} + \frac{\nabla_{\rm g}\cdot\nabla_{\rm R}}{2\mu_{\rm a}}\Big] + V\Big\}\psi_{\rm mol} = E_{\rm int}\psi_{\rm mol} \tag{2.8}$$

and

$$-\hbar^2\frac{\nabla^2_{\rm CM}}{2M}A_{\rm CM} = (E_{\rm tot} - E_{\rm int})A_{\rm CM}. \tag{2.9}$$

Equation (2.9) can be easily recognized to be the time-independent Schrödinger equation for a body of mass M freely moving in space with kinetic energy $(E_{\rm tot} - E_{\rm int})$. In conclusion, the non-relativistic Hamiltonian, in atomic units, for the internal motion of the hydrogen molecular ion is

$$H_{\rm int} = -\frac{\nabla^2_{\rm g}}{2} - \frac{\nabla^2_{\rm R}}{2\mu} - \frac{\nabla^2_{\rm g}}{8\mu} - \frac{\nabla_{\rm g}\cdot\nabla_{\rm R}}{2\mu_{\rm a}} + \frac{1}{R} - \frac{1}{r_{1\rm e}} - \frac{1}{r_{2\rm e}} \tag{2.10}$$

which can be expressed in a more compact way as

$$H_{\rm int} = H_{\rm BO} + \frac{1}{\mu}H_{\rm ad} + \frac{1}{\mu_{\rm a}}H_{\rm gu} \tag{2.11}$$

where

$$H_{\rm BO} = -\frac{\nabla^2_{\rm g}}{2} + \frac{1}{R} - \frac{1}{r_{1\rm e}} - \frac{1}{r_{2\rm e}}, \tag{2.12}$$

$$H_{\rm ad} = -\frac{\nabla^2_{\rm R}}{2} - \frac{\nabla^2_{\rm g}}{8} \tag{2.13}$$

and

$$H_{\rm gu} = -\frac{\nabla_{\rm g}\cdot\nabla_{\rm R}}{2}. \tag{2.14}$$

Equation (2.13) and, in the case of HD^+, (2.14) couple electronic and nuclear motions making it impossible to find exact eigenfunctions and eigenvalues for equation (2.10); in order to make the problem tractable some approximations can be made.

2.1.1 The Born-Oppenheimer approximation and its solution

The Born-Oppenheimer problem is solved by ignoring $H_{\rm ad}$ and $H_{\rm gu}$ in equation (2.8) and solving the Schrödinger equation for different values of R to generate a potential energy curve and a wavefunction that depends parametrically on R. The Born-Oppenheimer electronic equation

$$\Big(-\frac{\nabla_{\rm g}^2}{2}+\frac{1}{R}-\frac{1}{r_{1\rm e}}-\frac{1}{r_{2\rm e}}\Big)\phi_t(\boldsymbol{r}_{\rm g};R)=E_t(R)\phi_t(\boldsymbol{r}_{\rm g};R) \tag{2.15}$$

has to be solved. In (2.15) t is the electronic state; this three-dimensional equation represents the motion of a single electron around two fixed nuclei.

By using prolate spheroidal coordinates, equation (2.15) can be separated into three one-dimensional equations which may be solved exactly with series expansions [9]. The prolate spheroidal coordinates are defined as

$$\xi=\frac{r_{1\rm e}+r_{2\rm e}}{R} \quad \text{with} \quad 1\le\xi<\infty,$$

$$\eta=\frac{r_{1\rm e}-r_{2\rm e}}{R} \quad \text{with} \quad -1\le\eta\le 1$$

and χ represents the rotation of the electron about the internuclear axis ($0\le\chi<2\pi$). The transformation from cartesian to prolate coordinates allows (2.15) to be written as

$$\Big[\frac{\partial}{\partial\xi}(\xi^2-1)\frac{\partial}{\partial\xi}+\frac{\partial}{\partial\eta}(1-\eta^2)\frac{\partial}{\partial\eta}+\Big(\frac{1}{(\xi^2-1)}+\frac{1}{(1-\eta^2)}\Big)\frac{\partial^2}{\partial\chi^2}+2R\xi-p^2(\xi^2-\eta^2)\Big]\phi_t(\xi,\eta,\chi;R)=0 \tag{2.16}$$

where $p^2=-\frac{R^2}{2}[E_t(R)-\frac{1}{R}]$.

In the Hamiltonian operator of equation (2.16) there are no cross-derivatives between the coordinates, so the solution can be factorized as

$$\phi_t(\xi,\eta,\chi;R)=L(\xi;R)M(\eta;R)N(\chi) \tag{2.17}$$

to obtain three one-dimensional equations

$$\Big(\frac{\partial^2}{\partial\chi^2}+\Lambda^2\Big)N(\chi)=0, \tag{2.18}$$

$$\Big[\frac{\partial}{\partial\xi}(\xi^2-1)\frac{\partial}{\partial\xi}+A-\frac{\Lambda^2}{(\xi^2-1)}+2R\xi-p^2\xi^2\Big]L(\xi;R)=0, \tag{2.19}$$

$$\Big[\frac{\partial}{\partial\eta}(1-\eta^2)\frac{\partial}{\partial\eta}-A-\frac{\Lambda^2}{(1-\eta^2)}+p^2\eta^2\Big]M(\eta;R)=0 \tag{2.20}$$

where Λ^2 and A are the separation constants. Equation (2.18) can be solved analytically with the result

$$N(\chi)=\frac{1}{\sqrt{2\pi}}e^{i\Lambda\chi} \tag{2.21}$$

where $\Lambda=0,\pm1,\pm2,\ldots$.

For the solution of equation (2.19) the Hylleraas expansion [9] over associated Laguerre functions

$$L(\xi;R)=(\xi^2-1)^{\frac{|\Lambda|}{2}}e^{-\frac{x}{2}}\sum_{n=|\Lambda|}^{\infty}\frac{g_n(R)}{n!}\mathcal{L}_n^{(|\Lambda|)}(x) \tag{2.22}$$

can be used. In (2.22) $x=\alpha(\xi-1)$ and α is a non-linear variational parameter. Substitution of this solution in (2.19) leads to a recursion relation between the coefficients $g_n(R)$.

Equation (2.20) may be solved using an Hylleraas expansion [9] over associated Legendre functions

$$M(\eta;R)=\sum_{s=0}^{\infty}f_s(R)\mathcal{P}_{|\Lambda|+s}^{(|\Lambda|)}(\eta). \tag{2.23}$$

The solution of the electronic Born-Oppenheimer equation is achieved by determining $g_n(R), f_s(R)$ and $E_t(R)$ for a given state at a particular value of R and requiring that the separation constant A satisfies at the same time both the set of recursion relations in $g_n(R)$ and $f_s(R)$. This condition can be expressed as the matrix eigenvalue equations [10]

$$\boldsymbol{G}\boldsymbol{g}=-A\boldsymbol{g} \tag{2.24}$$

$$\boldsymbol{F}\boldsymbol{f}=A\boldsymbol{f}. \tag{2.25}$$

Solution of the Born-Oppenheimer equation yields an electronic potential energy curve

$$U(R)=E_t(R) \tag{2.26}$$

in which all the couplings between nuclear and electronic motions have been neglected. The radial Schrödinger equation for the nuclear motion is then

$$\Big\{ -\frac{d^2}{dR^2} + 2\mu\Big[U(R) - E_{vN}\Big] + \frac{N(N+1)}{R^2}\Big\}\chi_{vN}(R) = 0 \tag{2.27}$$

and its vibration-rotational eigenfunctions and eigenvalues may be found by Numerov-Cooley integration [11].

2.1.2 The adiabatic approximation

Adiabatic vibration-rotational energies may be obtained by correcting the potential by adding the expectation values of

$$\frac{1}{\mu}H_{\rm ad} \tag{2.28}$$

to the Born-Oppenheimer potential using the Born-Oppenheimer wavefunctions $\phi_t(\boldsymbol{r}_{\rm g}; R)$ [12]. Following the method suggested by Born and Huang [13], the complete molecular wavefunction can be expressed as a series expansion over the Born-Oppenheimer solutions $\phi_t(\boldsymbol{r}_{\rm g}; R)$ as follows

$$\psi_{\rm mol}(\boldsymbol{R}, \boldsymbol{r}_{\rm g}) = \sum_t F_t(\boldsymbol{R})\phi_t(\boldsymbol{r}_{\rm g}; R). \tag{2.29}$$

Substituting (2.29) into the Schrödinger equation for the internal motion (2.8), a set of coupled differential equations for the function $F_t(\boldsymbol{R})$ is obtained

$$H_{\rm int}\sum_t F_t(\boldsymbol{R})\phi_t(\boldsymbol{r}_{\rm g}; R) = E_{\rm int}\sum_t F_t(\boldsymbol{R})\phi_t(\boldsymbol{r}_{\rm g}; R). \tag{2.30}$$

This equation can be simplified by premultiplying by $\phi_s^*(\boldsymbol{r}_{\rm g}; R)$ and integrating over the electronic coordinate $\boldsymbol{r}_{\rm g}$ to obtain

$$E_s(R)F_s(\boldsymbol{R}) + \sum_t \int \phi_s^*(\boldsymbol{r}_{\rm g}; R)\Big[-\frac{\nabla_{\rm R}^2}{2\mu} - \frac{\nabla_{\rm g}^2}{8\mu} - \frac{\nabla_{\rm g}\cdot\nabla_{\rm R}}{2\mu_{\rm a}}\Big]F_t(\boldsymbol{R})\phi_t(\boldsymbol{r}_{\rm g}; R)d\boldsymbol{r}_{\rm g} = E_{\rm int}F_s(\boldsymbol{R}) \tag{2.31}$$

that can be rewritten as

$$E_s(R)F_s(\boldsymbol{R}) + \int \phi_s^*(\boldsymbol{r}_\mathrm{g};R)\Big[-\frac{\nabla_\mathrm{R}^2}{2\mu} - \frac{\nabla_\mathrm{g}^2}{8\mu} - \frac{\nabla_\mathrm{g}\cdot\nabla_\mathrm{R}}{2\mu_\mathrm{a}}\Big]F_s(\boldsymbol{R})\phi_s(\boldsymbol{r}_\mathrm{g};R)d\boldsymbol{r}_\mathrm{g}$$

$$+\sum_{t\neq s}\int \phi_s^*(\boldsymbol{r}_\mathrm{g};R)\Big[-\frac{\nabla_\mathrm{R}^2}{2\mu} - \frac{\nabla_\mathrm{g}^2}{8\mu} - \frac{\nabla_\mathrm{g}\cdot\nabla_\mathrm{R}}{2\mu_\mathrm{a}}\Big]F_t(\boldsymbol{R})\phi_t(\boldsymbol{r}_\mathrm{g};R)d\boldsymbol{r}_\mathrm{g} = E_\mathrm{int}F_s(\boldsymbol{R}). \tag{2.32}$$

In the Born-Oppenheimer equation the nuclei are treated as fixed charged points, so the wavefunctions $\phi_t(\boldsymbol{r}_\mathrm{g};R)$ are either symmetric or antisymmetric with respect to exchange of nuclei or with respect to electron inversion in the geometric centre of the nuclei; in the particular case of HD^+, the operator ∇_R is antisymmetric with respect to nuclear permutation while the operator ∇_g is antisymmetric for electron inversion. For this reason the following integrals allow the elimination of the coupling term $\nabla_\mathrm{R}\cdot\nabla_\mathrm{g}$ from the diagonal terms of equation (2.32)

$$\int \phi_s^*(\boldsymbol{r}_\mathrm{g};R)\nabla_\mathrm{R}\phi_s(\boldsymbol{r}_\mathrm{g};R)d\boldsymbol{r}_\mathrm{g} = 0,$$

$$\int \phi_s^*(\boldsymbol{r}_\mathrm{g};R)\nabla_\mathrm{g}\phi_s(\boldsymbol{r}_\mathrm{g};R)d\boldsymbol{r}_\mathrm{g} = 0, \tag{2.33}$$

$$\int \phi_s^*(\boldsymbol{r}_\mathrm{g};R)\nabla_\mathrm{g}\cdot\nabla_\mathrm{R}\phi_s(\boldsymbol{r}_\mathrm{g};R)d\boldsymbol{r}_\mathrm{g} = 0$$

so that it becomes

$$\Big\{E_s(R) - \frac{\nabla_\mathrm{R}^2}{2\mu} - \int \phi_s^*(\boldsymbol{r}_\mathrm{g};R)\Big[\frac{\nabla_\mathrm{R}^2}{2\mu} + \frac{\nabla_\mathrm{g}^2}{8\mu}\Big]\phi_s(\boldsymbol{r}_\mathrm{g};R)d\boldsymbol{r}_\mathrm{g}\Big\}F_s(\boldsymbol{R})$$

$$+\sum_{t\neq s}\Big\{\int \phi_s^*(\boldsymbol{r}_\mathrm{g};R)\Big[-\frac{\nabla_\mathrm{R}^2}{2\mu} - \frac{\nabla_\mathrm{g}^2}{8\mu} - \frac{\nabla_\mathrm{g}\cdot\nabla_\mathrm{R}}{2\mu_\mathrm{a}}\Big]\phi_t(\boldsymbol{r}_\mathrm{g};R)d\boldsymbol{r}_\mathrm{g}$$

$$-\int \phi_s^*(\boldsymbol{r}_\mathrm{g};R)\Big[-\frac{\nabla_\mathrm{R}}{\mu} - \frac{\nabla_\mathrm{g}}{2\mu_\mathrm{a}}\Big]\phi_t(\boldsymbol{r}_\mathrm{g};R)d\boldsymbol{r}_\mathrm{g}\cdot\nabla_\mathrm{R}\Big\}F_t(\boldsymbol{R}) = E_\mathrm{int}F_s(\boldsymbol{R}). \tag{2.34}$$

In the case of the Born-Oppenheimer approximation, equation (2.34) reduces to

$$\Big\{E_s(\boldsymbol{R}) - \frac{\nabla_\mathrm{R}^2}{2\mu}\Big\}F_s^\mathrm{BO}(\boldsymbol{R}) = E_\mathrm{int}^\mathrm{BO}F_s^\mathrm{BO}(\boldsymbol{R}). \tag{2.35}$$

Equation (2.34) is a set of coupled differential equations for which it is impossible to find the exact solution because it would be necessary to calculate the couplings between the infinite set of functions

$$F_t(\boldsymbol{R})\phi_t(\boldsymbol{r}_{\rm g};R).$$

The adiabatic approximation consists in considering just the diagonal coupling in the electronic state solving only

$$\Big\{E_s(R)-\frac{\nabla^2_{\rm R}}{2\mu}+\int\phi^*_s(\boldsymbol{r}_{\rm g};R)\frac{\nabla^2_{\rm g}}{8\mu}\phi_s(\boldsymbol{r}_{\rm g};R)d\boldsymbol{r}_{\rm g}$$

$$-\int\phi^*_s(\boldsymbol{r}_{\rm g};R)\frac{\nabla^2_{\rm R}}{2\mu}\phi_s(\boldsymbol{r}_{\rm g};R)d\boldsymbol{r}_{\rm g}\Big\}F^{\rm ad}_s(\boldsymbol{R})=E_{\rm int}F^{\rm ad}_s(\boldsymbol{R}). \tag{2.36}$$

The effect of this approximation is that the nuclear motion is now governed by the effective potential

$$U(R)=E_s(R)-\int\phi^*_s(\boldsymbol{r}_{\rm g};R)\frac{\nabla^2_{\rm g}}{8\mu}\phi_s(\boldsymbol{r}_{\rm g};R)d\boldsymbol{r}_{\rm g}-\int\phi^*_s(\boldsymbol{r}_{\rm g};R)\frac{\nabla^2_{\rm R}}{2\mu}\phi_s(\boldsymbol{r}_{\rm g};R)d\boldsymbol{r}_{\rm g} \tag{2.37}$$

which is isotope dependent because it depends on the reduced mass μ; on the other hand, the Born-Oppenheimer potential $E_s(R)$ is isotope independent. Substituting (2.37) into (2.27), χ_{vN} and E_{vN} are obtained as solutions of the radial Schrödinger equation for the nuclear motion.

The adiabatic approximation then, consists in retaining the diagonal correction improving the approximation given by the Born-Oppenheimer one, even though electronic and nuclear motions are still separated.

The adiabatic approximation is particularly successful when the choice is made to neglect the non-adiabatic coupling to the state of interest; namely when the ground electronic state of a molecule which does not couple with its first excited state, producing non-adiabatic effects, has to be studied. This is the case for the ground states of H_2^+ and D_2^+, but not for HD^+; in fact, in this case the

$$\frac{\nabla_{\rm g}\cdot\nabla_{\rm R}}{2\mu_{\rm a}} \tag{2.38}$$

term couples the ground (Σ_g^+) and the first excited (Σ_u^+) electronic states. In order to obtain accurate results for HD^+ it is necessary to perform non-adiabatic calculations especially for high vibrational levels. In fact if the behaviour of the adiabatic potential for these states at large R is considered, at very large R they have the same dissociation limit even though in reality the dissociation limits H^++D(1s) and H(1s)+D^+ are separated by 29.8 cm^{-1}. This is a degeneracy that can be resolved only by performing non-adiabatic calculations.

2.1.3 The matrix elements of the Hamiltonian

In order to apply the Hamiltonian (2.10) to the hydrogen molecular ion, explicit forms of the operators that appear in it are needed; these have to be expressed in terms of the internal coordinates of the system (R, ξ, η) since the dependence upon χ is going to disappear. First, the angular motion of the nuclei has to be separated and then the resulting matrix elements have to be expressed in terms of the internal coordinates. The angular motion of the nuclei is separated by transforming the frame system from the space-fixed axes system (X, Y, Z) to a frame of rotating molecule-fixed axes (x, y, z); to do it, two Euler angles need to be defined:

- ϕ, about the initial Z axis with $0 \leq \phi < 2\pi$;
- θ, about the resultant y axis with $0 \leq \theta < \pi$

from which the following transformation is obtained

$$\begin{pmatrix} x \\ y \\ z \end{pmatrix} = \begin{pmatrix} \cos\phi\cos\theta & \sin\phi\cos\theta & -\sin\theta \\ -\sin\phi & \cos\phi & 0 \\ \cos\phi\sin\theta & \sin\phi\sin\theta & \cos\theta \end{pmatrix} \begin{pmatrix} X \\ Y \\ Z \end{pmatrix}; \tag{2.39}$$

in (2.39) x, y, z are the new rotating axes. The new coordinates (R, θ, ϕ) are sufficient to describe the motion of the nuclei.

The above transformation has to be applied to the differential operators of the Hamiltonian (2.10). Applying transformation (2.39) to the nuclear Laplacian operator ∇_R^2 and using it in (2.35) and (2.36), the separation of the rotational motion of the molecule [12] is obtained. In a frame system so defined, the motion of the electron is governed by the

molecule-fixed potential

$$U(r_{1e}, r_{2e}) = -\frac{1}{r_{1e}} - \frac{1}{r_{2e}} \tag{2.40}$$

so, physically, it is convenient to transform the operators to a molecule-fixed electron coordinates system referring it to the geometric centre of the internuclear vector. Then

$$\begin{aligned} \frac{\partial}{\partial\phi}\Big)_{\mathrm{s}} &= \frac{\partial}{\partial\phi}\Big)_{\mathrm{m}} - i\cos\theta L_z + i\sin\theta L_x; \\ \frac{\partial}{\partial\theta}\Big)_{\mathrm{s}} &= \frac{\partial}{\partial\theta}\Big)_{\mathrm{m}} - iL_y; \\ \frac{\partial}{\partial R}\Big)_{\mathrm{s}} &= \frac{\partial}{\partial R}\Big)_{\mathrm{m}} \end{aligned} \tag{2.41}$$

where the subscript s indicates the partial differential operators referring to the electron coordinates in the space-fixed axes system (X, Y, Z) while the subscript m refers to the electron coordinates in the molecule-fixed electron coordinate system (R, θ, ϕ). From transformation (2.41) a form is obtained for the nuclear Laplacian operator ∇^2_{R} that depends explicitly on the components of the electron angular momentum in the rotating coordinate system (L_x, L_y, L_z) through the operators [12]

$$L^{\pm} = L_x \pm iL_y. \tag{2.42}$$

Following the same procedure, the operator coupling electron and nuclear motions $\nabla_{\mathrm{g}} \cdot \nabla_{\mathrm{R}}$ may be written as a function of L_x, L_y, L_z and, moreover, as a function of the components of the electron's momentum operator

$$\boldsymbol{P} = -i\nabla_{\mathrm{g}} \tag{2.43}$$

in the molecule-fixed coordinate system through [12]

$$P^{\pm} = P_x \pm iP_y. \tag{2.44}$$

The electronic Laplacian and the potential operators

$$\nabla^2_{\mathrm{g}} = \frac{\partial^2}{\partial x^2}\Big)_{\mathrm{m}} + \frac{\partial^2}{\partial y^2}\Big)_{\mathrm{m}} + \frac{\partial^2}{\partial z^2}\Big)_{\mathrm{m}}, \tag{2.45}$$

$$V = \frac{1}{R} - \frac{1}{r_{1e}} - \frac{1}{r_{2e}} \tag{2.46}$$

are both independent of the Euler angles ϕ and θ.

Now, the forms derived for all the operators of the total Hamiltonian (2.10) allow the rotational motion of the molecule to be separated. For this purpose the molecular wave-function is written as

$$\psi_{\text{mol}} = \sum_{\Lambda} \Omega^{N}_{M_N,\Lambda}(\theta,\phi,\chi) U^{N}_{\Lambda}(\xi,\eta,R) \tag{2.47}$$

where the functions U^{N}_{Λ} depend on the relative positions of the particles and

$$\Omega^{N}_{M_N,\Lambda} = \frac{1}{2\pi} e^{iM_N\phi} e^{i\Lambda\chi} d^{N}_{M_N,\Lambda}(\theta) \tag{2.48}$$

are the normalized symmetric top eigenfunctions; $\boldsymbol{N}$ is the total angular momentum in the space-fixed system, M_N is its component along the space-fixed Z axis and Λ is its component along the rotating molecule-fixed z axis.

The motion of the electron about the z axis is described by the angle χ

$$L_z = -i\frac{\partial}{\partial\chi}. \tag{2.49}$$

Substitution of (2.47) into (2.8) leads to the elimination of the Euler angles ϕ and θ. The matrix elements of the Hamiltonian can be indicated as

$$\langle NM_N\Lambda'|H|NM_N\Lambda\rangle = \langle\Lambda'|H|\Lambda\rangle \tag{2.50}$$

since N and M_N are good quantum numbers. From the expression of the differential operators [12] in the total Hamiltonian, the only non-zero matrix elements of H are those which satisfy the Λ selection rule

$$\Lambda - \Lambda' = \Delta\Lambda = 0, \pm 1 \tag{2.51}$$

that is, the only non-zero matrix elements of the Hamiltonian are [12]

$$\langle \Lambda|H|\Lambda\rangle = -\frac{1}{2}\langle \Lambda|\nabla_{\rm g}^2|\Lambda\rangle + V - \frac{1}{8\mu}\langle \Lambda|\nabla_{\rm g}^2|\Lambda\rangle$$

$$-\frac{1}{2\mu}\Big\{\frac{\partial^2}{\partial R^2} + \frac{2}{R}\frac{\partial}{\partial R} - \frac{1}{R^2}\Big[N(N+1) - \Lambda(\Lambda+1) + \langle \Lambda|L^+L^-|\Lambda\rangle\Big]\Big\}$$

$$-\frac{i}{2\mu_{\rm a}}\Big\{P_z\frac{\partial}{\partial R} + \frac{1}{2R}\langle \Lambda|P^+L^- - P^-L^+|\Lambda\rangle\Big\}, \tag{2.52}$$

$$\langle \Lambda-1|H|\Lambda\rangle = \sqrt{(N+\Lambda)(N-\Lambda+1)}\Big\{\frac{1}{2\mu R^2}\langle \Lambda-1|L^-|\Lambda\rangle + \frac{i}{4\mu_{\rm a}R}\langle \Lambda-1|P^-|\Lambda\rangle\Big\}, \tag{2.53}$$

$$\langle \Lambda+1|H|\Lambda\rangle = \sqrt{(N+\Lambda+1)(\Lambda-N)}\Big\{\frac{1}{2\mu R^2}\langle \Lambda+1|L^+|\Lambda\rangle - \frac{i}{4\mu_{\rm a}R}\langle \Lambda+1|P^+|\Lambda\rangle\Big\}. \tag{2.54}$$

At this point the total internal Hamiltonian (2.10) does not depend any more on ϕ and θ, having separated the rotational motion of the nuclei.

The final step is to express the above matrix elements as function of the internal coordinates (R, ξ, η, χ) of the system allowing the elimination of the coordinate χ. After some manipulations the final matrix elements useful to develop non-adiabatic calculations for $\Lambda = 0, \pm 1$, namely between Σ and Π basis functions respectively, are [12]

$$\langle 0_{\rm g}'|H|0_{\rm g}\rangle = -\frac{2X_0}{R^2} + \frac{1}{R}\Big[1 - \frac{4\xi}{(\xi^2-\eta^2)}\Big] - \frac{1}{2\mu R^2}\Big\{\frac{\partial}{\partial R}\Big(R^2\frac{\partial}{\partial R}\Big) - 2Y\frac{\partial}{\partial R}R + (\xi^2+\eta^2)X_0 - N(N+1)\Big\}, \tag{2.55}$$

$$\langle 0_{\rm u}|H|0_{\rm g}\rangle = -\frac{1}{\mu_{\rm a}R^2}\Big\{Z\frac{\partial}{\partial R}R - \xi\eta X_0\Big\}, \tag{2.56}$$

$$\langle \pm 1_{\rm g}|H|0_{\rm g}\rangle = \pm\frac{\sqrt{N(N+1)}}{2\mu R^2}B, \tag{2.57}$$

$$\langle \pm 1_{\rm u}|H|0_{\rm g}\rangle = \mp\frac{\sqrt{N(N+1)}}{2\mu_{\rm a}R^2}A \tag{2.58}$$

where

$$X_\Lambda = \frac{1}{\xi^2-\eta^2}\Big\{\frac{\partial}{\partial\xi}(\xi^2-1)\frac{\partial}{\partial\xi} + \frac{\partial}{\partial\eta}(1-\eta^2)\frac{\partial}{\partial\eta}\Big\} - \frac{\Lambda^2}{(\xi^2-1)(1-\eta^2)}, \tag{2.59}$$

$$Y = \frac{1}{\xi^2-\eta^2}\Big\{\xi(\xi^2-1)\frac{\partial}{\partial\xi} + \eta(1-\eta^2)\frac{\partial}{\partial\eta}\Big\}, \tag{2.60}$$

$$Z = \frac{1}{\xi^2 - \eta^2}\left\{\eta(\xi^2 - 1)\frac{\partial}{\partial \xi} + \xi(1 - \eta^2)\frac{\partial}{\partial \eta}\right\}, \tag{2.61}$$

$$A = \frac{\sqrt{(\xi^2 - 1)(1 - \eta^2)}}{\xi^2 - \eta^2}\left\{\xi\frac{\partial}{\partial \xi} - \eta\frac{\partial}{\partial \eta}\right\}, \tag{2.62}$$

$$B = \frac{\sqrt{(\xi^2 - 1)(1 - \eta^2)}}{\xi^2 - \eta^2}\left\{\eta\frac{\partial}{\partial \xi} - \xi\frac{\partial}{\partial \eta}\right\} \tag{2.63}$$

and the subscripts g and u derive from the dependence of the single operators of the Hamiltonian on η; for the diagonal operators even in η the rules are

$$g \leftrightarrow g, \quad u \leftrightarrow u, \quad u \nleftrightarrow g \tag{2.64}$$

while if the diagonal operators are odd in η the rules change to

$$g \nleftrightarrow g, \quad u \nleftrightarrow u, \quad u \leftrightarrow g; \tag{2.65}$$

on the other hand for the off-diagonal operators in A, the matrix elements of the even operators in η satisfy (2.65), while those of the odd operators obey (2.64).

2.2 Non-adiabatic calculations

As already mentioned, it is impossible to find the exact solution of equation (2.34) because it would require the solution of an infinite set of coupled differential equations. One solution [14] is to try to reduce the problem by just considering the coupling with a finite number of other states and hope that the Born expansion (2.29) converges rapidly. This method has been used for the lowest vibrational levels but if there is the will to increase the number of levels studied, longer Born expansions are needed.

To perform more efficient and accurate non-adiabatic calculations, other techniques have to be developed.

2.2.1 Some possible approaches

Variational calculations

Within this method [15, 16] the eigenvalues of the complete Hamiltonian (2.8) are sought by variational adjustment of the trial wavefunction

$$\Psi = \sum_{i=0}^{i_m} \sum_{j=0,2}^{j_m} \sum_{k=0}^{k_m} c_{ijk}\phi_{ijk}(R,\xi,\eta) + \sum_{i=0}^{i'_m} \sum_{j=1,3}^{j'_m} \sum_{k=0}^{k'_m} c_{ijk}\phi_{ijk}(R,\xi,\eta). \tag{2.66}$$

In (2.66) the first summations are enough to describe an homonuclear molecule and the second summations have to be added in order to study an heteronuclear system; the basis functions of the expansion are

$$\phi_{ijk}(R,\xi,\eta) = e^{-\alpha\xi}\cosh(\beta\eta)\xi^i\eta^j R^{-3/2} e^{-\frac{1}{2}x^2} H_k(x) \tag{2.67}$$

where $H_k(x)$ are Hermite polynomials, $x = \gamma(R-\delta)$, i, j, k are integers and $\alpha, \beta, \gamma, \delta$ are adjustable non-linear parameters chosen to minimize the energy.

Variational-pertubation calculations

In this method [17–20] the non-adiabatic effects are treated as a perturbation of the adiabatic approximation so that the adiabatic wavefunctions can be used as a starting point for the development of the calculations. An adiabatic Hamiltonian is defined

$$H^{\mathrm{ad}} = \sum_n E_n^{\mathrm{ad}} |\psi_n^{\mathrm{ad}}\rangle\langle\psi_n^{\mathrm{ad}}| \tag{2.68}$$

where E_n^{ad} are the adiabatic energies and $|\psi_n^{\mathrm{ad}}\rangle$ is a complete set of adiabatic eigenfunctions of the form

$$\psi_n^{\mathrm{ad}}(\boldsymbol{R}, \boldsymbol{r}_{\mathrm{g}}) = \phi_n^{\mathrm{BO}}(\boldsymbol{r}_{\mathrm{g}}; R) F_n^{\mathrm{ad}}(\boldsymbol{R}). \tag{2.69}$$

$F_n^{\mathrm{ad}}(\boldsymbol{R})$ are the solutions of the radial Schrödinger equation with $U(R)$ being the adiabatic potential (see equations (2.27) and (2.37)).

The total Hamiltonian can now be separated into an adiabatic part and a non-adiabatic term treated as a perturbation

$$H = H^{\mathrm{ad}} + H^{\mathrm{nad}} \tag{2.70}$$

so that

$$H|\psi_n^{\mathrm{ad}}\rangle = E_n^{\mathrm{ad}}|\psi_n\rangle + H^{\mathrm{nad}}|\psi_n\rangle \tag{2.71}$$

and since

$$\langle\psi_n^{\mathrm{ad}}|H^{\mathrm{ad}}|\psi_n^{\mathrm{ad}}\rangle = E_n^{\mathrm{ad}} \tag{2.72}$$

the first-order energy correction is

$$\langle\psi_n^{\mathrm{ad}}|H^{\mathrm{nad}}|\psi_n^{\mathrm{ad}}\rangle = 0. \tag{2.73}$$

To find the second-order energy correction, ψ^{ad} is treated as the zero-order eigenfunction and the first-order eigenfunction is written as

$$\psi_n = \psi_n^{\mathrm{ad}} + \psi_n^{'} \tag{2.74}$$

where $\psi_n^{'}$ satisfies the equation

$$(H^{\mathrm{ad}} - E_n^{\mathrm{ad}})\psi_n^{'} = -H^{\mathrm{nad}}\psi_n^{\mathrm{ad}}. \tag{2.75}$$

The second-order energy correction is given by

$$E^{''} = \langle\psi_n^{'}|H^{\mathrm{nad}}|\psi_n^{\mathrm{ad}}\rangle = \langle\psi_n^{'}|H - E_n^{\mathrm{ad}}|\psi_n^{\mathrm{ad}}\rangle. \tag{2.76}$$

To first-order the ground state couples only to excited Σ and Π states. The non-adiabatic corrections are completely independent for each coupling

$$E^{''} = \sum_{\Lambda\alpha} E_{\Lambda\alpha}^{''} \tag{2.77}$$

where Λ is the projection of the orbital angular momentum on the internuclear axis and α includes g and u characters. For the homonuclear molecular ions the coupling between states of different g/u symmetry is zero and this method gives very good results, but for HD^+ the results compared with experiments become worse at the approach of the dissociation limit

because the coupling between $1s\sigma_g$ and $2p\sigma_u$ states increases at large internuclear distances and can no longer be treated as a perturbation.

2.2.2 The theory of the transformed Hamiltonian for HD^+

The electronic part of the Schrödinger equation needs to be solved very accurately in prolate spheroidal coordinates. When the internal Schrödinger equation is expressed in prolate spheroidal coordinates, very complicated nuclear motion terms appear (see equations (2.55) to (2.58)); some of them consist of cross-derivative terms between electronic and nuclear coordinates. For this reason when non-adiabatic calculations are performed, many problems arise from the complexity of the equations; then, it is convenient to simplify the theory being careful not to lose accuracy in the results.

The main theoretical properties to be satisfied from the transformed Hamiltonian theory are the following:

-) the electronic Schrödinger equation has to be accurately and easily solved;
-) the nuclear motion effects have to be included;
-) all the properties of HD^+ and its isotopomers have to be calculated accurately for all the levels of the ground electronic state.

The first condition is complied with by the development of a theory in which the Schrödinger equation is solved in prolate spheroidal coordinates, but in order to satisfy the second property a more sophisticated theory has to be used. If the first two conditions are satisfied also the third will be with high probability.

The transformed Hamiltonian theory for HD^+ [21–23] answers all the requirements listed above. The core of the theory is to transform the Schrödinger equation in such a way that complicated nuclear motion terms involving cross-derivatives between nuclear and electronic coordinates do not appear in the transformed Hamiltonian; the new energy operator is, in this way, able to take account of those terms within a transformed potential energy operator, which does not contain any derivatives. As a consequence, some nuclear

motion effects which before the transformation appeared as non-adiabatic effects, are now accounted for in the adiabatic part of the problem.

Because of the different nuclear masses in HD^+, the g/u symmetry breaking term

$$-\frac{\nabla_g \cdot \nabla_R}{2\mu_a} \tag{2.78}$$

has to be treated to obtain an intermediate transformed Hamiltonian, which is similar to that for H_2^+ and D_2^+; a further transformation is then made to give a final transformed Hamiltonian. As will be seen, it is possible to choose the intermediate transformation [21,22] so that the mass asymmetry is mainly accounted for through effective nuclear charges.

The intermediate transformation

The starting point of the transformed Hamiltonian theory is to rewrite the Hamiltonian (2.10) as

$$H_{int} = T_e + \frac{1}{\mu} H_{ad} + \frac{1}{\mu_a} H_{gu} + V \tag{2.79}$$

where the kinetic energy operator T_e is

$$T_e = \frac{1}{2}\nabla_g^2, \tag{2.80}$$

the potential energy operator is

$$V = \frac{1}{R} - \frac{1}{r_{1e}} - \frac{1}{r_{2e}} \tag{2.81}$$

and the reduced mass constants and the other kinetic operators are defined in section 2.1. In order to remove the coupling term

$$\frac{1}{\mu_a} H_{gu}, \tag{2.82}$$

the Schrödinger equation is transformed as

$$H' = e^{iS} H_{int} e^{-iS} \tag{2.83}$$

where S is an hermitian operator and the exponentials are to be interpreted as the corresponding power series expansions. The expansion of equation (2.83) gives

$$H^{'} = H_{\rm int} + [iS, H_{\rm int}] + \frac{1}{2!}[iS,[iS,H_{\rm int}]] + \frac{1}{3!}[iS,[iS,[iS,H_{\rm int}]]] + \ldots . \tag{2.84}$$

The hermitian operator S is given by

$$S = S_{\rm g} + S_{\rm u} \tag{2.85}$$

where $S_{\rm g}$ and $S_{\rm u}$ are, respectively, even and odd operators with respect to inversion of the electron coordinates in the geometric centre of nuclei; they are explicitly given by

$$iS_{\rm g} = a(\boldsymbol{R}\cdot\nabla_{\rm R}) + b(\boldsymbol{r}_{\rm g}\cdot\nabla_{\rm g}) \tag{2.86}$$

and

$$iS_{\rm u} = c(\boldsymbol{r}_{\rm g}\cdot\nabla_{\rm R}) + d(\boldsymbol{R}\cdot\nabla_{\rm g}) \tag{2.87}$$

where a, b, c, d are real parameters. The four real parameters are chosen to be [21,22]

$$a = 0, \quad b = 0, \quad c = \tanh^{-1}\left[\frac{\mu}{\mu_{\rm a}(2\mu+1)}\right], \quad d = \frac{c}{4} \tag{2.88}$$

and to the first order in (nuclear mass)$^{-1}$

$$c = \frac{1}{2\mu_{\rm a}}, \quad d = \frac{1}{8\mu_{\rm a}}. \tag{2.89}$$

The reason for this choice is explained as follows.

Even though there are many transformations able to eliminate the coupling term, this one avoids having divergent potential energy terms which are uncomfortable to treat. Avoiding such terms decreases the possible choices for the transformation employed. The electron-nuclear potential energy terms should not be affected by the transformation apart from multiplicative factors

$$e^{iS}\left(\frac{1}{r_{\rm nc}}\right)e^{-iS} = \frac{Z_{\rm n}}{r_{\rm nc}} \tag{2.90}$$

where n=1,2 and $Z_{\rm n}$ may be seen as effective nuclear charges. A simple condition for this to happen is that iS, $\boldsymbol{r}_{1\rm e}(=\boldsymbol{r}_{\rm g}+\frac{1}{2}\boldsymbol{R})$ and $\boldsymbol{r}_{2\rm e}(=\boldsymbol{r}_{\rm g}-\frac{1}{2}\boldsymbol{R})$ satisfy the following commutation

rules

$$[iS, \boldsymbol{r}_{1c}] = \mathrm{k}_1 \boldsymbol{r}_{1c} \tag{2.91}$$

and

$$[iS, \boldsymbol{r}_{2c}] = -\mathrm{k}_2 \boldsymbol{r}_{2c} \tag{2.92}$$

where k_1 and k_2 are constants. Taking the general form of iS (see equations (2.85), (2.86) and (2.87)) the commutators become

$$[iS, \boldsymbol{r}_{1c}] = \Big(\frac{1}{2}c + b\Big)\boldsymbol{r}_{1c} + \Big(\frac{1}{2}a + d - \frac{1}{4}c - \frac{1}{2}b\Big)\boldsymbol{R} \tag{2.93}$$

and

$$[iS, \boldsymbol{r}_{2c}] = -\Big(\frac{1}{2}c - b\Big)\boldsymbol{r}_{2c} + \Big(-\frac{1}{2}a + d - \frac{1}{4}c + \frac{1}{2}b\Big)\boldsymbol{R}. \tag{2.94}$$

The simplest way to satisfy (2.91) and (2.92) is to set

$$a = b = 0 \quad \text{and} \quad d = \tfrac{1}{4}c$$

so that k_1=k_2 and a completely odd transformation is chosen. If $c = \omega$ and $d = \frac{1}{4}\omega$, iS is chosen to be

$$iS = \omega\Big[(\boldsymbol{r}_g \cdot \nabla_R) + \frac{1}{4}(\boldsymbol{R} \cdot \nabla_g)\Big] \tag{2.95}$$

which leads to the elimination of

$$\frac{1}{\mu_a} H_{gu}. \tag{2.96}$$

With iS expressed as (2.95) the explicit form for the transformed Hamiltonian H' [21, 22] can be evaluated to be

$$\begin{aligned} H' = T_e &+ \Big\{\Big[2 + \frac{1}{\mu}\Big]\cosh(\omega) - \frac{1}{\mu_a}\sinh(\omega) - 2\Big\}H_{ad} \\ &+ \Big\{-\Big[2 + \frac{1}{\mu}\Big]\sinh(\omega) + \frac{1}{\mu_a}\cosh(\omega)\Big\}H_{gu} + V' \end{aligned} \tag{2.97}$$

from which ω must satisfy the equation

$$-\Big[2 + \frac{1}{\mu}\Big]\sinh(\omega) + \frac{1}{\mu_a}\cosh(\omega) = 0 \tag{2.98}$$

which leads to

$$\omega = \tanh^{-1}\Big(\frac{1}{p}\Big) \tag{2.99}$$

where

$$p = \Big(2 + \frac{1}{\mu}\Big)\mu_{\rm a}. \tag{2.100}$$

Using in (2.97) the properties of the hyperbolic trigonometric functions

$$\sinh(\omega) = \frac{1}{\sqrt{p^2 - 1}} \tag{2.101}$$

and

$$\cosh(\omega) = \frac{p}{\sqrt{p^2 - 1}} \tag{2.102}$$

the new expression for $H^{'}$ is

$$H^{'} = T_{\rm e} + \frac{1}{\mu_{\rm eff}} H_{\rm ad} + V^{'} \tag{2.103}$$

which is formally similar to the Hamiltonian for H_2^+ and D_2^+; in (2.103) $\mu_{\rm eff}$ plays the role of an effective nuclear reduced mass

$$\frac{1}{\mu_{\rm eff}} = \frac{1}{\mu_{\rm a}}\sqrt{p^2 - 1} - 2 \simeq \frac{1}{\mu} - \frac{1}{4\mu_{\rm a}^2} + \mathcal{O}\Big(\frac{1}{\mu\mu_{\rm a}^2}\Big). \tag{2.104}$$

Having eliminated

$$\frac{1}{\mu_{\rm a}} H_{\rm gu} \tag{2.105}$$

multiplying the relative electron position vectors by the same constant, the transformed potential energy $V^{'}$ [21,22] becomes

$$V^{'} = \frac{1}{R\sqrt{1 + 2\beta\Big(\frac{r_{\rm g}\cdot R}{R^2}\Big) + 4\gamma\Big(\frac{r_{\rm g}^2 + \frac{1}{4}R^2}{R^2}\Big)}} - \frac{Z_1}{r_{1\rm e}} - \frac{Z_2}{r_{2\rm e}} \tag{2.106}$$

where

$$\beta = \frac{1}{\sqrt{p^2 - 1}} \simeq \frac{1}{2\mu_{\rm a}} + \mathcal{O}\Big(\frac{1}{\mu\mu_{\rm a}}, \frac{1}{\mu_{\rm a}^2}\Big), \tag{2.107}$$

$$\gamma = \frac{p\beta - 1}{2} \simeq \frac{1}{16\mu_{\rm a}^2} + \mathcal{O}\Big(\frac{1}{\mu\mu_{\rm a}^2}\Big), \tag{2.108}$$

$$Z_1 = e^{-\frac{\omega}{2}} = \sqrt[4]{\frac{p-1}{p+1}} \simeq 1 - \frac{1}{4\mu_{\rm a}} + \mathcal{O}\Big(\frac{1}{\mu\mu_{\rm a}}, \frac{1}{\mu_{\rm a}^2}\Big), \tag{2.109}$$

$$Z_2 = e^{\frac{\omega}{2}} = \sqrt[4]{\frac{p+1}{p-1}} \simeq 1 + \frac{1}{4\mu_{\rm a}} + \mathcal{O}\Big(\frac{1}{\mu\mu_{\rm a}}, \frac{1}{\mu_{\rm a}^2}\Big). \tag{2.110}$$

The entire transformation of the Hamiltonian has been performed in cartesian coordinates but its expression has to be written in terms of the internal prolate spheroidal coordinates. While $T_{\rm e}$, $H_{\rm ad}$ and the electron-nuclear potential energy have similar forms as in the untransformed Hamiltonian (see equation (2.55)), the transformed internuclear potential energy operator is quite different and it becomes [21]

$$V' = -\frac{2}{R}\Big[\frac{(Z_1+Z_2)\xi + (Z_2 - Z_1)\eta}{\xi^2 - \eta^2}\Big] + \frac{1}{R\sqrt{1 + \beta\xi\eta + \gamma(\xi^2+\eta^2)}} \tag{2.111}$$

which contains an inseparable term that does not allow the exact solution of the Schrödinger equation

$$(T_{\rm e} + V')\phi_t = E\phi_t. \tag{2.112}$$

At this stage it is possible to solve the Schrödinger equation associated with the Hamiltonian (2.103) in the adiabatic approximation [21,22,24]. The transformed Hamiltonian in prolate spheroidal coordinates for the Σ states is

$$H' = -\frac{2}{\kappa R^2}X_0 - \frac{1}{2\mu_{\rm eff}R^2}\Big\{\frac{\partial}{\partial R}\Big(R^2\frac{\partial}{\partial R}\Big) - 2Y\frac{\partial}{\partial R}R + (\xi^2+\eta^2-2)X_0 - N(N+1)\Big\} + V' \tag{2.113}$$

where X_0 and Y are defined in (2.59) and (2.60), the mass dependent constant $\mu_{\rm eff}$ is given in terms of μ and $\mu_{\rm a}$ (see equation (2.104)) and

$$\frac{1}{\kappa} = 1 + \frac{1}{2\mu_{\rm eff}}. \tag{2.114}$$

In the Schrödinger equation

$$\Big(-\frac{2}{\kappa R^2}X_0 + V'\Big)\psi_0 = E_0\psi_0, \tag{2.115}$$

no derivatives with respect to R appear and it can be solved variationally for a range of values of R. Then the adiabatic correction to E_0 is given by

$$E_{\rm ad} = -\frac{1}{2\mu_{\rm eff}}\langle\psi_0|\frac{\partial^2}{\partial R^2}+\frac{2}{R}\frac{\partial}{\partial R}-\frac{2}{R^2}Y\frac{\partial}{\partial R}R+\frac{1}{R^2}(\xi^2+\eta^2-2)X_0-\frac{1}{R^2}N(N+1)|\psi_0\rangle. \quad (2.116)$$

Equation (2.113) is not separable because of the presence of the transformed internuclear potential; a solution could be found in expanding the unseparable term contained in $V^{'}$ as a Taylor series

$$\frac{1}{R\sqrt{1+\beta\xi\eta+\gamma(\xi^2+\eta^2)}} = \frac{1}{R}\Big\{1-\frac{1}{2}\Big[\beta\xi\eta+\gamma(\xi^2+\eta^2)\Big]+\frac{3}{8}\beta^2\xi^2\eta^2\Big\}+\mathcal{O}\Big(\frac{1}{\mu\mu_{\rm a}^2},\frac{1}{\mu_{\rm a}^3}\Big) \quad (2.117)$$

and developing a variational method that requires only the evaluation of two-dimensional integrals involving separable integrands, all of which may be evaluated analytically. The solution of equation (2.113) can be expressed as

$$\psi_0 = \sum_i c_i\phi_i \quad (2.118)$$

with the ϕ_i basis functions modelled on the Hylleraas expansion [9] that were used in the development of the Born-Oppenheimer electronic equation (see section 2.1.1 on page 9). The new basis functions associated with the Σ states, which do not depend on R, are

$$\phi_i = \frac{1}{\sqrt{2\pi}}e^{-\frac{\alpha(\xi-1)}{2}}\mathcal{L}_{m_i}[\alpha(\xi-1)]\mathcal{P}_{n_i}(\eta), \quad (2.119)$$

where the convention $\mathcal{L}_{m_i}^{(0)}(x) = \mathcal{L}_{m_i}(x)$ is used. In (2.119), $\mathcal{L}_{m_i}[\alpha(\xi-1)]$ and $\mathcal{P}_{n_i}(\eta)$ are Laguerre and Legendre polynomials respectively of order m_i and n_i, and α is treated as a non-linear variational parameter. The subscripts m_i and n_i are positive integers (m_i (n_i) = 0, 1, 2, ... m_{max} (n_{max})) such that the combination between m_i and n_i is unique for each value of i. Using the variational principle for the linear parameters c_i of the expansion leads to the matrix equation

$$(\mathbf{H}-E_0\mathbf{S})\mathbf{c} = \mathbf{0} \quad (2.120)$$

where

$$H_{ij} = \int\phi_i\Big(-\frac{2}{\kappa R^2}X_0+V^{'}\Big)\phi_j d\tau, \quad (2.121)$$

$$S_{ij} = \int \phi_i \phi_j d\tau, \tag{2.122}$$

and

$$d\tau = \frac{1}{4}\pi R^3(\xi^2 - \eta^2)d\xi d\eta. \tag{2.123}$$

Since the operators in (2.115) are hermitian, **H** and **S** are symmetric matrices. The matrix elements (2.121) and (2.122) may be evaluated analytically in terms of

$$\int_0^\infty x^k e^{-x} \mathcal{L}_m(x)\mathcal{L}_n(x)dx \tag{2.124}$$

where $x = \alpha(\xi - 1)$ and

$$\int_{-1}^{+1} \eta^k \mathcal{P}_m(\eta)\mathcal{P}_n(\eta)d\eta. \tag{2.125}$$

In order to compute the vibration-rotational levels in the adiabatic approximation, the radial Schrödinger equation

$$\Big\{ -\frac{1}{2\mu_{\text{eff}}}\Big[\frac{d^2}{dR^2} + \frac{2}{R}\frac{d}{dR} - \frac{1}{R^2}N(N+1)\Big] + W(R)\Big\}F_{vN}(R) = E_{vN}F_{vN}(R) \tag{2.126}$$

has to be solved; in (2.126) the adiabatic potential is

$$W(R) = E_0(R) + E_{\text{ad}}(R), \tag{2.127}$$

where $F_{vN}(R)$ are the radial eigenfunctions and E_{vN} are the energies of the level with vibrational quantum number v and rotational quantum number N. Substituting

$$F_{vN}(R) = \frac{1}{R}\chi_{vN}(R) \tag{2.128}$$

in (2.126), the following expression for the radial Schrödinger equation is obtained

$$\Big\{ -\frac{d^2}{dR^2} + 2\mu_{\text{eff}}\Big[W(R) - E_{vN}\Big] + \frac{N(N+1)}{R^2}\Big\}\chi_{vN}(R) = 0 \tag{2.129}$$

(compare with (2.27)); this can be solved numerically using the Numerov-Cooley algorithm [11] as implemented by Le Roy [7]. The potential energy curves obtained [21, 22, 24] are used later in studying the isotopic dependence of the bond length.

The final transformation

So far, the non-adiabatic coupling of the states due to the operator

$$-\frac{1}{\mu_{\text{eff}}R^2}\Big\{\frac{\partial}{\partial R}(R^2\frac{\partial}{\partial R}) - 2Y\frac{\partial}{\partial R}R + (\xi^2+\eta^2-2)X_0\Big\} \tag{2.130}$$

has been ignored; it contains a term, which is present for H_2^+ and D_2^+ also, formed by cross-derivatives between electronic and nuclear coordinates, difficult to calculate non-adiabatically. Another transformation of the Hamiltonian has to be performed. The matrix elements of the transformed Hamiltonian are formally similar to those reported in (2.55) to (2.58). Since the

$$2Y\frac{\partial}{\partial R}R \tag{2.131}$$

term appears in the diagonal matrix elements in Λ of $H^{'}$, this term is considered in the form it has in (2.113); $H^{'}$ is rewritten as

$$H^{'} = -\frac{2\rho}{mR^2}X_0 - \frac{1}{2\mu_{\text{eff}}R^2}\Big\{\frac{\partial}{\partial R}(R^2\frac{\partial}{\partial R}) - 2Y\frac{\partial}{\partial R}R\Big\} + V^{'} \tag{2.132}$$

where

$$\frac{1}{m} = 1 + \frac{1}{4\mu_{\text{eff}}} \tag{2.133}$$

and

$$\rho = 1 + \frac{m}{4\mu_{\text{eff}}}(\xi^2+\eta^2-1). \tag{2.134}$$

As before, the Hamiltonian $H^{'}$ is transformed as

$$H^{''} = e^{i\Theta}H^{'}e^{-i\Theta} \tag{2.135}$$

so that the wavefunction $\psi^{'}$ becomes

$$\psi^{''} = e^{i\Theta}\psi^{'}. \tag{2.136}$$

It will be seen that the objective is achieved if Θ is chosen to be

$$\Theta = -if(\rho)\Big(R\frac{\partial}{\partial R} + 3\Big) \tag{2.137}$$

with

$$f(\rho) = -\frac{1}{2}\ln\rho, \tag{2.138}$$

H'' is hermitian and the transformation (2.135) is unitary. The volume element $d\tau$ in prolate spheroidal coordinates is now

$$d\tau = \frac{R^5}{8}(\xi^2 - \eta^2)dRd\xi d\eta d\chi. \tag{2.139}$$

After some manipulations [21, 23] the transformed Hamiltonian H'' may be expressed in terms of the first and second derivatives with respect to ρ, $f'(\rho)$ and $f''(\rho)$, as

$$H'' = e^{-2f}\Big\{ -\frac{2\rho}{mR^2}X_0 + \frac{1}{\mu_{\text{eff}}R^2}\Big[\Big(3\rho f' + 2\rho(\rho-1)f'' - 10\rho(\rho-1)(f')^2 - 6(\rho-1)f'\Big)\frac{\partial}{\partial R}R$$

$$+2\Big(3\rho f' + 2\rho(\rho-1)f'' - 4\rho(\rho-1)(f')^2 + 2\rho f'Y\Big) + (1+2\rho f')Y\frac{\partial}{\partial R}R \tag{2.140}$$

$$-\frac{1}{2}\Big(1 + 4\rho(\rho-1)(f')^2 + 4(\rho-1)f'\Big)\frac{\partial}{\partial R}\Big(R^2\frac{\partial}{\partial R}\Big)\Big]\Big\} + e^{-f}V'$$

where

$$V' \propto \frac{1}{R} \tag{2.141}$$

and since Θ has no derivatives with respect to ξ and η,

$$e^{i\Theta}V'e^{-i\Theta} = e^{-f(\rho)}V'. \tag{2.142}$$

In (2.140) the cross-derivative term

$$Y\frac{\partial}{\partial R}R \tag{2.143}$$

is eliminated if

$$1 + 2\rho f'(\rho) = 0 \tag{2.144}$$

which is a differential equation with solution

$$f(\rho) = -\frac{1}{2}\ln\rho + constant. \tag{2.145}$$

Choosing the constant of integration to be zero,

$$e^{-f} = \sqrt{\rho},$$

$$f' = -\frac{1}{2\rho}, \tag{2.146}$$

$$f'' = \frac{1}{2\rho^2}.$$

Substituting (2.146) into (2.140) H'' becomes

$$H'' = -\frac{2\rho^2}{mR^2}X_0 - \frac{\rho}{\mu_{\text{eff}}R^2}(2Y+3) - \frac{1}{2\mu_{\text{eff}}}\Big(\frac{\partial^2}{\partial R^2} + \frac{5}{R}\frac{\partial}{\partial R} + \frac{3}{R^2}\Big) + \sqrt{\rho}V' \tag{2.147}$$

which is hermitian. By making the substitution

$$\psi'' = R^{-\frac{5}{2}}\phi_t \tag{2.148}$$

in

$$H''\psi'' = E\psi'' \tag{2.149}$$

the new transformed Schrödinger equation

$$H_t\phi_t = E\phi_t \tag{2.150}$$

is obtained where

$$H_t = -\frac{2\rho^2}{mR^2}X_0 - \frac{\rho}{\mu_{\text{eff}}R^2}(2Y+3) + \sqrt{\rho}V' + \frac{3}{8\mu_{\text{eff}}R^2} - \frac{1}{2\mu_{\text{eff}}}\frac{\partial^2}{\partial R^2}; \tag{2.151}$$

this Hamiltonian is hermitian if ϕ_t is normalized using the volume element

$$d\tau = \frac{1}{8}(\xi^2 - \eta^2)dRd\xi d\eta d\chi. \tag{2.152}$$

This form of the Hamiltonian is able to reproduce the correct dissociation energies for HD^+ [21, 23]. The diagonal matrix elements for the Σ states are

$$H_t = -\frac{2\rho^2}{mR^2}X_0 - \frac{\rho}{\mu_{\text{eff}}R^2}(2Y+3) + \sqrt{\rho}V' + \frac{3}{8\mu_{\text{eff}}R^2} - \frac{1}{2\mu_{\text{eff}}}\frac{\partial^2}{\partial R^2} + \frac{\rho}{2\mu_{\text{eff}}R^2}N(N+1). \tag{2.153}$$

In H_t, then, there are no cross-derivatives between the bond length coordinate R and the electronic coordinates ξ and η; this means that all the nuclear motion effects, apart from the non-adiabatic coupling due to

$$-\frac{1}{2\mu_{\rm eff}}\frac{\partial^2}{\partial R^2}, \tag{2.154}$$

may be accounted for in the adiabatic approximation.

In conclusion, if the final transformed Hamiltonian is written as

$$H_t = -\frac{1}{2\mu_{\rm eff}}\frac{\partial^2}{\partial R^2} + H_e \tag{2.155}$$

the matrix elements used to study the properties of HD^+ are the following

$$\langle 0'_{g,u}|H_e|0_{g,u}\rangle = -\frac{2\rho^2}{mR^2}X_0 - \frac{\rho}{\mu_{\rm eff}R^2}(2Y+3) + \sqrt{\rho}V' + \frac{3}{8\mu_{\rm eff}R^2} + \frac{\rho}{2\mu_{\rm eff}R^2}N(N+1), \tag{2.156}$$

$$\langle \pm 1'_{g,u}|H_e|\pm 1_{g,u}\rangle = -\frac{2\rho^2}{mR^2}X_1 - \frac{\rho}{\mu_{\rm eff}R^2}(2Y+3) + \sqrt{\rho}V' + \frac{3}{8\mu_{\rm eff}R^2} + \frac{\rho}{2\mu_{\rm eff}R^2}[N(N+1)-2], \tag{2.157}$$

and

$$\langle \pm 1_{g,u}|H_e|0_{g,u}\rangle = \pm\frac{\rho}{2\mu_{\rm eff}R^2}\sqrt{N(N+1)}B. \tag{2.158}$$

To ensure the hermiticity of H_e

$$\langle 0_{g,u}|H_e|\pm 1_{g,u}\rangle = \mp\frac{\rho}{2\mu_{\rm eff}R^2}\sqrt{N(N+1)}\Big(B + \frac{\xi\eta}{\sqrt{(\xi^2-1)(1-\eta^2)}}\Big). \tag{2.159}$$

Since the Hamiltonian has been transformed to remove the g/u coupling from the kinetic energy part of the problem, the matrix elements between g and u functions only involve the transformed potential energy

$$\langle 0'_{g,u}|H_e|0_{u,g}\rangle = \sqrt{\rho}V', \tag{2.160}$$

$$\langle \pm 1'_{g,u}|H_e|\pm 1_{u,g}\rangle = \sqrt{\rho}V', \tag{2.161}$$

and

$$\langle \pm 1'_{g,u}|H_e|0_{u,g}\rangle = 0. \tag{2.162}$$

From equations (2.150) and (2.153) the transformed Schrödinger equation can be solved in an adiabatic approximation, neglecting the coupling between rotational and electronic angular momenta. To do this, the equation

$$\Big[-\frac{2\rho^2}{mR^2}X_0-\frac{\rho}{\mu_{\rm eff}R^2}(2Y+3)+\frac{3}{8\mu_{\rm eff}R^2}+\sqrt{\rho}V'\Big]\phi_0=E_0\phi_0 \tag{2.163}$$

has to be considered where the potential V' is given by (2.111). Equation (2.163) does not contain any derivatives with respect to R and it is solved variationally for a range of values of R following the same method explained before (see page 25 to page 27). In calculating the adiabatic correction $E_{\rm ad}$, for $N>0$ the rotational contribution is approximated by setting $\rho=1$ for convenience, in solving the vibration-rotational problem. Then, for $A=0$, the adiabatic correction is given by

$$E_{\rm ad}=-\frac{1}{2\mu_{\rm eff}}\langle\psi_0|\frac{\partial^2}{\partial R^2}-\frac{N(N+1)}{R^2}|\psi_0\rangle. \tag{2.164}$$

The vibration-rotational energies E_{vN} and the vibrational wavefunctions $\chi_{vN}(R)$ are calculated from the radial equation

$$\Big\{-\frac{d^2}{dR^2}+\frac{1}{R^2}N(N+1)+2\mu_{\rm eff}\Big[E_0(R)+E_{\rm ad}(R)-E_{vN}\Big]\Big\}\chi_{vN}(R)=0 \tag{2.165}$$

and solved numerically using the Numerov-Cooley algorithm [11].

Transformed eigenfunctions and transformed properties

Since the Hamiltonian is transformed, as explained before, through

$$H_{\rm t}=e^{i\Theta}H'e^{-i\Theta} \tag{2.166}$$

and its eigenvalues remain the same, the eigenvectors are also transformed

$$\psi_{\rm t}=e^{i\Theta}\psi'. \tag{2.167}$$

For this reason, when calculating properties other than the energy from the transformed wavefunction, transformed operators have to be used.

In the case of the bond length, its most general form, namely for HD^+ in prolate spheroidal coordinates after the intermediate transformation [21] is

$$R' = R\sqrt{1 + \beta\xi\eta + \gamma(\xi^2 + \eta^2)} \tag{2.168}$$

where β and γ are the mass factors indicated in equations (2.107) and (2.108) respectively. In the specific case of the homonuclear species H_2^+ and D_2^+, equation (2.168) reduces to

$$R' = R. \tag{2.169}$$

When the final transformation is applied, the form of the transformed bond length is

$$R_t = e^{i\Theta} R' e^{-i\Theta} = e^{f(\rho)} R = \rho^{-1/2} R \tag{2.170}$$

where ρ, Θ and $f(\rho)$ are defined respectively in (2.134), (2.137) and (2.138). Starting with (2.170) it is possible to transform the R dependent part of any other operator of interest.

The electron density at the nuclei is one of the other properties of interest for this project, since it appears in the expression of the relativistic correction (see chapter 8). In prolate spheroidal coordinates the expressions for the electron density at the nuclei 1 and 2 are given respectively by

$$\delta(\boldsymbol{r}_{1e}) = \frac{4\delta(\xi - 1)\delta(\eta + 1)}{\pi R^3(\xi^2 - \eta^2)}, \tag{2.171}$$

$$\delta(\boldsymbol{r}_{2e}) = \frac{4\delta(\xi - 1)\delta(\eta - 1)}{\pi R^3(\xi^2 - \eta^2)}. \tag{2.172}$$

After the first transformation the following expression arises [21]

$$\delta'(\boldsymbol{r}_{ne}) = \frac{4Z_n^3\delta(\xi - 1)\delta(\eta \pm 1)}{\pi R^3(\xi^2 - \eta^2)} \tag{2.173}$$

where $n = 1, 2$ refers to the nuclei and Z_n are the effective nuclear charges of equations (2.109) and (2.110).

Since from equation (2.173) $\delta'(\boldsymbol{r}_{ne}) \propto (1/R^3)$, in prolate spheroidal coordinates the second and final transformation gives

$$\delta_t(\boldsymbol{r}_{ne}) = e^{i\Theta}\delta'(\boldsymbol{r}_{ne})e^{-i\Theta} = e^{i\Theta}\frac{1}{R^3}e^{-i\Theta}\delta'(\boldsymbol{r}_{ne})R^3 = \rho^{3/2}\delta'(\boldsymbol{r}_{ne}) \tag{2.174}$$

at nuclei 1 and 2 where ρ is given by (2.134).

Chapter 3

Calculation methods

3.1 Introduction

In order to perform non-adiabatic calculations, the approach used is, first, a variational method following the work of Moss and Sadler [6] in which just some levels for $v \leq 4$ are studied. Although it might be possible to achieve satisfactory results for higher vibrational levels, the variational method is limited by the number of basis functions needed. For this reason a scattering approach is mainly used in this work; this allows the study of non-adiabatic properties of H_2^+, D_2^+ and HD^+ for all the vibration-rotational levels. For HD^+ use of the intermediate transformed Hamiltonian (see page 21) to determine adiabatic corrections for some properties allows a valid comparison with the other two molecules, avoiding the effect of mass asymmetry.

In addition, as the scattering method does not produce any wavefunctions, the Hutson method [25] is used to determine the expectation values of the properties of interest.

Even though most of the integrals needed may be evaluated analytically, some of them require numerical integration for singular integrands; the last section of this chapter is dedicated to an explanation of this topic.

3.2 The variational method

The variational calculations use a linear combination of products of electronic and vibrational functions of the form [6]

$$\psi_{\rm mol}(\xi,\eta,R) = \sum_i c_i \phi_i(\xi,\eta)\psi_i(R). \tag{3.1}$$

The electronic part of the solution, $\phi_i(\xi,\eta)$, includes both Σ and Π functions. From the matrix elements for H_2^+ and D_2^+ in equations (2.55) to (2.58), the dependence on χ disappears and just the variables ξ, η, R remain with the volume element

$$d\tau = \frac{R^5}{8}(\xi^2-\eta^2)d\xi d\eta dR. \tag{3.2}$$

As in [23,24] the electronic functions are modelled on the Hylleraas expansion

$$\phi_i(\xi,\eta) = e^{-\frac{\alpha(\xi-1)}{2}}(\xi^2-1)^{\frac{|\Lambda|}{2}}\mathcal{L}_{m_i}^{(|\Lambda|)}[\alpha(\xi-1)]\mathcal{P}_{n_i}^{(|\Lambda|)}(\eta). \tag{3.3}$$

In [23,24] Π functions were not used, that is the coupling of electronic and rotational angular momenta was not included. There the electronic problem was solved at each value of R and the non-linear parameter α was optimized, so that α was taken as a discrete function of R. In [6] Π functions were added to the electronic basis to account for the $\Sigma-\Pi$ coupling and vibrational functions were included, so that a potential energy function was not forthcoming and a property value at each value of R was not determined; that is averaging over vibration took place. Single values of the non-linear parameters α_Σ and α_Π are used for the Σ and Π electronic functions and they are optimized. For high vibrational levels, where average bond lengths can be greater than 10 a_0, the use of single values of α_Σ and α_Π is not satisfactory. The number of basis functions needed to allow for this becomes too large for the method to be reliable. In [6] different values of α_Σ and α_Π were used as N increased, but even so the results were only considered to be acceptable for low vibrational levels.

The vibrational part of the problem is modelled on the Fues-type functions [26]

$$\psi_i(R) = \frac{1}{R}e^{-\frac{y}{2}}y^{\frac{\beta+1}{2}}\mathcal{L}_{k_i}^{(\beta)}(y) \tag{3.4}$$

where $\mathcal{L}_{k_i}^{(\beta)}(y)$ are associated Laguerre polynomials and

$$y = \epsilon_{k_i} R\delta \tag{3.5}$$

with

$$\epsilon_{k_i} = \frac{4\gamma}{2k_i + \beta + 1}, \tag{3.6}$$

$$\beta = 2\sqrt{\gamma + N(N+1) + \frac{1}{4}} \tag{3.7}$$

and

$$\gamma = \frac{k\mu}{\delta^2}. \tag{3.8}$$

As before, μ is the reduced nuclear mass and k and δ are seen as non-linear variational parameters. The orders of the associated polynomials m_i, n_i and k_i are integers so that the combination of them is unique for a particular A state. The Fues functions (3.4) are the solutions of the Schrödinger equation in which the Fues potential appears

$$V = \frac{k}{2}\Big(\frac{R - R_{\mathrm{e}}}{R}\Big)^2 \tag{3.9}$$

where k is a force constant and R_{e} is the equilibrium bond length; the parameter δ may be interpreted loosely as $1/R_e$. This potential is more realistic than the harmonic potential

$$V = \frac{k}{2}\Big(\frac{R - R_{\mathrm{e}}}{R_{\mathrm{e}}}\Big)^2. \tag{3.10}$$

The required electronic matrix elements may be evaluated analytically using the integrals (2.124) and (2.125), which may be expressed [24] in terms of

$$\int_0^\infty x^k e^{-x} \mathcal{L}_m^{(k)}(x) \mathcal{L}_n^{(k)}(x) dx = \frac{\delta_{mn}(n+k)!}{n!} \tag{3.11}$$

by using the relation [27]

$$\mathcal{L}_m^{(k)}(x) = \mathcal{L}_m^{(k+1)}(x) - \mathcal{L}_{m-1}^{(k+1)}(x). \tag{3.12}$$

In particular for the $\Pi - \Pi$ matrix elements in the ξ variable

$$\int_0^\infty x^k e^{-x} \mathcal{L}_m^{(1)}(x) \mathcal{L}_n^{(1)}(x) dx \tag{3.13}$$

with

$$\mathcal{L}_m^{(1)}(x) = \sum_{j=0}^{m} \mathcal{L}_j^{(0)}(x); \tag{3.14}$$

for the $\Sigma - \Pi$ integrals

$$\mathcal{L}_m^{(0)}(x) = \mathcal{L}_m^{(1)}(x) - \mathcal{L}_{m-1}^{(1)}(x). \tag{3.15}$$

For the $\Sigma - \Pi$ matrix elements the ξ integrals involved, through (3.15), are

$$\int_0^\infty x^k e^{-x} \mathcal{L}_m^{(1)}(ax) \mathcal{L}_n^{(1)}(bx) dx \tag{3.16}$$

where the arguments of the associated Laguerre polynomials differ because the non-linear parameters, α_Σ and α_Π, are different. The two associated Laguerre polynomials of (3.16) may be expressed as linear combinations of associated Laguerre polynomials with argument x [28]

$$\mathcal{L}_m^{(1)}(ax) = \sum_{j=0}^{m} \frac{(m+1)!}{(m+1-j)!} a^{m-j} (1-a)^j \mathcal{L}_{m-j}^{(1)}(x) \tag{3.17}$$

which reduces evaluation of integral (3.16) to that of integrals (3.13).

For the integrals involving η

$$\int_{-1}^{+1} \eta^k \mathcal{P}_m^{(1)}(\eta) \mathcal{P}_n^{(1)}(\eta) d\eta \tag{3.18}$$

has to be considered, both for $\Pi - \Pi$ and $\Sigma - \Pi$. By expressing η^k as a linear combination of Legendre polynomials, (3.18) may be written in term of integrals of triple products of Legendre polynomials

$$\int_{-1}^{+1} \mathcal{P}_k(\eta) \mathcal{P}_m(\eta) \mathcal{P}_n(\eta) d\eta. \tag{3.19}$$

The integrals over the linear variable R are of the form

$$\int_0^\infty z^{\beta+k} e^{-z} \mathcal{L}_m^{(\beta)}(az) \mathcal{L}_n^{(\beta)}(bz) dz \tag{3.20}$$

and they can be analytically evaluated after manipulations similar to the ones considered earlier, using more general relations [27, 28].

The calculations to solve the non-adiabatic problem are performed by a program solving the linear variational problem for given values of the vibrational and rotational quantum numbers. The non-linear variational parameters (table 3.1) $\alpha_\Sigma, \alpha_\Pi$ appearing in the electronic basis functions, and k and δ in the vibrational Fues basis functions, were optimized by trial and error for the vibrationless levels. The number of functions is constrained by placing maximum values on m_i, n_i and k_i in equations (3.3) and (3.4) and on the sums $(m_i + n_i)$ and $(m_i + n_i + k_i)$, the maximum acceptable numbers of electronic basis functions and total basis functions allowed, respectively.

Cation	α_Σ	α_Π	k	δ
H_2^+	3.44	3.60	0.655	0.77
D_2^+	3.54	3.30	0.600	0.69
HD^+	3.50	3.47	0.650	0.70

Table 3.1: Variational parameters optimized by trial and error for the $v = 0$ levels.

3.3 The scattering method

As already noted, the transformed Hamiltonian for HD^+ (2.155) is formally the same as the Hamiltonian for H_2^+ and D_2^+ apart from the μ_{eff} which substitutes μ. These Hamiltonians are similar to the ones used in the scattering problem with R playing the role of the scattering coordinate. If the matrix elements of (2.155) between the functions (2.119) are considered, a set of coupled differential equations in R is obtained; this set can be used with an inelastic quantum-mechanical scattering theory.

The scattering method [8] is based on the idea of expanding the dependence of the wavefunction on all but one of the coordinates (R), in terms of a complete set of basis

functions, in order to form a set of coupled differential equations and imposing the correct bound state boundary conditions on the solutions. A body-fixed coordinate system rotating with the molecule is employed. The boundary conditions are different from the usual ones of scattering theory in which the wavefunction for the scattering coordinate must converge to zero just for $R = 0$; here it must go to zero both for $R = 0$ and $R = \infty$ and this is referred to as 'closed channels' in the scattering theory.

The artificial scattering method used throughout this work consists of adding two 'open' artificial scattering channels at large R, to the set of coupled channels arising from the coupled differential equations of the bound state problem. These two extra channels have lower asymptotic energies than the bound state channel and both correspond asymptotically to scattering states. The program computes the transition matrix elements T_{ij} between these two channels for a given scattering energy. By including artificial potential matrix elements, the two open channels are forced to notice the closed bound state channels so that the former are coupled to the latter but they are not to each other. Moreover, the T_{ij} matrix elements have first order poles as a function of scattering energy; these poles occur at the exact bound state energies. Since the behaviour of T_{ij} is well defined near the bound state energies, these may be easily located.

These equations are solved by propagating the solution using a log-derivative method [29]. Briefly, in a one-dimensional system the log-derivative matrix is defined as

$$\mathrm{y}(x) = \frac{\mathrm{d}}{\mathrm{d}x}\ln\psi(x) = \frac{\psi^{'}(x)}{\psi(x)} \tag{3.21}$$

where $\psi(x)$ is the eigenfunction of the matrix Schrödinger equation

$$\left[\frac{\mathrm{d}^2}{\mathrm{d}x^2} + \mathrm{V}(x)\right]\psi(x) = \mathbf{0}. \tag{3.22}$$

The matrix Ricatti equation

$$\mathrm{y}^{'}(x) + \mathrm{V}(x) + \mathrm{y}^2(x) = \mathbf{0} \tag{3.23}$$

is obtained by differentiating (3.21) and using (3.22) to eliminate the second derivative term that cannot be integrated using numerical techniques for solving differential equations

because $\mathbf{y}(x)$ diverges for some x values. The algorithm has the following form

$$\mathbf{y}_n(x) = \Big(\frac{1}{\mathbf{I} + h\mathbf{y}_{n-1}(x)}\Big)\mathbf{y}_{n-1}(x) - \frac{h}{3}w_n\mathbf{u}_n \tag{3.24}$$

where $\mathbf{I}$ is the unitary matrix and h is the spacing between integration points: $\mathbf{u}_n$ is the form assumed by the potential according to whether n is odd or even

$$\begin{aligned} \mathbf{u}_n &= V(x_n) && n = 0, 2, 4, \ldots, N \\ \mathbf{u}_n &= \Big[\mathbf{I} + \tfrac{h^6}{6}V(x_n)\Big]^{-1} V(x_n) && n = 1, 3, 5, \ldots, N-1 \end{aligned}$$

and w_n are the weights

$$\begin{aligned} w_n &= 1 \quad \text{if} \quad n = 0, N \\ w_n &= 2 \quad \text{if} \quad n = 2, 4, 6, \ldots, N-2 \\ w_n &= 3 \quad \text{if} \quad n = 1, 3, 5, \ldots, N-1. \end{aligned}$$

The truncated error is

$$\mathbf{y}(x_N) = \mathbf{y}_N + \mathbf{C}h^4 + \mathcal{O}(h^6) \tag{3.25}$$

where $\mathbf{C}$ is an unknown constant matrix, $\mathcal{O}(h^6)$ is a matrix of order h^6, $\mathbf{y}(x_N)$ is the exact value and $\mathbf{y}_N$ is the approximate value computed by the method. Only at the final integration point $n = N$, the numerical value of $\mathbf{y}_n$ is a good approximation to the value $\mathbf{y}(x_N)$. By defining the quantity

$$\mathbf{z}_n = h\mathbf{y}_n, \tag{3.26}$$

the program solves one iteration step; the matrix $\mathbf{y}_N$ is then recovered in the final calculation by

$$\mathbf{y}_N = \frac{\mathbf{z}_N}{h}. \tag{3.27}$$

What is obtained as solution of the problem are the transition probabilities of the scattering channels; these are the matrix elements of the $\mathbf{T}$ matrix linked to the scattering matrix $\mathbf{S}$ by the expression

$$\mathbf{S} = \mathbf{I} - i\mathbf{T}. \tag{3.28}$$

The T matrix elements have a complicated form [8] but the aspect on which the attention has to be focused is just one, the first order pole in the vicinity of every bound state eigenvalue of the problem

$$T^N_{\beta\to\gamma} \propto \frac{1}{E - E'_i}. \tag{3.29}$$

In (3.29) N is the total angular momentum, β and γ are the two artificial channels, E'_i are the bound states of the problem and E is the eigenvalue of the state of interest. Thus, these matrix elements can be monitored for different scattering energies and the exact energy of the state of interest can be studied by making some iterations.

This method was first implemented for $H_2^+(v,0)$ in [30] and subsequently used for HD^+, H_2^+ and D_2^+.

3.4 The Hutson method

The variational method gives wavefunctions from which expectation values may be determined, but the scattering method does not. However, to calculate the expectation value of an operator W, a method reported by Hutson [25] may be used.

Knowing the solutions of the Schrödinger equation associated with an unperturbed Hamiltonian

$$H^{(0)}\psi_i^{(0)} = E_i^{(0)}\psi_i^{(0)}, \tag{3.30}$$

the Hamiltonian $H^{(0)}$ is perturbed to give a new energy operator of the form

$$H = H^{(0)} + \lambda W \tag{3.31}$$

associated with the equation

$$H\psi_i = E_i\psi_i \tag{3.32}$$

where W is the operator corresponding to the property of interest. From the Rayleigh-Schrödinger perturbation theory the eigenvalues can be written as

$$E_i(\lambda) = E_i^{(0)} + \lambda\langle\psi_i^{(0)}|W|\psi_i^{(0)}\rangle + \lambda^2 \sum_{i\neq j} \frac{\langle\psi_i^{(0)}|W|\psi_j^{(0)}\rangle\langle\psi_j^{(0)}|W|\psi_i^{(0)}\rangle}{E_i^{(0)} - E_j^{(0)}} + \mathcal{O}(\lambda^3)$$

$$= E_i^{(0)} + \lambda\langle W\rangle + \lambda^2 k + \mathcal{O}(\lambda^3) \tag{3.33}$$

where $\langle W\rangle$ is the expectation value of the property of interest. A rearrangement of (3.33) gives

$$\frac{E_i(\lambda) - E_i^{(0)}}{\lambda} = \langle W\rangle + \lambda k + \mathcal{O}(\lambda^2). \tag{3.34}$$

Linear regression of $(E_i(\lambda) - E_i^{(0)})/\lambda$ on λ gives, as the intercept, the desired expectation value $\langle W\rangle$. By choosing the values of λ used (typically 3) carefully, accurate expectation values may be found. In the case of the electric dipole polarizability of H_2^+ and D_2^+ (see chapter 7) the expectation value vanishes and it is the coefficient of λ^2 that is of interest; in that case $(E_i(\lambda) - E_i^{(0)})/\lambda^2$ is regressed on λ^2.

3.5 Numerical integration

While the results for the dissociation energy, the bond length and the dipole polarizability are obtained through analytical integration, the matrix elements of some other properties reported in this work involve singular and/or non-separable integrands and numerical integration is necessary. In particular, a method similar to that proposed in [31] by Carrington and Kennedy is used where the basic idea is to evaluate the integrals excluding spherical volumes of smaller and smaller radii, and to extrapolate the results to a spherical volume of zero radius.

In that work, the integrals were evaluated by double quadrature. As reported in figure 3.1, the range of integration was divided between a sphere of radius 2 (A) corresponding to $1 \leq \xi \leq 3$, an outer region (C) from $\xi = 3$ to $\xi = \infty$ and the remaining area between the sphere and C (B=B_1+B_2+B_3). Over the outer region C products of 32-points Gauss-Laguerre (over ξ) and 16-points Gauss-Legendre (over η) quadratures were used. Over the

quadrant region A Carrington and Kennedy used the following transformation

$$\xi = 1 + \lambda sin\mu$$

$$\eta = -1 + \lambda cos\mu \tag{3.35}$$

to improve the convergence of the integrals. This part was further divided into anular regions and a product of 24-points over λ by 16-points over η Gauss-Legendre quadratures for each region was used. By decreasing of a power of 10 at every step the magnitude of λ (from 2×10^{-5} to 2×10^{-7}), the contribution to the integral over the range from the innermost value of λ to the edge of the excluded sphere with the same λ value for $\mu = 0$, was evaluated through an 8-points (λ) and 16-points (μ) Gauss-Legendre double quadratures.

The remaining region to integrate, B, was divided into the three sub-regions:

1) B_1, for $-1 \leq \eta \leq (-1 + \sqrt{2})$ and ξ varying on the edge of the sphere;

2) B_2, for $1 \leq \xi \leq (1 + \sqrt{2})$ and η varying on the edge of the sphere;

3) B_3, the remaining square.

Over these three regions was used, respectively, a double Gauss-Legendre quadrature with 8-ξ-points by 16-η-points, 16-ξ-points by 8-η-points and 8-ξ-points by 8-η-points.

In this work the singularities are also treated but in a different way. The alternative approach is schematically reported in figure 3.2 in the case of one singularity in the point $(\xi = 1, \eta = -1)$ and in figure 3.3 in the case of two singularities in the points $(\xi = 1, \eta = -1)$ and $(\xi = 1, \eta = 1)$. In figure 3.2 the range of integration has been divided between the following regions:

1) A, upper delimited by the straight line of equation $\eta = 1 - \xi$ while $1 \leq \xi \leq 2$;

2) B, corresponding to $1 - \xi \leq \eta \leq 1$ and $1 \leq \xi \leq 2$;

3) C, from ξ=2 to ξ=3;

4) D, from ξ=3 to $\xi = \infty$.

As in the method of Carrington and Kennedy and explained above, multiple-points Gauss-Laguerre (over ξ) and Gauss-Legendre (over η) are used. On region A, 24-points double quadratures are used for integration both on η and ξ; regions B and C are integrated with 12-points quadratures and on region D 8-points and 16-points quadratures are used

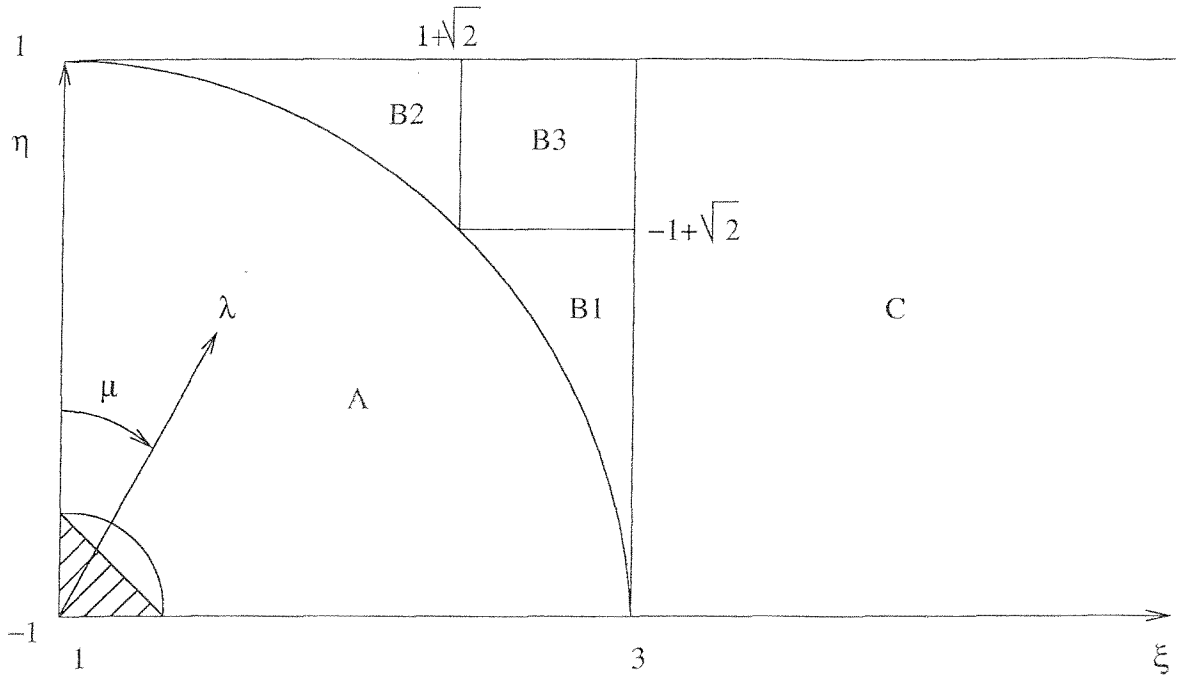

Figure 3.1: Subdivision of the integration range $1 \leq \xi < \infty$ and $-1 \leq \eta \leq 1$ for the numerical evaluation of singular integrands (after [31]). The dashed area represents the excluded volume.

respectively on η and ξ.

The convergence of this alternative method was tested and the results obtained with both the methods are consistent.

In the case of singularities in the points $(\xi = 1, \eta = -1)$ and $(\xi = 1, \eta = 1)$ (see figure 3.3) a similar approach is used. In this case the region A is divided in the two sub-regions:

1) A_1, corresponding to A in figure 3.2;

2) A_2, which is the mirrored one confined by the straight line $\eta = (\xi - 1)$ while $1 \leq \xi \leq 2$. Now region B is given by $(1 - \xi) \leq \eta \leq (\xi - 1)$ while $1 \leq \xi \leq 2$. For H_2^+ and D_2^+ the contribution to the integral from region A_1 is the same as the one from region A_2 for many properties, this allowing simplification of program coding.

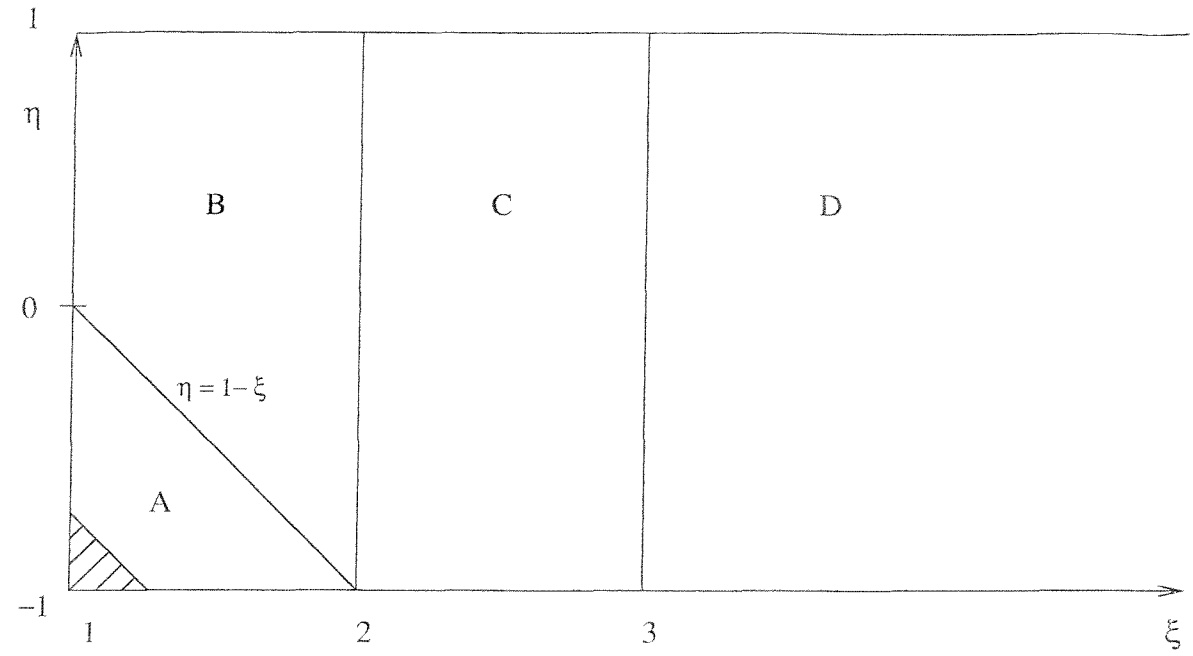

Figure 3.2: Subdivision of the integration range $1 \leq \xi < \infty$ and $-1 \leq \eta \leq 1$ for the numerical evaluation of singular integrands with the approach followed in this work: this is the case of one singularity in the point $(\xi = 1, \eta = -1)$. The dashed area represents the excluded volume.

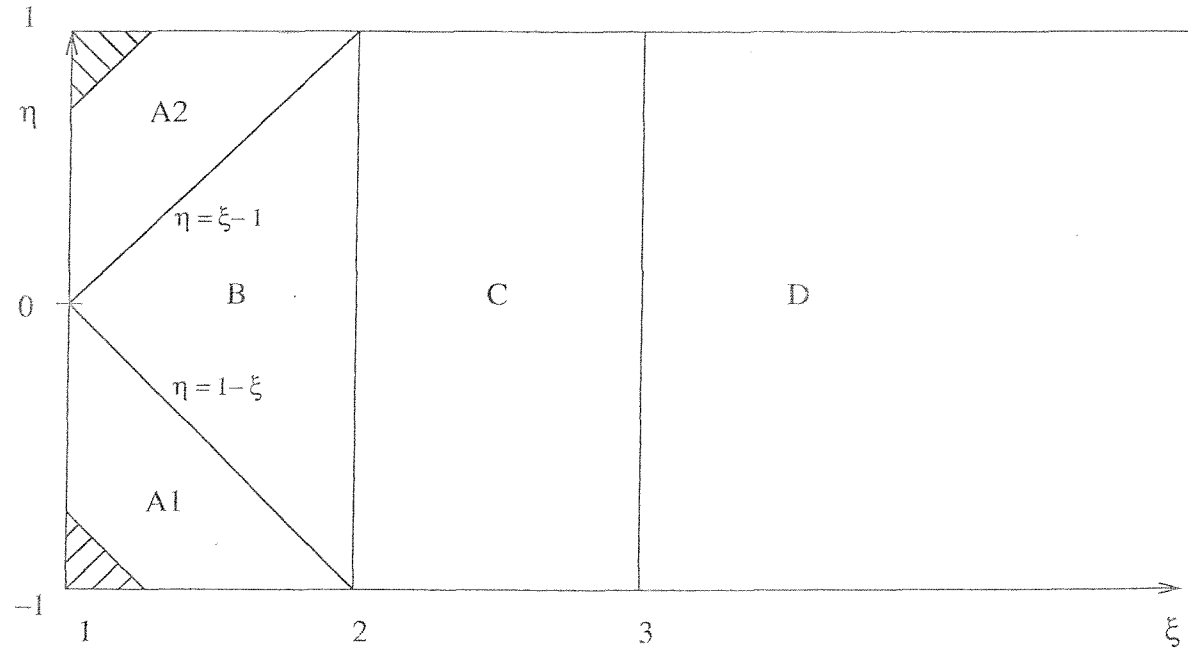

Figure 3.3: Subdivision of the integration range $1 \leq \xi < \infty$ and $-1 \leq \eta \leq 1$ for the numerical evaluation of singular integrands with the approach followed in this work: this is the case of two singularities in the points $(\xi = 1, \eta = -1)$ and $(\xi = 1, \eta = 1)$. The dashed areas represent the excluded volumes.

3.6 Tests on the accuracy of the results

The accuracy and the convergence of the results reported in this work were tested for each level. In particular in using the LEVEL program, the attention was focused on the integration step and in the variational approach, the convergence of the results were tested by increasing the number of basis functions (up to 748 for Σ and up to 480 for Π). In using the scattering method attention was paid not just in the number of basis functions used (up to 225 for Σ and up to 84 for Π) but also in the step and in the numbers of integration points.

Chapter 4

Results: adiabatic and non-adiabatic dissociation energies for H_2^+, D_2^+ and HD^+

4.1 Introduction

Accurate dissociation energies for many bound and quasibound vibration-rotational levels have been calculated for the ground electronic states of H_2^+ [2], D_2^+ [3] and HD^+ [4]. Adiabatic and non-adiabatic corrections to the dissociation energies have been studied [32,33] and attempts made to reproduce the dissociation energies using an effective Hamiltonian. Although the effective parameters obtained scaled between H_2^+, D_2^+ and HD^+ according to their reduced masses [33], scaling of the adiabatic and non-adiabatic corrections to the dissociation energies was not considered; this chapter [34] is dedicated to this topic.

While the Born-Oppenheimer and the adiabatic dissociation energies may be generated straightforwardly using standard programs, the non-adiabatic values for bound levels are computed through the theory and the calculation methods exposed in the previous chapters.

The results for the dissociation energies are given in wavenumber units; the only fundamental constants used are the ratios of the masses of the proton and the deuteron to that of the electron and the conversion factor from hartree to wavenumber (see table 4.1). For all the reported results the 1986 constants [35] are used, since earlier work used these.

Constant	Value
Proton-electron mass ratio (m_p/m_e)	1 836.152 701
Deuteron-electron mass ratio (m_d/m_e)	3 670.483 014
Hartree (E_h)	219 474.630 67 cm^{-1}

Table 4.1: Values of the fundamental constants used in this work [35].

4.2 The adiabatic correction to the dissociation energy

The adiabatic corrections to the dissociation energies for H_2^+, D_2^+ and HD^+ are studied using the LEVEL program [7] which allows the solution of the Schrödinger equation for bound and quasibound levels. The molecular properties of interest may be studied using potential energy curves for the three molecules; the same Born-Oppenheimer potential curve is used for all the three molecules and specific ones for the adiabatic potential for each of them. In discussing the adiabatic correction, two different approaches have to be recalled: the *standard* and the *partitioned* adiabatic corrections [22,32]. As already noted, the adiabatic corrections are diagonal in the electronic state and arise because of the finite masses of the nuclei. They can be seen as the response of the nuclei to the instantaneous position of the electron; in this way the uniformity of motion of the centre of mass of the three-body system is maintained.

By using the adiabatic potential (2.37) in equation (2.36) the adiabatic approximation is well determined. For homonuclear cations like H_2^+ and D_2^+ this approximation does not give the correct dissociation limit for large values of R; in other words, the energy does not tend to that of the atom with the appropriate reduced mass for the electron. The adiabatic correction may be made to vanish in the limit $R \to \infty$ because the expectation values of

$$\frac{\nabla_R^2}{2} \quad \text{and} \quad \frac{\nabla_g^2}{8}$$

are the same [36]. Thus, the Hamiltonian at dissociation may be rewritten as

$$H = \left[H_{BO} - \frac{\nabla_g^2}{4\mu}\right] + \frac{1}{\mu}\left[-\frac{\nabla_R^2}{2} + \frac{\nabla_g^2}{8}\right] = H_{BO}^{\frac{m_e}{m+1}} + \frac{1}{\mu}H_{part}. \tag{4.1}$$

Now, for an homonuclear molecule, the electron kinetic energy term involves the electron

reduced mass

$$\frac{m}{m+1} = \frac{1}{1+\frac{1}{2\mu}} \tag{4.2}$$

which is correct for a one-electron atom with a nucleus of mass m. A new operator

$$\frac{1}{\mu} H_{\text{part}}$$

is introduced, instead of

$$\frac{1}{\mu} H_{\text{ad}}$$

and whose expectation value is equal to zero at the dissociation limit. This approach is called '*partitioned* adiabatic method'. For HD^+ this partitioning may also be made with the intermediate transformed Hamiltonian to give the correct dissociation limits [21].

The adiabatic and partitioned corrections to the Born-Oppenheimer dissociation energies are obtained for the ground electronic states of the three molecules. The behaviour of the correction to the dissociation energies (in cm^{-1}) is studied versus the vibrational quantum numbers to check that the shape is the same apart from a scaling factor due to the different masses of the cations. The adiabatic correction makes the dissociation energies decrease; in figure 4.1 the partitioned adiabatic correction to the dissociation energies for rotationless levels of the ground electronic states of the three isotopomers is plotted against the vibrational quantum numbers. The behaviour of this correction, which decreases for low vibrational quantum numbers and then increases, is evident. In order to take into account the differences in the reduced masses of the molecules, the curve referring to D_2^+ is scaled by the factor of $m_d/m_p \approx 2$ and the one referring to HD^+ is scaled by the factor of $2m_d/(m_p + m_d) \approx 4/3$.

If the plot is against dissociation energies, rather than vibrational quantum numbers, the three curves are coincident, as shown in figure 4.2. Which dissociation energies are used is not of importance, since the corrections are insignificant compared with the dissociation energies themselves.

Note that for HD^+ use of the intermediate transformed Hamiltonian to give adiabatic corrections to the dissociation energies would include an extra 14.91 cm^{-1} for all levels except for those very close to dissociation, since the dissociation limits of the ground and the first excited states are in reality separated by 29.8 cm^{-1}. This is because inclusion of g/u symmetry breaking gives the correct dissociation limit of a deuterium atom plus a proton, while for both the ground and excited electronic states the Born-Oppenheimer and the adiabatic approximations give the same dissociation limit of an average of those of the hydrogen atom and the deuterium atom. The electronic g/u symmetry breaking becomes significant only close to dissociation.

For a nonzero rotational quantum number the curves are similar, but when the scaled corrections for a constant N are plotted against dissociation energies, the curves do not coincide, the difference increasing with N and becoming quite apparent for N=8 (see figure 4.3) and evident for N=16 (see figure 4.4). However, it is possible to mantain the coincidence by choosing a different N for each isotopomer. For example, the curves for H_2^+, $N = 8$, D_2^+, $N = 11$, and HD^+, $N = 9$, coincide (see figure 4.5), as do H_2^+, $N = 16$, D_2^+, $N = 23$ and HD^+, $N = 18$ (see figure 4.6).

Similar behaviour is observed for levels with the same v but different N when the scaled corrections to the dissociation energies are plotted against dissociation energies themselves. For v=0 the curves almost coincide (see figure 4.7), but the differences increase markedly with v (see figure 4.8), and this can not be remedied by choosing different v for each isotopomer. It appears that, in plotting corrections against dissociation energies, isotopic scaling is completely successful only for levels with N=0 or levels with v=0.

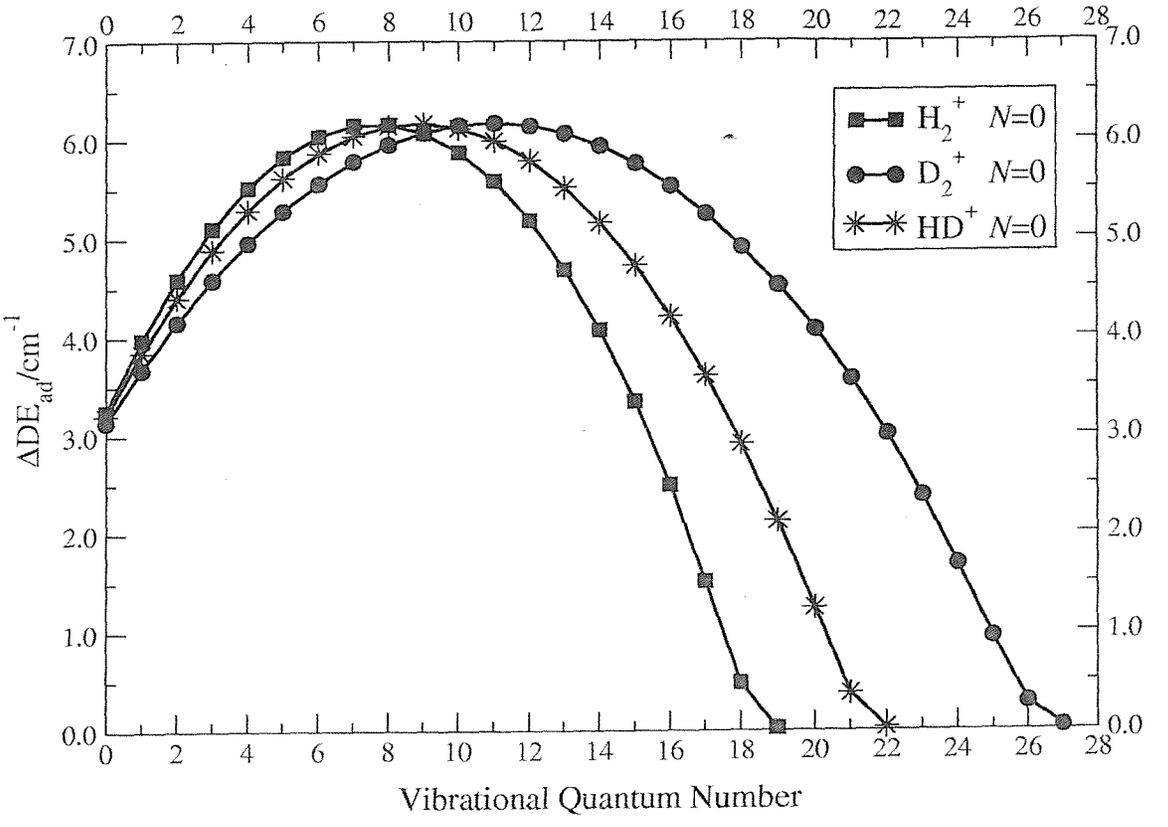

Figure 4.1: Partitioned corrections (partitioned − BO) for H_2^+ and D_2^+ and standard adiabatic correction (standard − BO) for HD^+ to the dissociation energy for N=0 against vibrational quantum numbers; a scaling factor of 2 to D_2^+ and of 4/3 to HD^+ is applied.

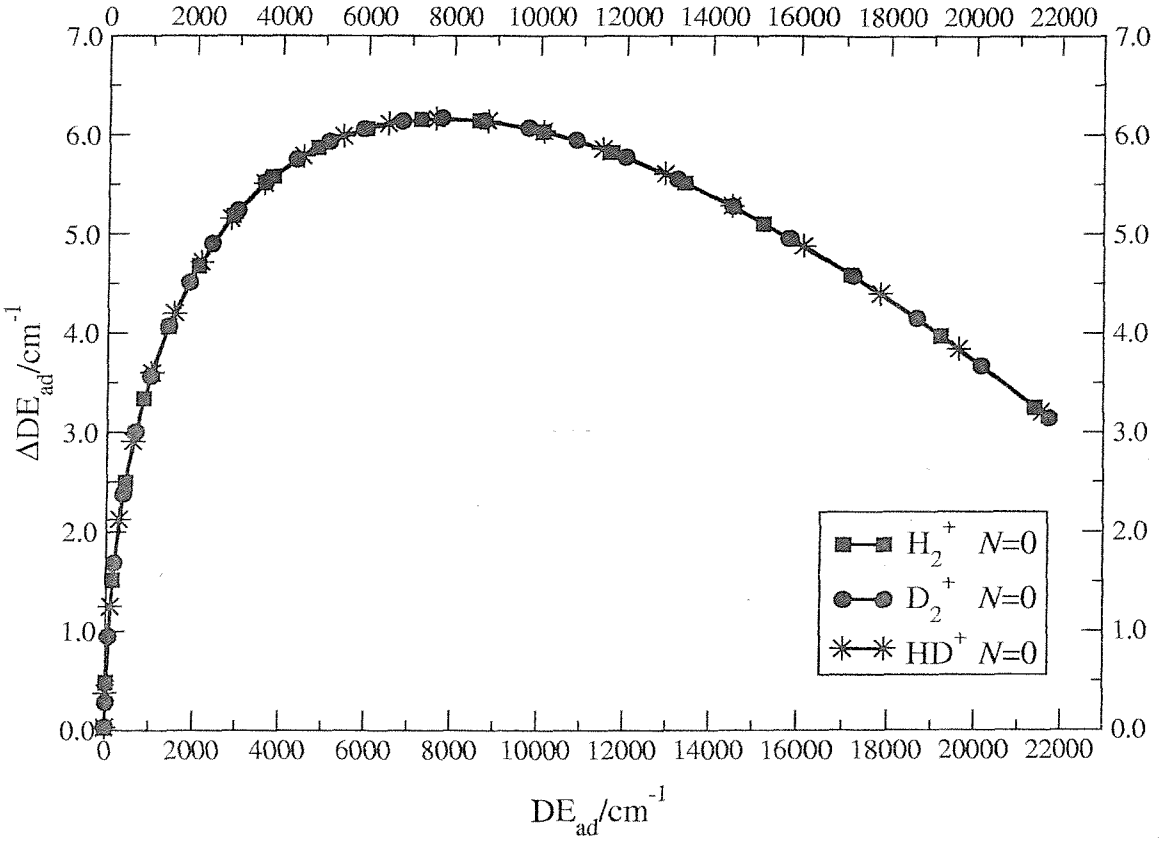

Figure 4.2: Partitioned corrections (partitioned − BO) for H_2^+ and D_2^+ and standard adiabatic correction (standard − BO) for HD^+ to the dissociation energy for N=0 against dissociation energies; a scaling factor of 2 to D_2^+ and of 4/3 to HD^+ is applied.

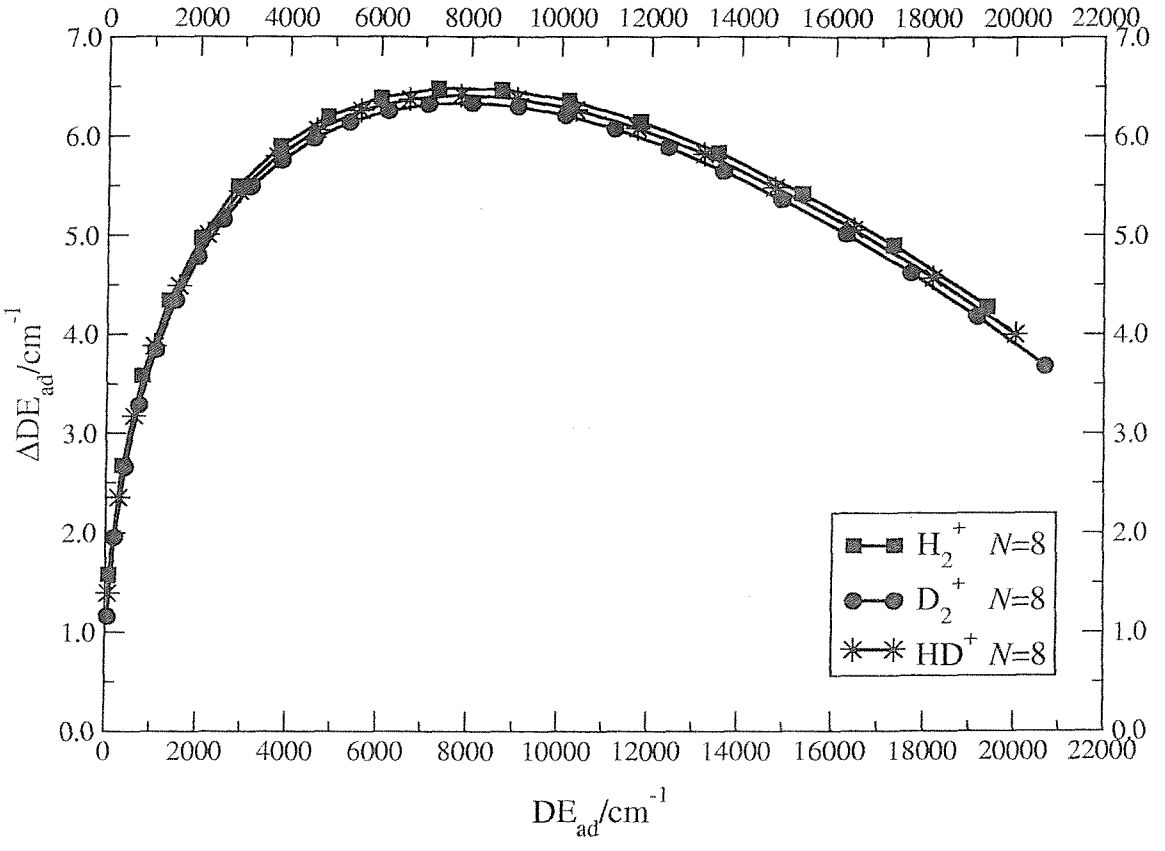

Figure 4.3: Partitioned corrections (partitioned − BO) for H_2^+ and D_2^+ and standard adiabatic correction (standard − BO) for HD^+ to the dissociation energy for N=8 against dissociation energies; a scaling factor of 2 to D_2^+ and of 4/3 to HD^+ is applied.

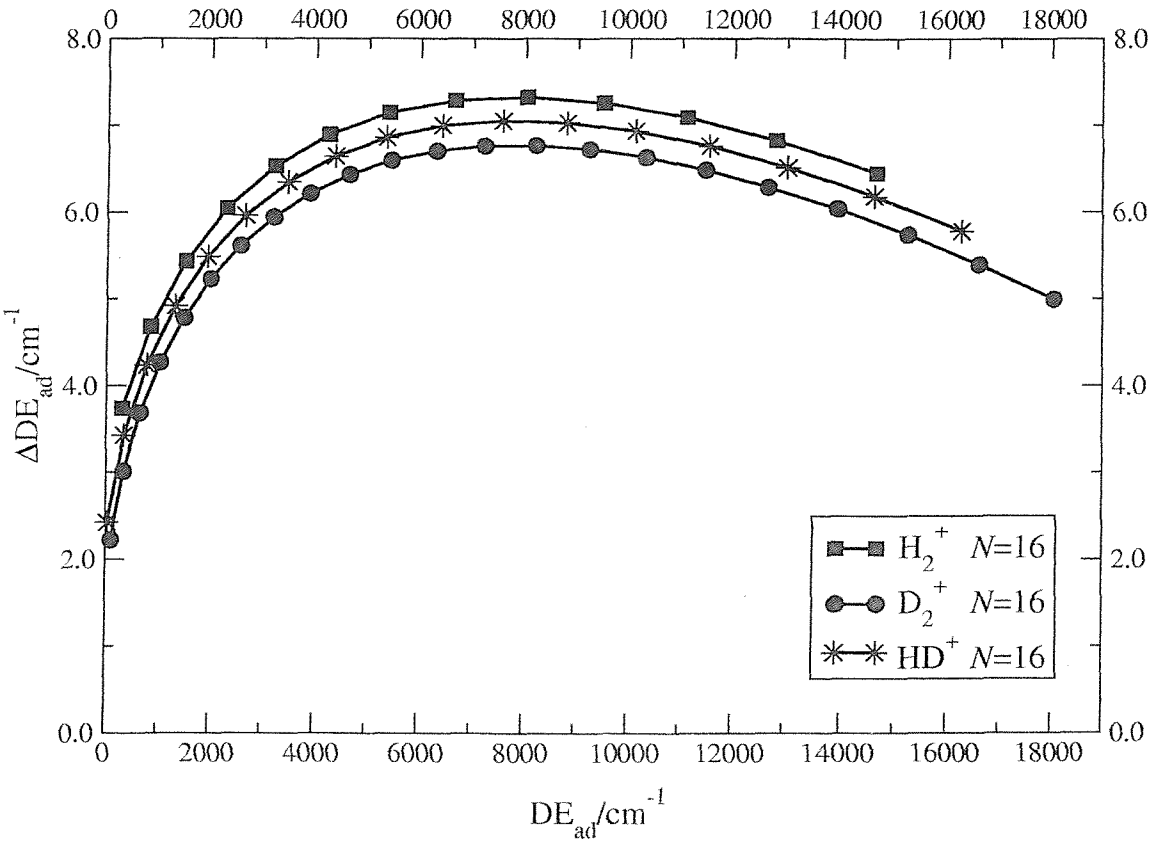

Figure 4.4: Partitioned corrections (partitioned − BO) for H_2^+ and D_2^+ and standard adiabatic correction (standard − BO) for HD^+ to the dissociation energy for N=16 against dissociation energies; a scaling factor of 2 to D_2^+ and of 4/3 to HD^+ is applied.

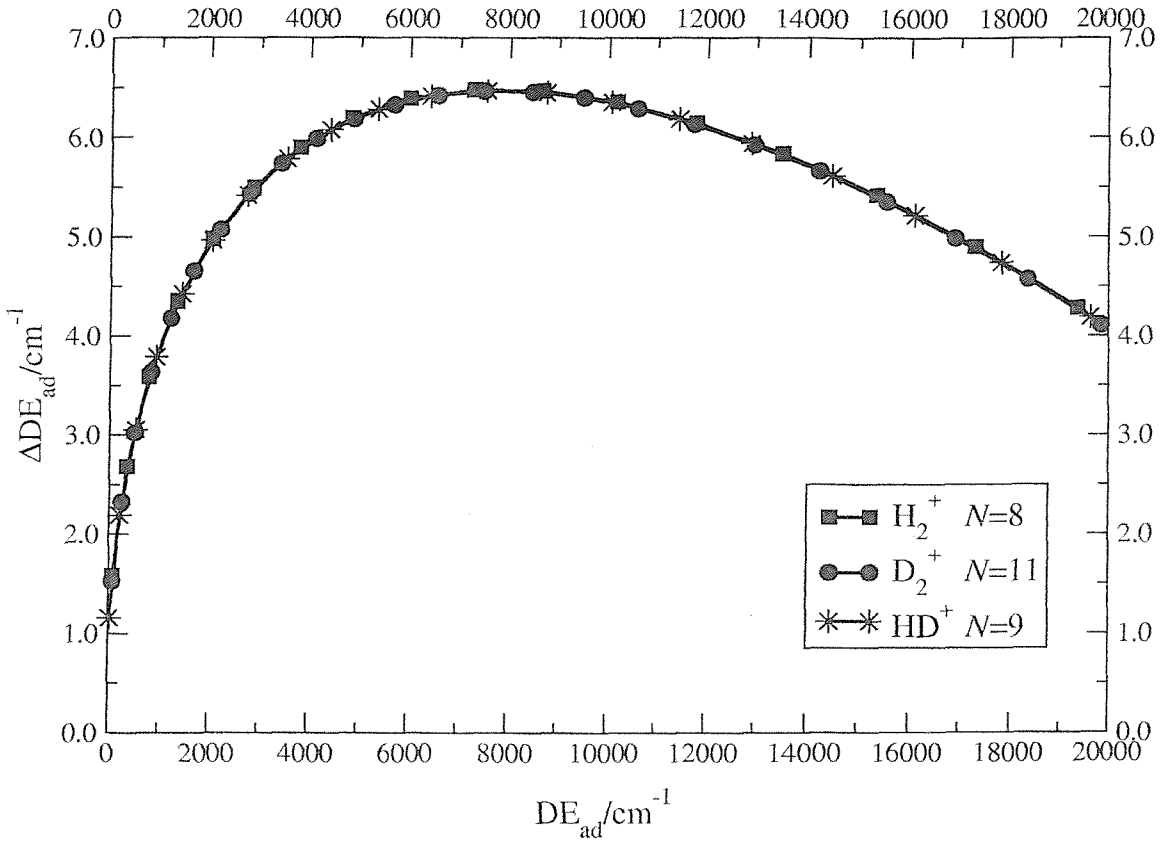

Figure 4.5: Partitioned corrections (partitioned − BO) for H_2^+ and D_2^+ and standard adiabatic correction (standard − BO) for HD^+ to the dissociation energy for N=8, N=11 and N=9 respectively against the dissociation energies; a scaling factor of 2 to D_2^+ and of 4/3 to HD^+ is applied.

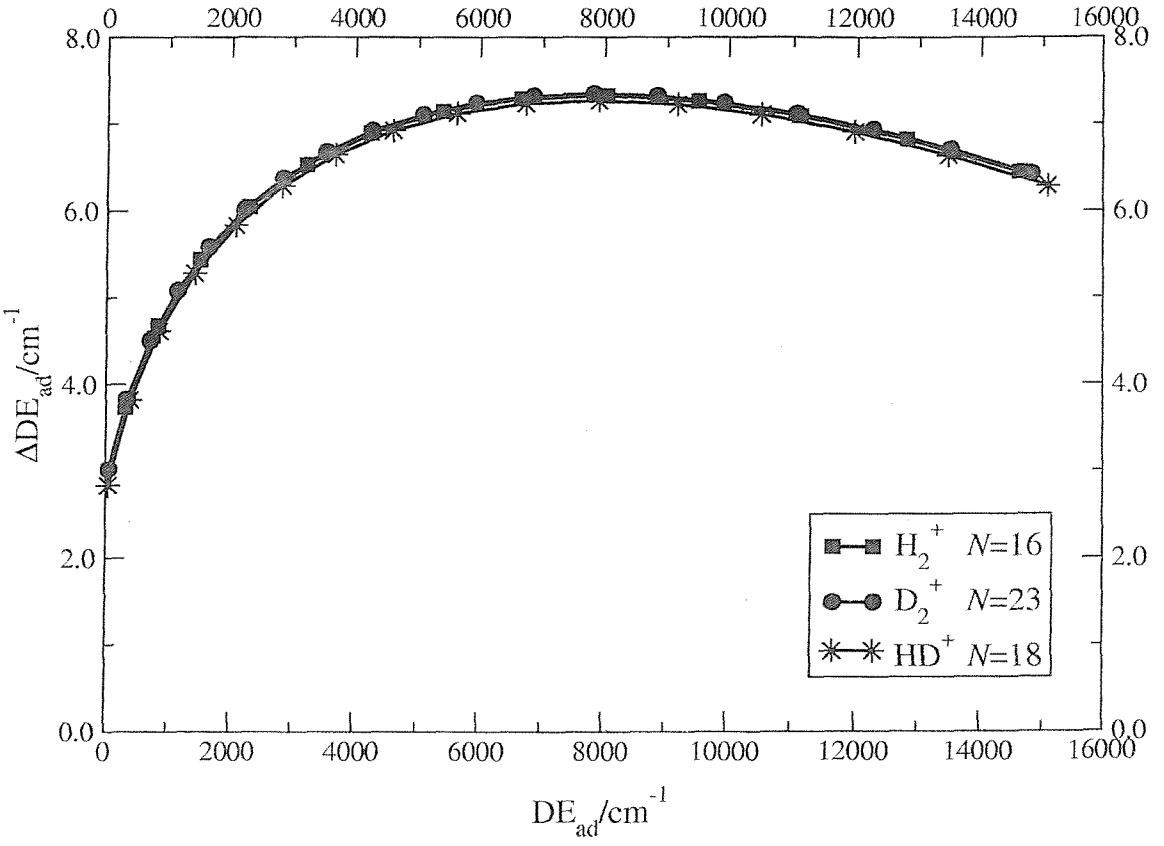

Figure 4.6: Partitioned corrections (partitioned − BO) for H_2^+ and D_2^+ and standard adiabatic correction (standard − BO) for HD^+ to the dissociation energy for N=16, N=23 and N=18 respectively against dissociation energies; a scaling factor of 2 to D_2^+ and of 4/3 to HD^+ is applied.

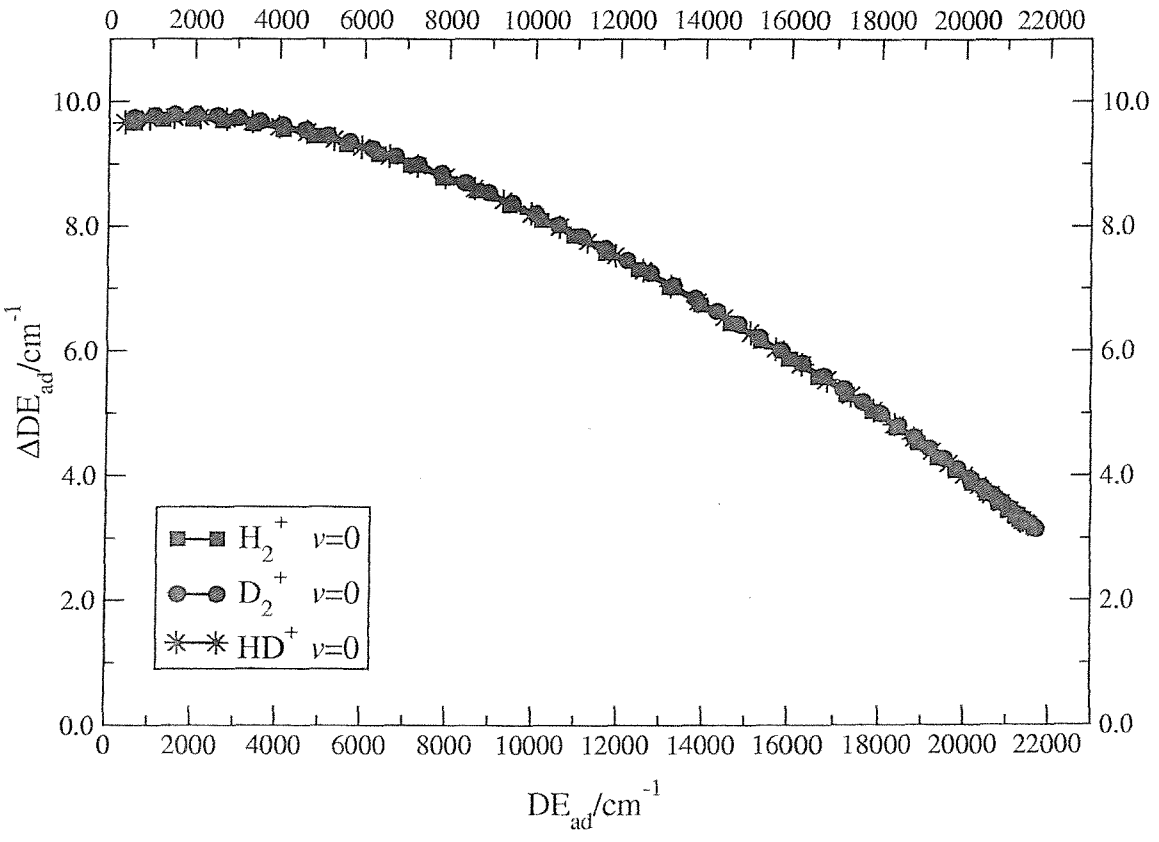

Figure 4.7: Partitioned corrections (partitioned − BO) for H_2^+ and D_2^+ and standard adiabatic correction (standard − BO) for HD^+ to the dissociation energy for v=0 against dissociation energies; a scaling factor of 2 to D_2^+ and of 4/3 to HD^+ is applied.

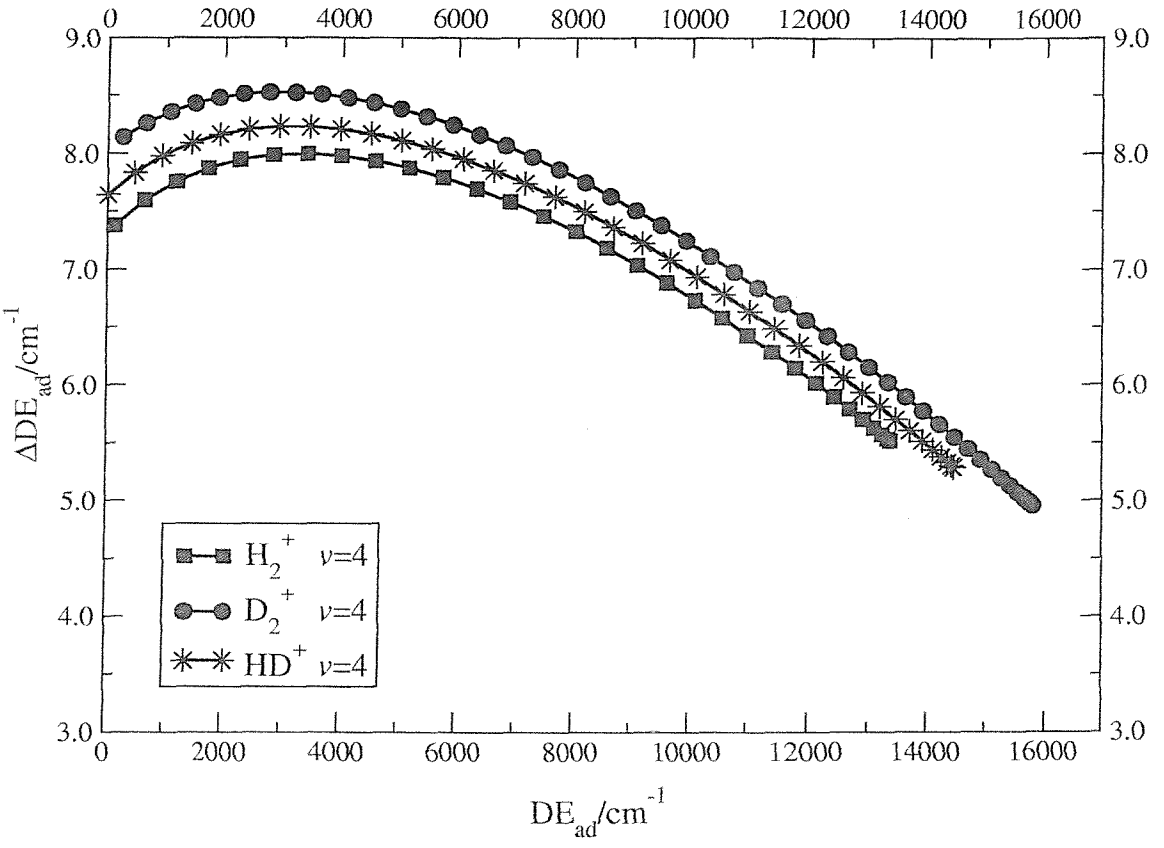

Figure 4.8: Partitioned corrections (partitioned − BO) for H_2^+ and D_2^+ and standard adiabatic correction (standard − BO) for HD^+ to the dissociation energy for v=4 against dissociation energies; a scaling factor of 2 to D_2^+ and of 4/3 to HD^+ is applied.

4.3 The non-adiabatic correction to the dissociation energy

Using the non-adiabatic dissociation energies of the three isotopomers [2–4], the scaled non-adiabatic corrections (non-adiabatic – adiabatic) to the dissociation energies for rotationless levels may be plotted against vibrational quantum numbers as reported in figure 4.9.

In the case of HD^+ the adiabatic dissociation energies are those obtained using the intermediate transformed Hamiltonian, so that g/u electronic symmetry breaking is not included in the comparison with H_2^+ and D_2^+. As for the adiabatic correction, the curves coincide if dissociation energies are used instead of vibrational quantum numbers (figure 4.10). The exceptions are HD^+, v=20, and, in particular, v=21; it is the v=20 level for which an anomalous bond length correction is found (see chapter 5 and [37]).

For nonzero N and for plots for constant v, similar scaling behaviour to that for adiabatic corrections is observed for most levels. In general for high lying levels the correction decreases in magnitude as v and/or N increases, that is as dissociation is approached. Other HD^+ levels that do not follow this trend may be recognized from plots similar to that in figure 4.9 for other values of N (see for example figure 4.11). Those identified are (21,0-3), (20,0-6) and (19,7-9); details of these results are reported in table 4.2.

An explanation for this anomalous behaviour for HD^+ non-adiabatic corrections is desirable. It seems unlikely that the fully non-adiabatic energies themselves are at fault, since they have been used to calculate transition frequencies that agree with experiment and to predict new transition frequencies that have been observed subsequently [1–4]. The most likely source of the anomaly must then lie in the intermediate transformed Hamiltonian calculations for HD^+. As explicitly reported in [38], in determining the potential energy curve it was apparent that the g/u symmetry breaking is negligible at bond lengths less than 10 a_0, but by 15 a_0 almost complete mixing of the g ground electronic state and the u first excited electronic state has occured (see figure 4.12).

In [38] the g/u symmetry breaking correction was calculated from

$$\Delta E_{\mathrm{g/u}}(R) = E_0(R, Z_1, Z_2) - E_0(R, 1, 1) \tag{4.3}$$

where $E_0(R,1,1)$ are the Born-Oppenheimer eigenvalues and $E_0(R,Z_1,Z_2)$ are the eigenvalues of the zeroth-order Hamiltonian

$$H_0 = -\frac{\nabla_g^2}{2} - \frac{Z_1}{r_{1e}} - \frac{Z_2}{r_{2e}} + \frac{1}{R} \tag{4.4}$$

where Z_1 and Z_2 are the effective nuclear charges (2.109) and (2.110), which assume the values of 0.999 931 956 and 1.000 068 044, respectively for HD^+. Equation (4.4) arises from (2.103) where the transformed potential operator V' was reduced to $1/R$ since all the other terms are considered as perturbations, as is the adiabatic term.

The HD^+ levels that show anomalies all have significant contributions to their properties from internuclear separations in this range, 10-15 a_0, as can be seen from the vibration-rotational wavefunctions which become more and more important with large bond lengths as dissociation is approached (see figures 4.13 and 4.14). A detailed discussion about the non-adiabatic correction to the bond lengths is given in the next chapter.

It is realized that the intermediate transformed Hamiltonian does not handle the g/u symmetry breaking as successfully as hoped in the region of rapid change. For the homonuclear isotopomers the non-adiabatic corrections are accounted for by the final transformation of the Hamiltonian and the mixing of electronic states by the $(\partial^2/\partial R^2)$ operator in equation (2.155). It seems likely that the implicit assumption that for HD^+ these corrections and the effects of g/u symmetry breaking are additive is flawed, and the effects of this non-additivity become prominent in the region of rapid change in g/u mixing. Also g/u symmetry breaking might not be fully accounted for by the intermediate transformed Hamiltonian.

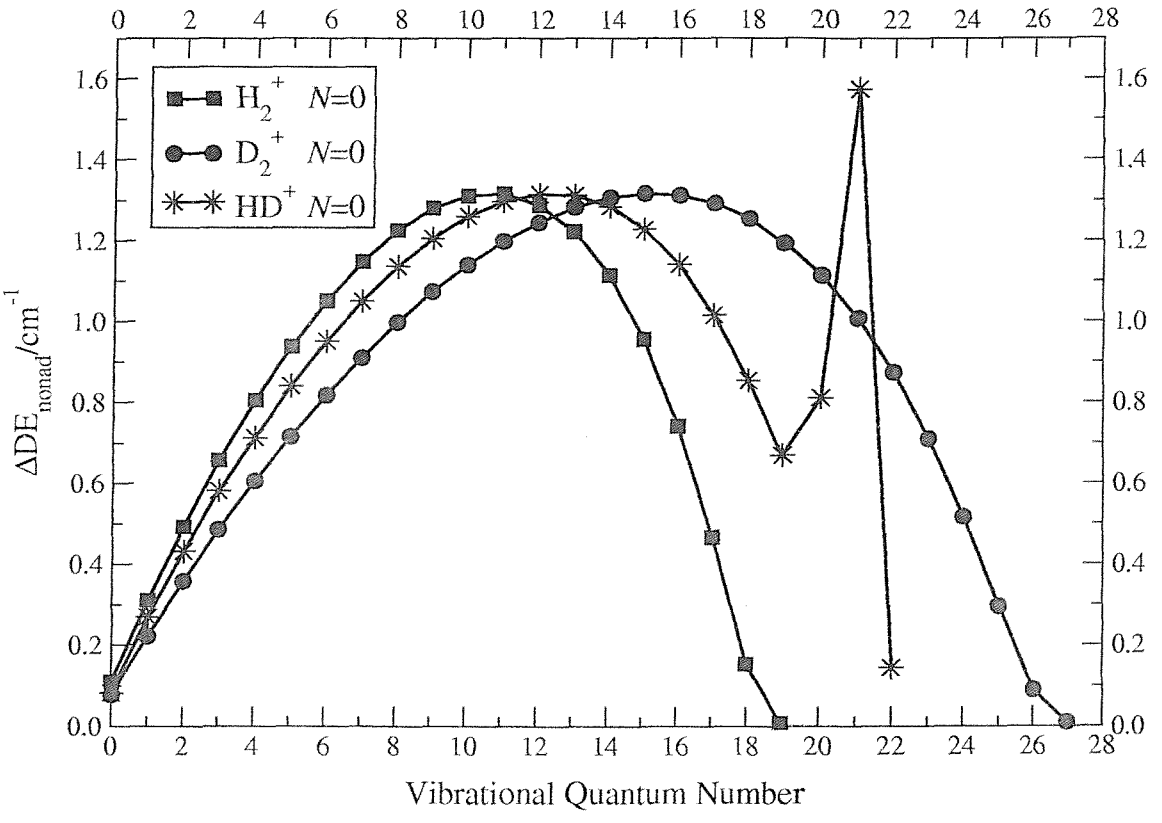

Figure 4.9: Non-adiabatic corrections to the dissociation energies (non-adiabatic − adiabatic for H_2^+ and D_2^+, and non-adiabatic − intermediate transformed adiabatic for HD^+) plotted against vibrational quantum numbers for N=0 levels; the D_2^+ and HD^+ corrections are scaled by factors of 2 and 4/3, respectively.

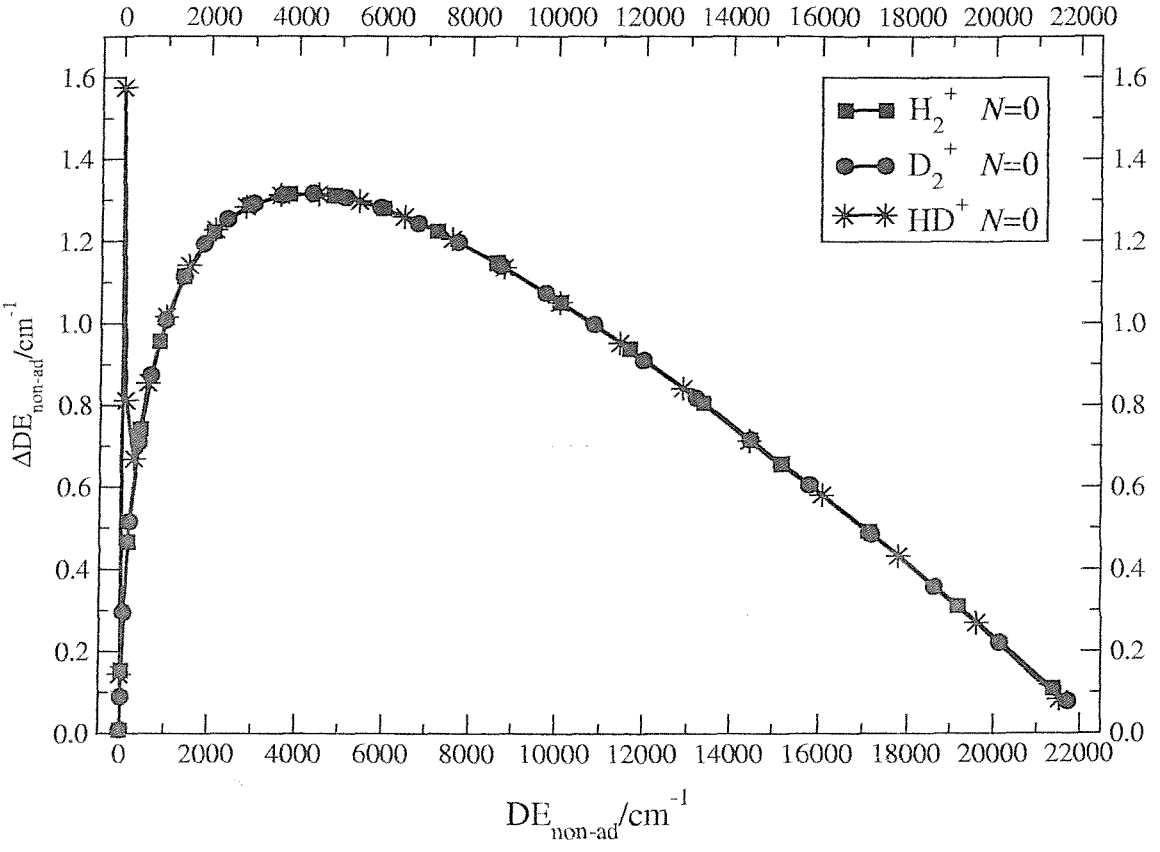

Figure 4.10: Non-adiabatic corrections to the dissociation energies (non-adiabatic − adiabatic for H_2^+ and D_2^+, and non-adiabatic − intermediate transformed adiabatic for HD^+) plotted against dissociation energies for N=0 levels; the D_2^+ and HD^+ corrections are scaled by factors of 2 and 4/3, respectively.

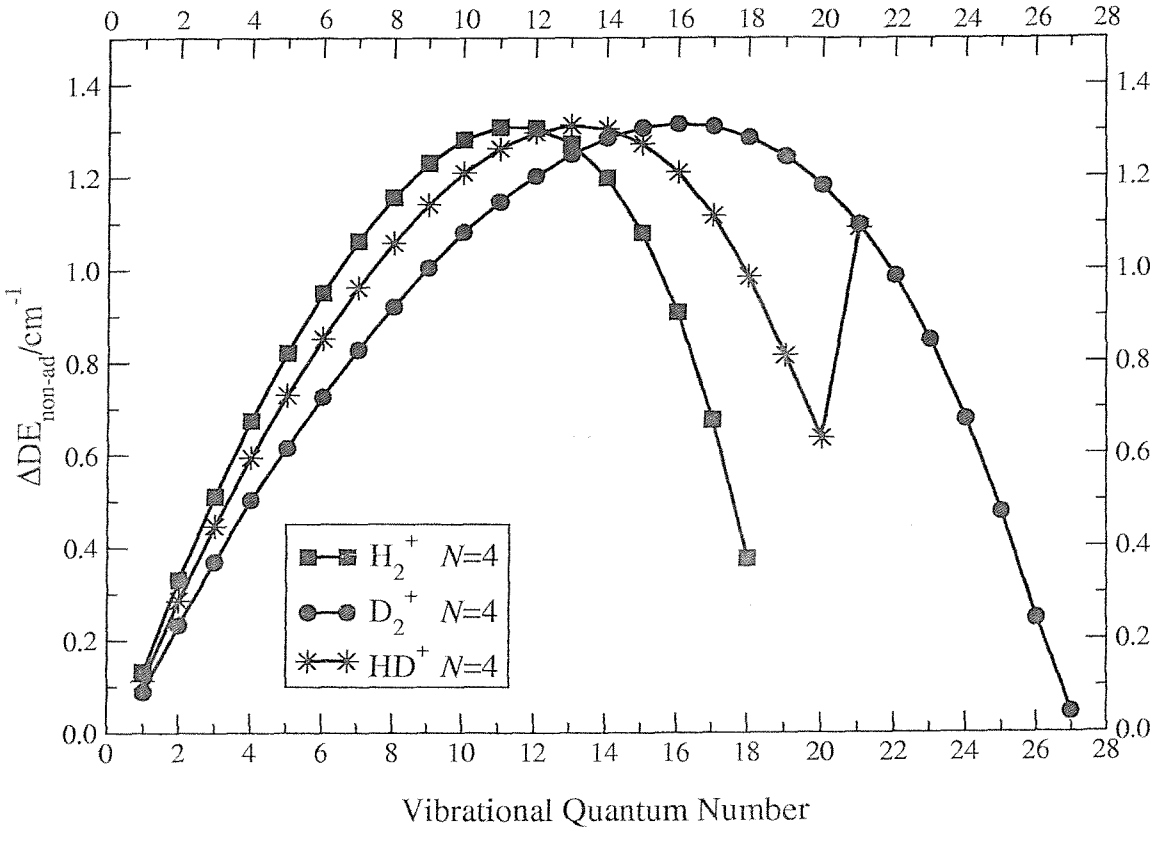

Figure 4.11: Non-adiabatic corrections to the dissociation energies (non-adiabatic − adiabatic for H_2^+ and D_2^+, and non-adiabatic − intermediate transformed adiabatic for HD^+) plotted against dissociation energies for N=4 levels; the D_2^+ and HD^+ corrections are scaled by factors of 2 and 4/3, respectively.

(v,N)	DE_{non-ad}/cm^{-1}	$\Delta DE_{non-ad}/cm^{-1}$
(17,12)	202.883 8	0.542 8
(17,13)	103.349 3	0.501 3
(17,14)	8.227 1	0.465 1
(18,8)	266.992 0	0.527 0
(18,9)	196.857 2	0.499 2
(18,10)	125.091 8	0.472 8
(18,11)	53.987 6	0.461 6
(19,0)	292.117 2	0.502 2
(19,1)	284.292 7	0.499 7
(19,2)	268.845 8	0.493 8
(19,3)	246.182 4	0.485 4
(19,4)	216.916 3	0.477 3
(19,5)	181.878 4	0.468 4
(19,6)	142.134 5	0.465 5
(19,7)	99.023 2	0.477 2
(19,8)	54.237 6	0.526 6
(19,9)	10.046 6	0.649 6
(20,0)	94.075 4	0.609 4
(20,1)	88.998 7	0.624 7
(20,2)	79.086 2	0.660 2
(20,3)	64.831 0	0.722 0
(20,4)	47.010 1	0.818 1
(20,5)	26.764 0	0.948 0
(20,6)	5.861 9	1.038 9
(21,0)	10.215 7	1.180 7
(21,1)	8.552 5	1.116 5
(21,2)	5.551 3	0.963 3
(21,3)	1.836 3	0.674 3
(22,0)	0.430 9	0.107 9
(22,1)	0.115 7	0.058 7

Table 4.2: HD^+: non-adiabatic dissociation energies and non-adiabatic corrections (non-adiabatic – intermediate transformed adiabatic) for selected vibration-rotational levels of the ground electronic state. In general, for high lying levels, the non-adiabatic correction to the dissociation energy decreases with the approach of dissociation. In this table the levels that do not follow this trend are reported.

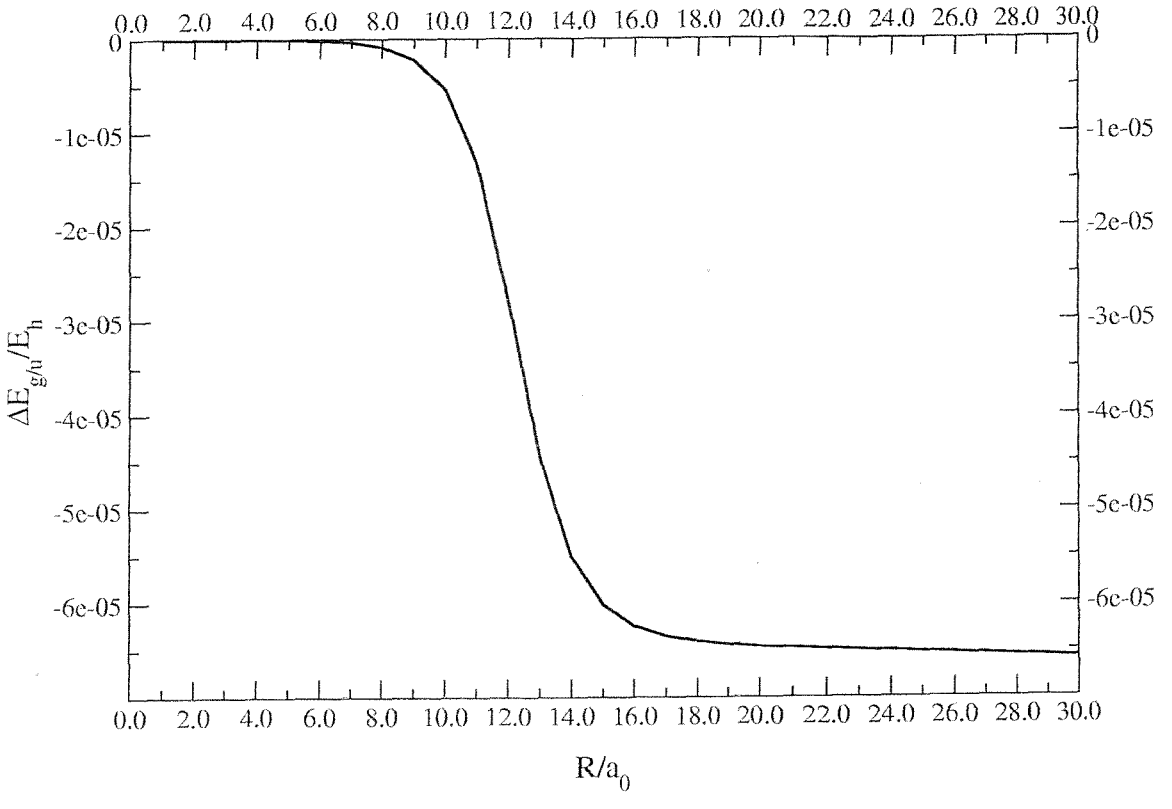

Figure 4.12: Symmetry breaking correction arising from equation (4.3) for the ground electronic state of HD^+ obtained from the results in [38].

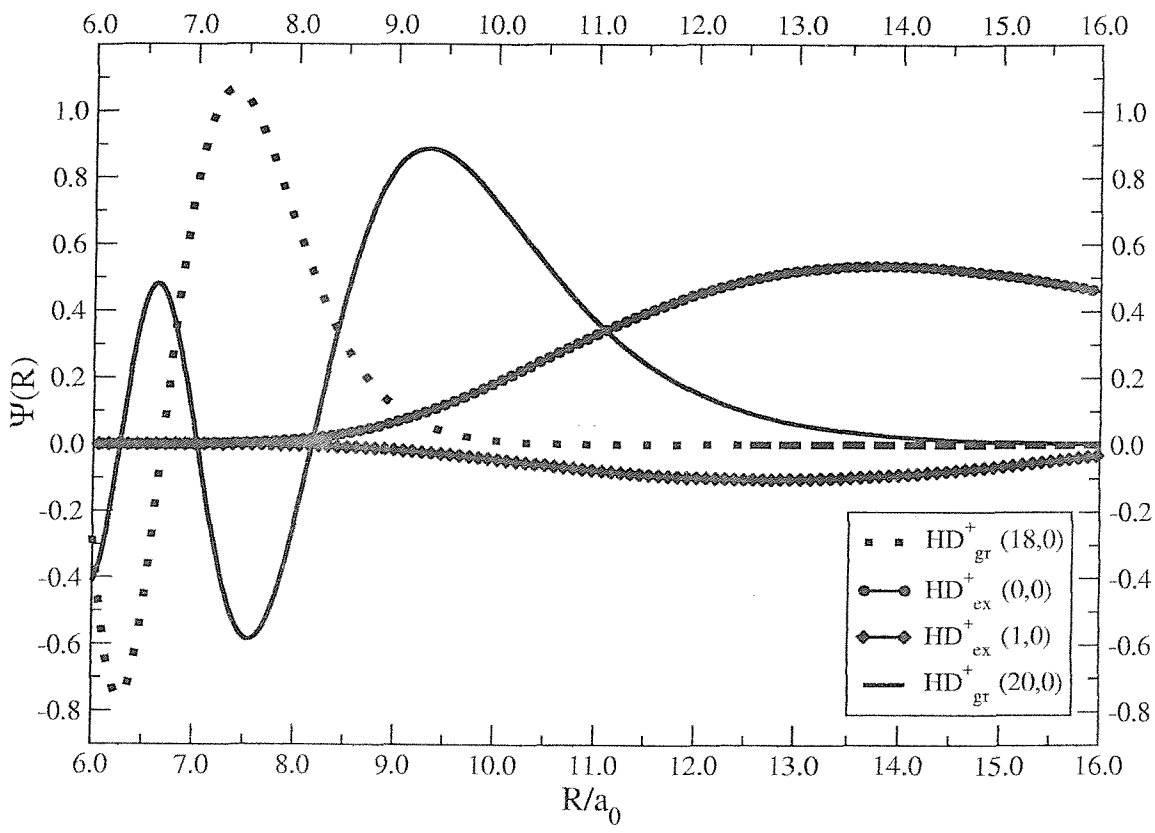

Figure 4.13: HD^+: details of the vibrational wavefunctions for the well-behaved level (18,0) and the anomalous level (20,0); the latter curve has significant amplitude in the region of the g/u symmetry breaking (10-15 a_0) as do the wavefunctions for (0,0) and (1,0) of the first excited state.

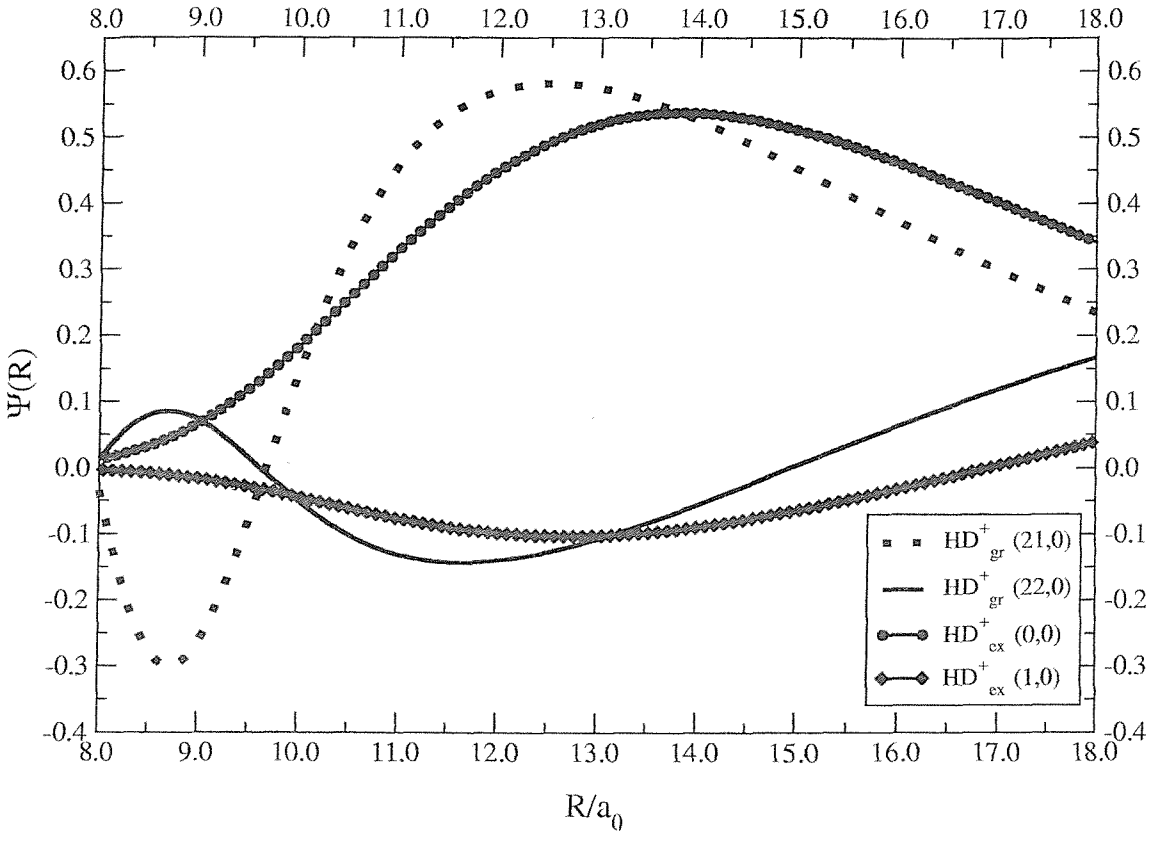

Figure 4.14: HD^+: details of the vibrational wavefunctions for the anomalous levels (21,0) and (22,0) of the ground electronic state with (0,0) and (1,0) levels of the first excited electronic state.

4.4 Conclusions

In this chapter a study of vibration-rotational levels of the ground electronic states of H_2^+, D_2^+ and HD^+ is reported with attention confined to the bound levels. It is shown how for v=0 and/or for N=0 it is possible to predict the adiabatic corrections to the dissociation energies for D_2^+ and HD^+ starting from those of H_2^+, through scaling factors based on the relative reduced masses. However, scaling becomes increasingly less successful as v (for constant N) or N (for constant v) increase. The same comments are true for the non-adiabatic corrections except for the few high lying levels of HD^+ that are found to be atypical.

Near the dissociation limit, the dissociation energy corrections are expected to reduce in magnitude as v increases, but out of line are certain levels with dissociation energies between 99.0 and 1.8 cm^{-1} and bond lengths between 7.9 and 15.7 a_0.

These results are perhaps not entirely unexpected; as reported in [37], the Born-Oppenheimer potential is the same for all the three isotopomers, and the adiabatic correction to the potential is first order and proportional to the inverse of the reduced mass. It is less expected for the non-adiabatic corrections which mix in excited electronic states.

Although it is not strictly possible to refer to a non-adiabatic potential, it can be argued [37] that the non-adiabatic correction will increase the dissociation energies for all levels and, as a consequence, will reduce the bond lengths, as reported in the next chapter.

Chapter 5

Results: adiabatic and non-adiabatic bond lengths for H_2^+, D_2^+ and HD^+

5.1 Introduction

In this chapter the results obtained for the adiabatic and non-adiabatic corrections to the bond lengths of the ground electronic states of H_2^+, D_2^+ and HD^+ [34] are exposed. As for the dissociation energies, the scaling of the corrections, both adiabatic and non-adiabatic, to the bond lengths for the three different isotopomers is considered.

One of the motivations for this work is that an anomalous non-adiabatic correction to the bond length was previously noted [37] for the v=20, N=0 level of HD^+ ground electronic state, in that it was opposite in sign with respect to all the other rotationless levels. The corresponding corrections to the expectation values $\langle R^2 \rangle$ and $\langle R^{-2} \rangle$ were also anomalous, suggesting that the calculations were not spurious. It is here reported that HD^+ in other vibration-rotational high lying levels also has corrections to $\langle R \rangle$ that are anomalous in having the unexpected sign, namely v=20, N=1-5 and v=19, N=7-9.

All the results for the bond length are given in atomic units and the fundamental constants listed in table 4.1 are used.

5.2 The adiabatic correction to the bond length

Abiabatic corrections to the bond length were considered and previously discussed for rotationless levels [37]. For levels with dissociation energies of more than about 5000 cm^{-1} they (adiabatic − Born-Oppenheimer) are positive, but for levels less than that they become negative, although their magnitude does not become significant until within about 2000 cm^{-1} of the dissociation limit.

The position for bond length corrections is similar to that for dissociation energy corrections (see previous chapter). If for rotationless levels the scaled corrections for D_2^+ and HD^+ are plotted against dissociation energies, the curves coincide with that for H_2^+, as shown in figure 5.1. Note that the bond length corrections for HD^+ do not allow for g/u symmetry breaking but, if the intermediate transformed Hamiltonian is used, then the scaled HD^+ curve still coincides with the corresponding scaled curves for the H_2^+ and D_2^+, except for the very highest levels ($v \geq 19$) where g/u electronic symmetry breaking is significant (see figure 5.2).

For a given non-zero rotational quantum number the scaled curves are slightly displaced from those for N=0, but so long as N is not too high, for example for N=8 (figure 5.3), those for different isotopomers still coincide. However, for even higher N, for example 16 (figure 5.4), this is no longer true, although the curves for H_2^+, N=16, and D_2^+, N=20, do as shown in figure 5.5.

For fixed v=0 the scaled curves do not quite coincide (figure 5.6), but for increasing fixed v the differences become much more pronounced, as explicitly reported in figure 5.7.

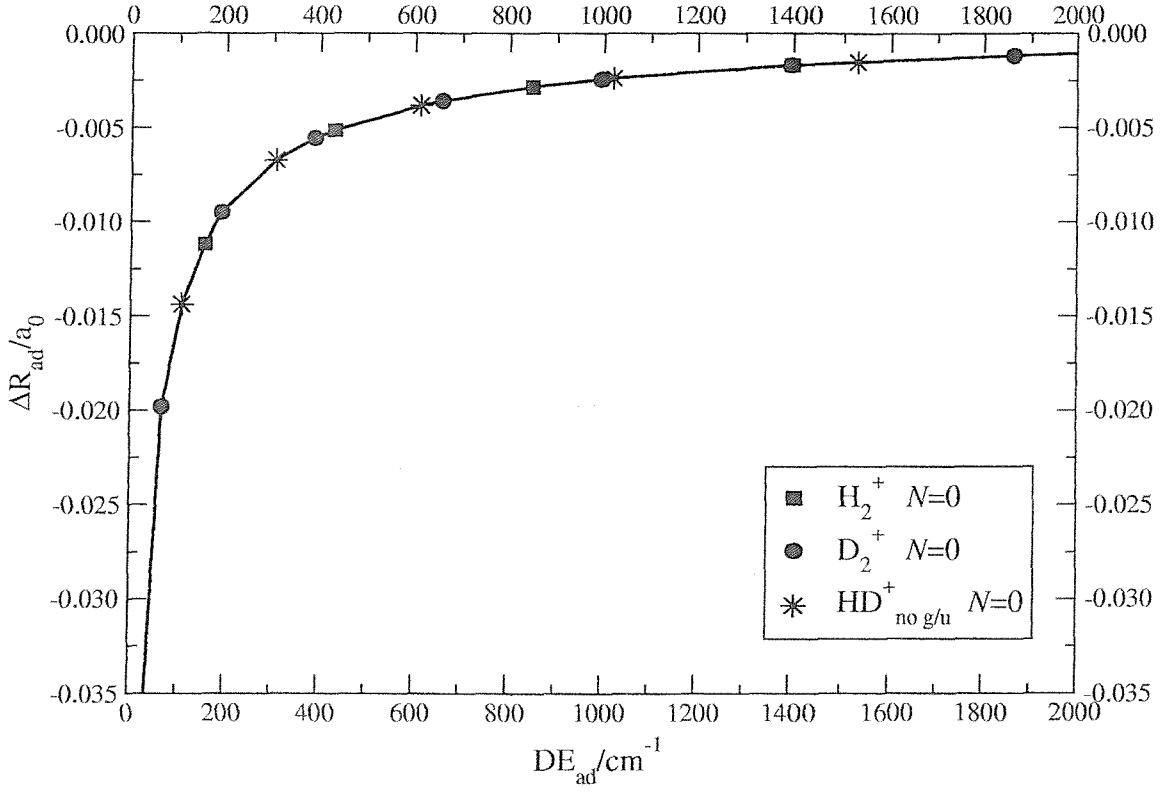

Figure 5.1: Partitioned corrections (partitioned − BO) for H_2^+ and D_2^+ and standard adiabatic correction (standard − BO) for HD^+ to the bond length for N=0 against dissociation energies; a scaling factor of 2 to D_2^+ and of 4/3 to HD^+ is applied.

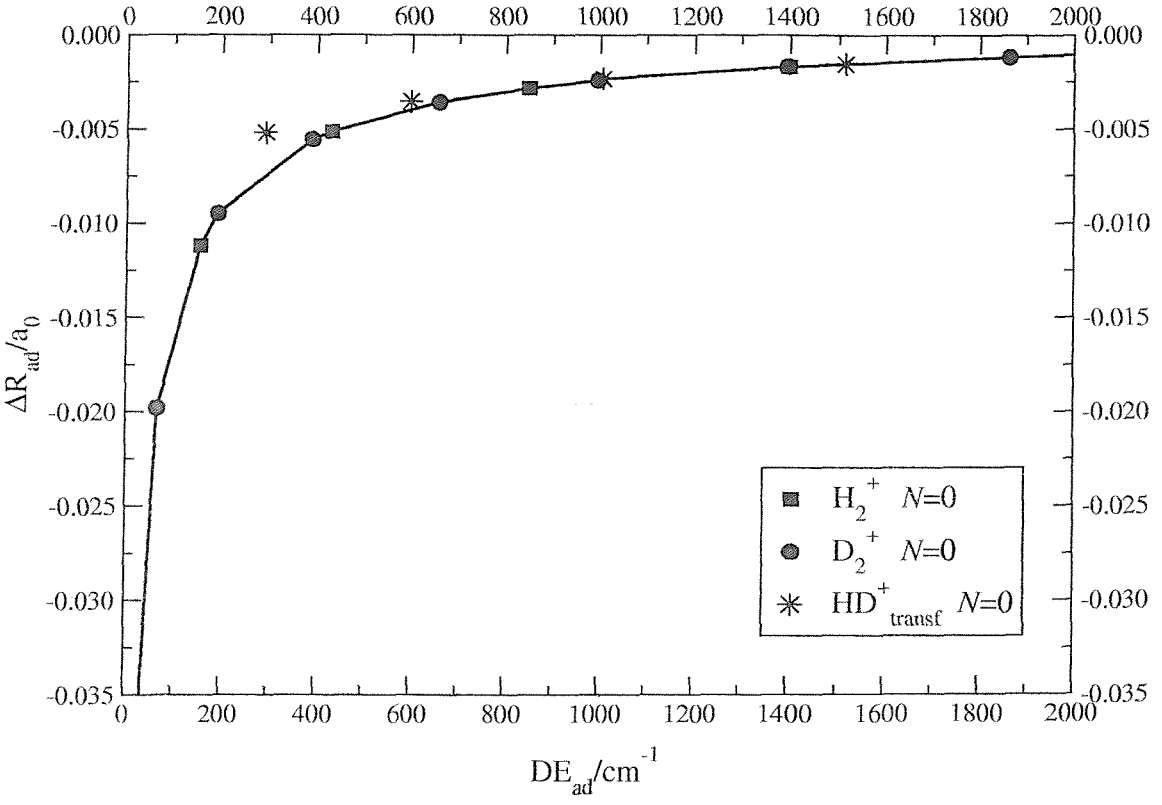

Figure 5.2: Partitioned corrections (partitioned − BO) for H_2^+ and D_2^+ and intermediate transformed adiabatic correction (transformed − BO) for HD^+ to the bond length for N=0 against dissociation energies; a scaling factor of 2 to D_2^+ and of 4/3 to HD^+ is applied.

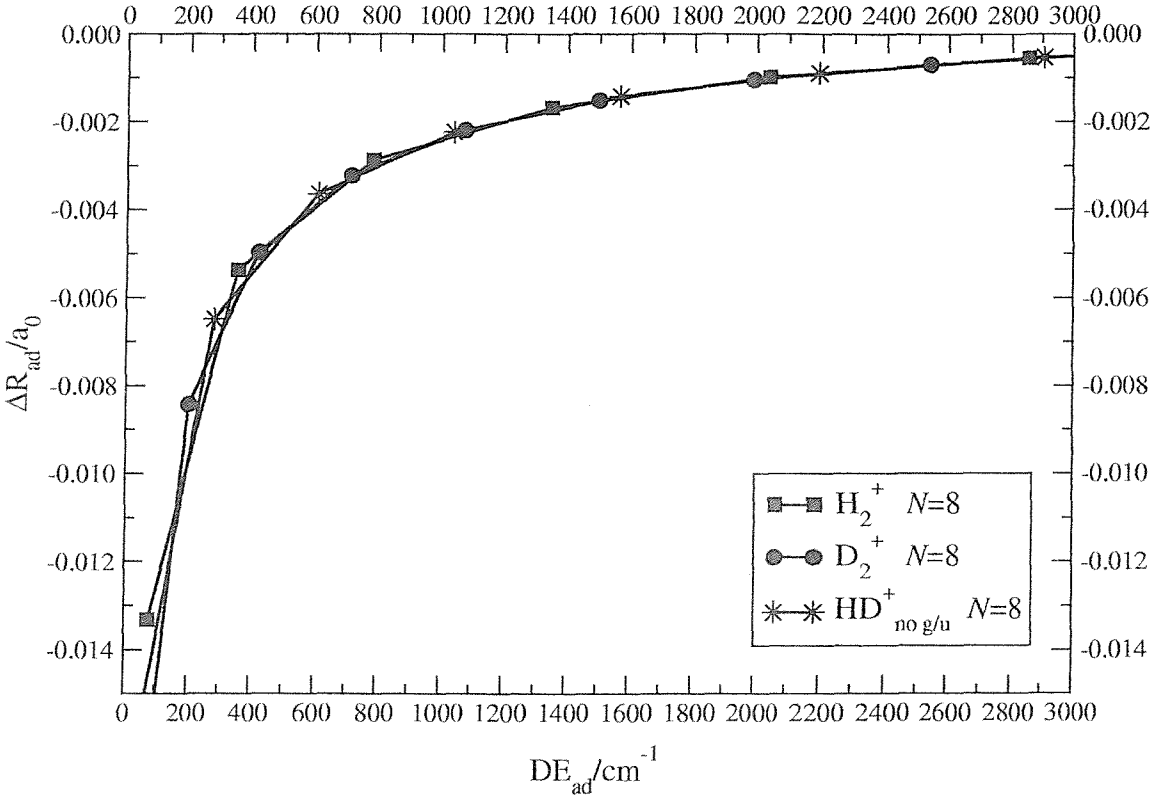

Figure 5.3: Partitioned corrections (partitioned − BO) for H_2^+ and D_2^+ and standard adiabatic correction (standard − BO) for HD^+ to the bond length for N=8 against dissociation energies; a scaling factor of 2 to D_2^+ and of 4/3 to HD^+ is applied.

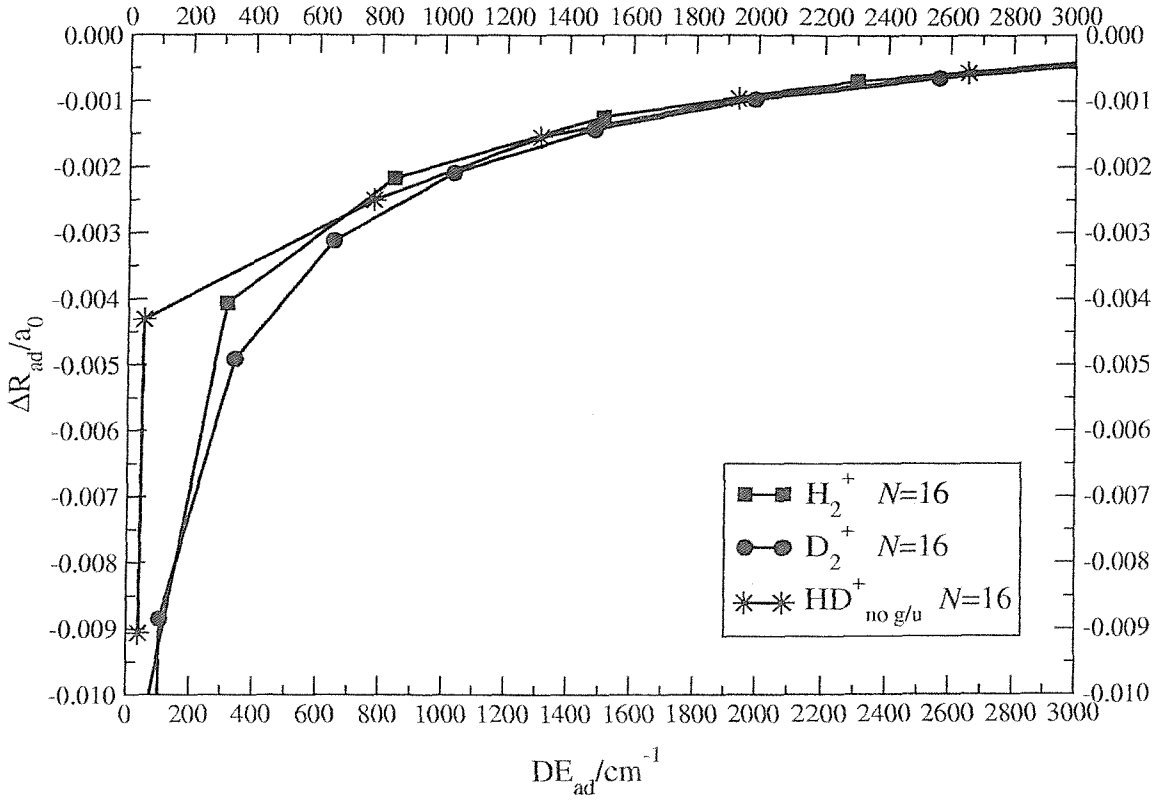

Figure 5.4: Partitioned corrections (partitioned − BO) for H_2^+ and D_2^+ and standard adiabatic correction (standard − BO) for HD^+ to the bond length for N=16 against dissociation energies; a scaling factor of 2 to D_2^+ and of 4/3 to HD^+ is applied.

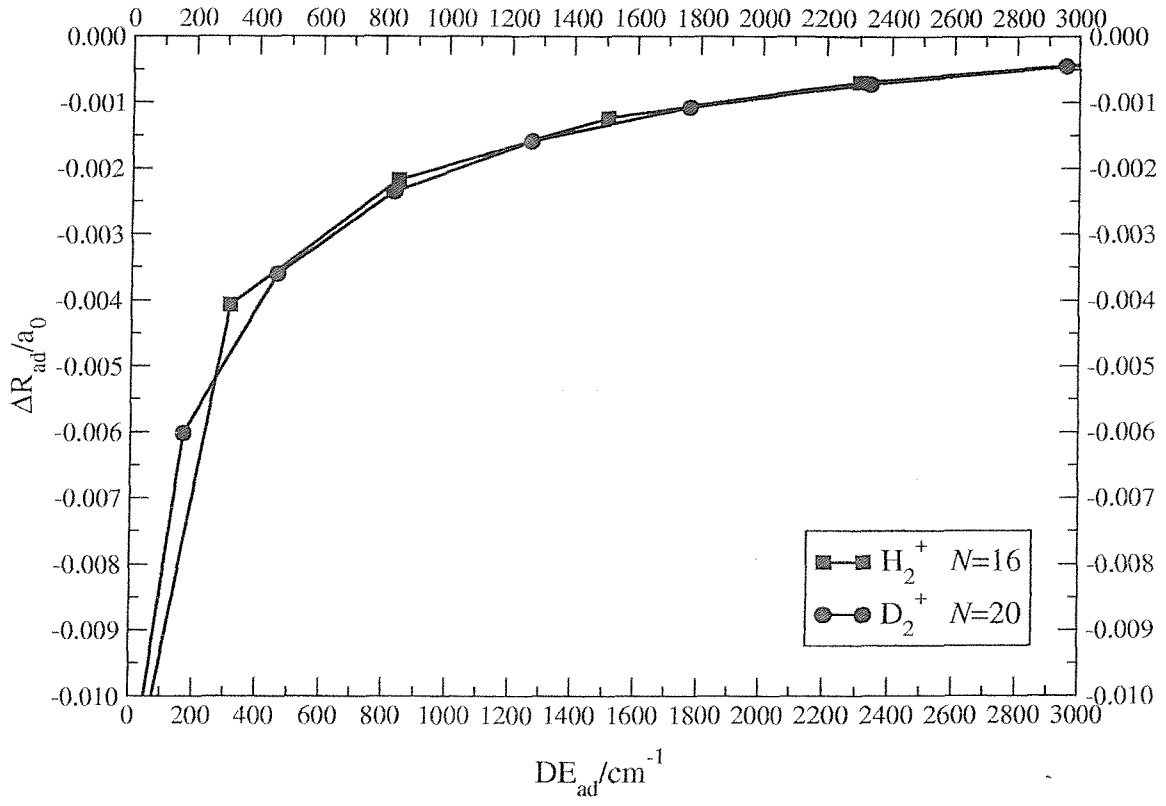

Figure 5.5: Partitioned corrections (partitioned − BO) for H_2^+ and D_2^+ to the bond length for N=16 and N=20 respectively against dissociation energies; a scaling factor of 2 to D_2^+ is applied.

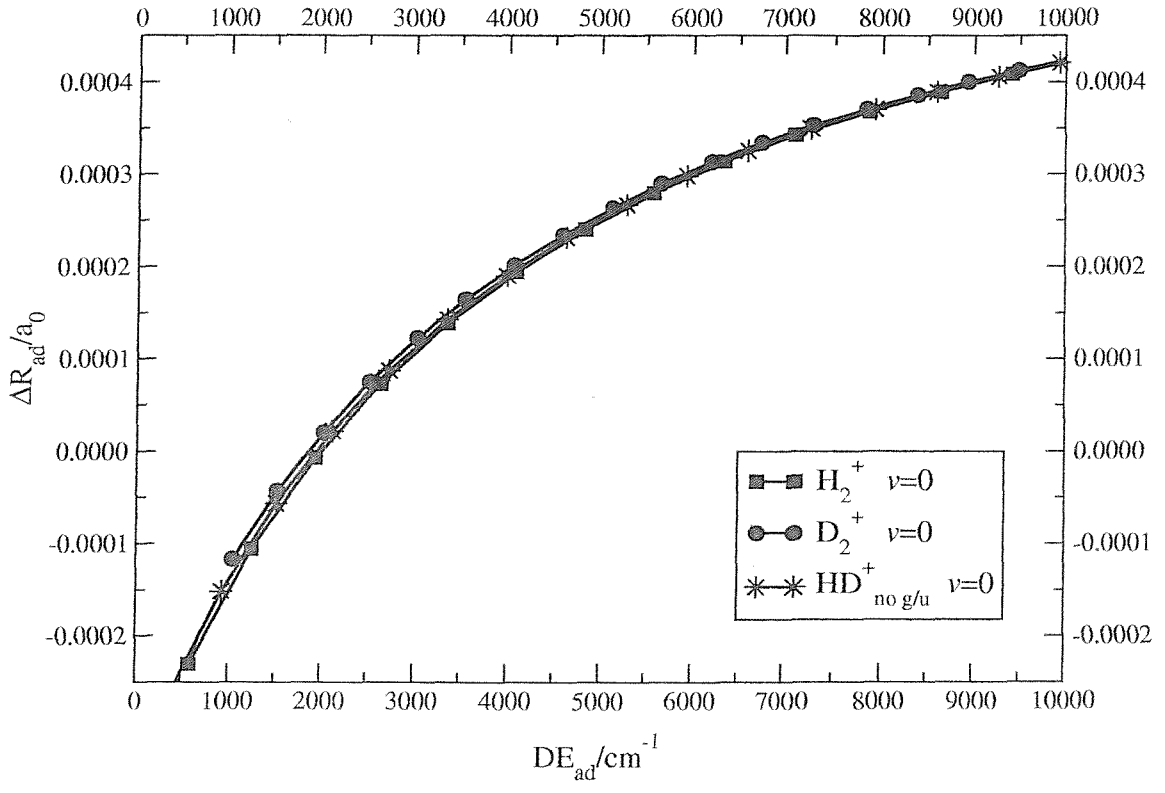

Figure 5.6: Partitioned corrections (partitioned – BO) for H_2^+ and D_2^+ and standard adiabatic correction (standard – BO) for HD^+ to the bond length for v=0 against dissociation energies; a scaling factor of 2 to D_2^+ and of 4/3 to HD^+ is applied.

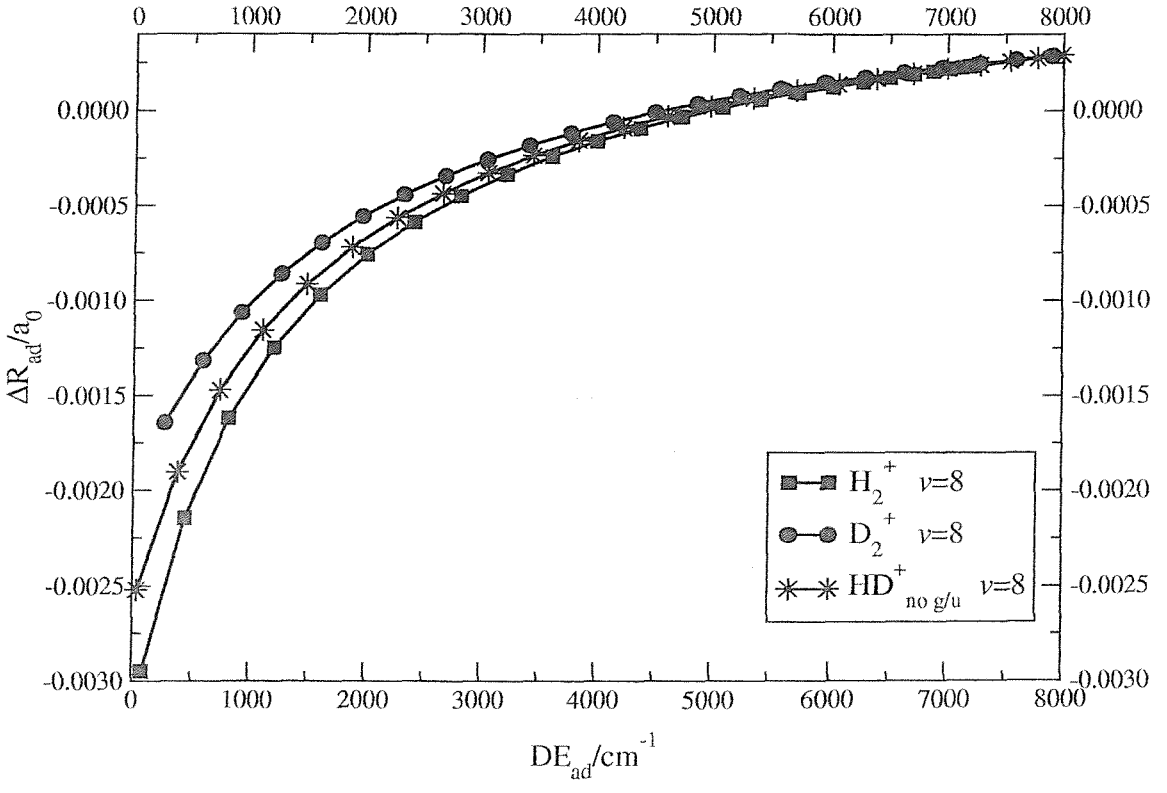

Figure 5.7: Partitioned corrections (partitioned − BO) for H_2^+ and D_2^+ and standard adiabatic correction (standard − BO) for HD^+ to the bond length for v=8 against dissociation energies; a scaling factor of 2 to D_2^+ and of 4/3 to HD^+ is applied.

5.3 The non-adiabatic correction to the bond length

Even confining interest to the bound vibration-rotational levels of the ground electronic states of the three isotopomers, there are many hundreds, as appears explicit from the grids of figures 5.8, 5.9 and 5.10; in these grids all the levels are indicated, for which the non-adiabatic values of the bond length and the relative non-adiabatic corrections are studied. All the results obtained are explicitly reported in tables 5.1 (H_2^+), 5.2 (D_2^+) and 5.3 (HD^+) since these were not published and they are not as easily reproduced as the adiabatic ones.

As might be expected, in general the corrections are negative and increase in magnitude with vibrational and rotational quantum numbers. As for the adiabatic corrections, scaling works well for low N (see figure 5.11), but for high N (figure 5.12) it is necessary to use different rotational quantum numbers for the three ions for reasonably successful scaling, as happens for example by plotting H_2^+, N=16 corrections with D_2^+, N=20, against dissociation energies (figure 5.13).

In the case of the bond length, the correction will depend on the first order correction to the wavefunction, proportional to the inverse of the reduced mass. As noted above, the scaling is less successful with increasing N for constant v (figures 5.14, 5.15 and 5.16) or increasing v for constant N, but is presumably a reflection of the different ways in which rotation and vibration depend on masses and bond lengths.

However, for HD^+, a number of high-lying levels show anomalies in that the magnitude of the correction decreases with increasing v and/or N; these include (19,1 - 6), (18,10 - 11) and (17,14), but it is conceivable that there are other such levels that lie close to dissociation with higher N and lower v. In addition there are some levels that show the same anomaly as v=20, N=0, in that the correction is actually positive rather than negative; these levels are (19,7 - 9) and (20,0 - 5). Figure 5.17 illustrates the behaviour for N=0 levels for all the three molecules, while details for relevant levels of HD^+ are given in table 5.4, as a selection of the results of the complete tables 5.1 (H_2^+), 5.2 (D_2^+) and 5.3 (HD^+).

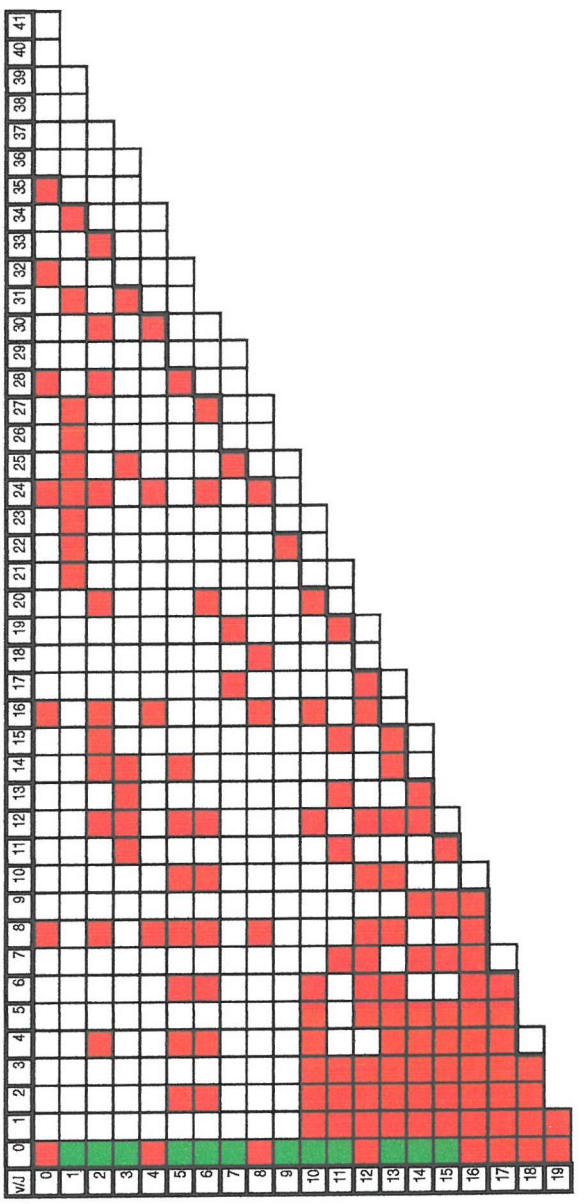

Figure 5.8: H_2^+: non-adiabatic levels studied and reported in this work; the green boxes indicate the levels for which the results were already published; the red ones the levels studied ex-novo in this work. The thick line separates the bound levels from the quasi-bound.

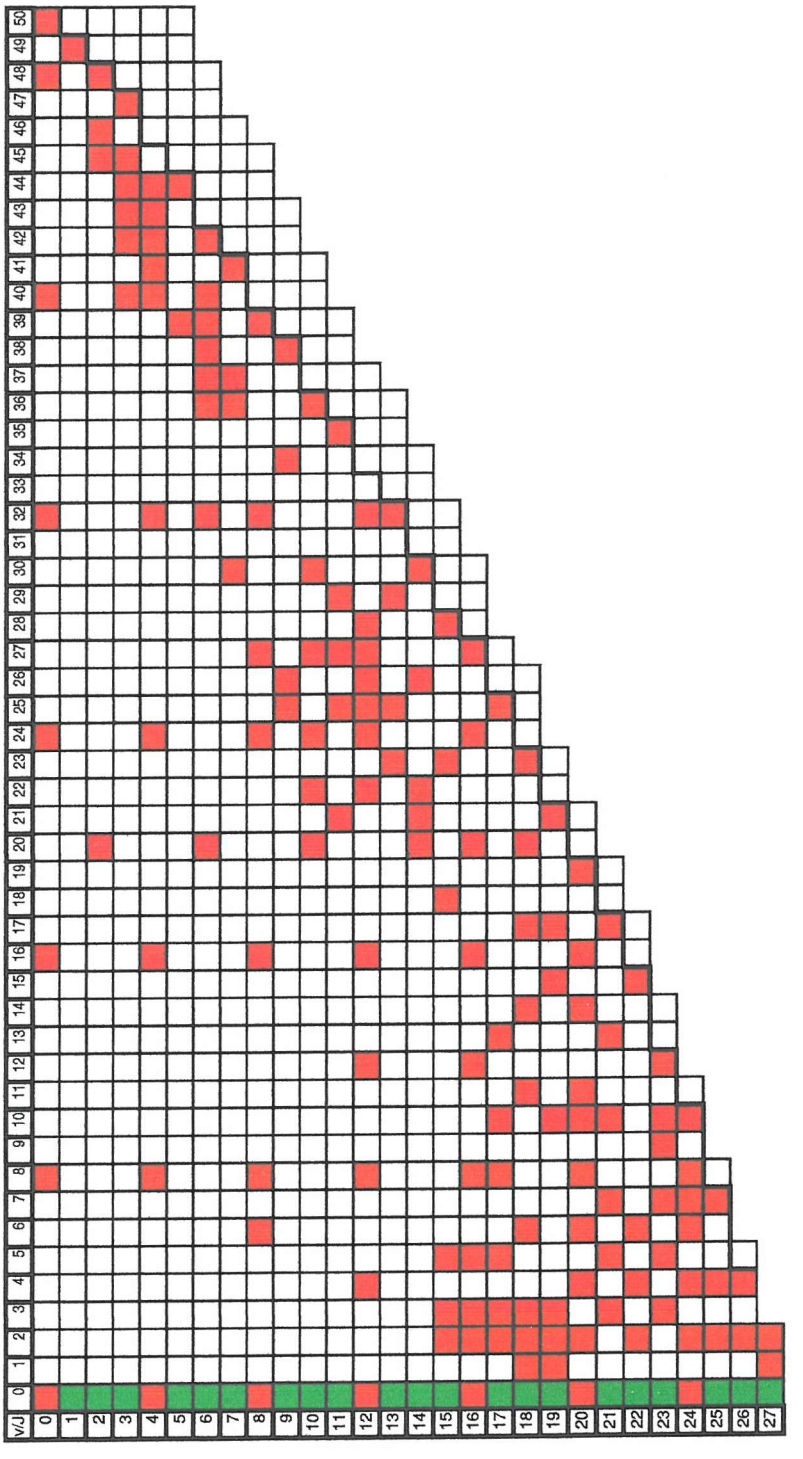

Figure 5.9: D_2^+: non-adiabatic levels studied and reported in this work; the green boxes indicate the levels for which the results were already published; the red ones the levels studied ex-novo in this work. The thick line separates the bound levels from the quasi-bound.

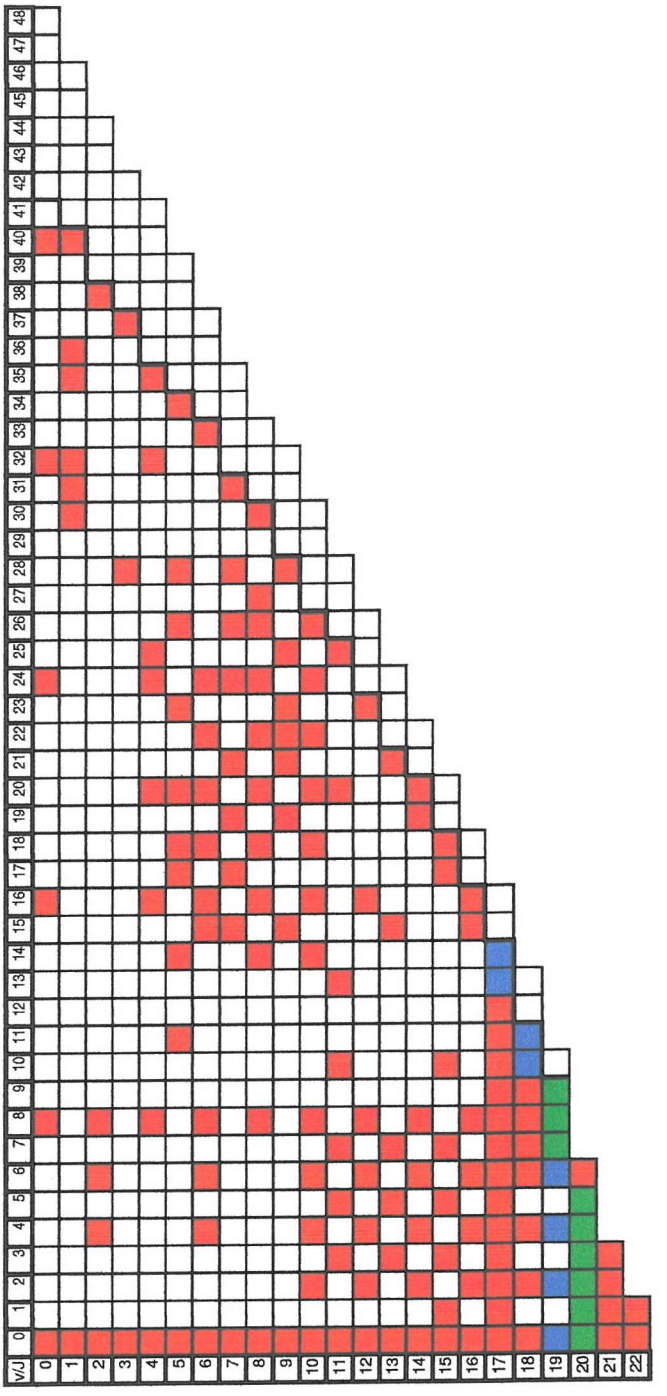

Figure 5.10: HD^+: non-adiabatic levels studied and reported in this work; the green boxes indicate the levels for which a positive non-adiabatic correction to the bond length is obtained; the blue ones indicate an increase in the correction; the red ones the other levels studied ex-novo in this work. The thick line separates the bound levels from the quasi-bound.

Table 5.1: H_2^+: non-adiabatic bond lengths and non-adiabatic corrections (non-adiabatic − partitioned).

(v, N)	$\langle R\rangle_{\mathrm{non-ad}}/a_0$	$\langle \Delta R\rangle_{\mathrm{non-ad}}/a_0$	(v, N)	$\langle R\rangle_{\mathrm{non-ad}}/a_0$	$\langle \Delta R\rangle_{\mathrm{non-ad}}/a_0$
(0,0)	2.063 914	-0.000 006	(4,0)	2.640 771	-0.000 061
(0,8)	2.159 449	-0.000 007	(4,8)	2.757 315	-0.000 067
(0,16)	2.410 200	-0.000 013	(4,16)	3.074 110	-0.000 087
(0,24)	2.800 677	-0.000 025	(4,24)	3.619 422	-0.000 148
(0,28)	3.053 667	-0.000 037	(4,30)	4.326 199	-0.000 329
(0,32)	3.359 333	-0.000 056	(5,0)	2.803 481	-0.000 080
(0,35)	3.640 960	-0.000 082	(5,2)	2.813 930	-0.000 081
(1,0)	2.119 125	-0.000 017	(5,4)	2.838 241	-0.000 082
(1,21)	2.803 642	-0.000 037	(5,6)	2.876 266	-0.000 085
(1,22)	2.859 398	-0.000 039	(5,8)	2.927 843	-0.000 088
(1,23)	2.917 838	-0.000 042	(5,10)	2.992 878	-0.000 093
(1,24)	2.979 100	-0.000 045	(5,12)	3.071 433	-0.000 099
(1,25)	3.043 360	-0.000 049	(5,14)	3.163 842	-0.000 107
(1,26)	3.110 836	-0.000 053	(5,28)	4.407 691	-0.000 376
(1,27)	3.181 801	-0.000 058	(6,0)	2.976 383	-0.000 103
(1,31)	3.508 962	-0.000 087	(6,2)	2.987 589	-0.000 104
(1,34)	3.822 150	-0.000 130	(6,4)	3.013 687	-0.000 106
(2,0)	2.339 751	-0.000 030	(6,6)	3.054 587	-0.000 109
(2,4)	2.369 114	-0.000 031	(6,8)	3.110 231	-0.000 114
(2,8)	2.444 200	-0.000 033	(6,10)	3.180 683	-0.000 121
(2,12)	2.562 526	-0.000 037	(6,12)	3.266 254	-0.000 130
(2,14)	2.637 230	-0.000 040	(6,20)	3.784 779	-0.000 205
(2,15)	6.678 416	-0.000 042	(6,24)	4.204 455	-0.000 313
(2,16)	2.722 168	-0.000 044	(6,27)	4.678 420	-0.000 522
(2,20)	2.923 628	-0.000 054	(7,0)	3.161 577	-0.000 131
(2,24)	3.172 076	-0.000 070	(7,17)	3.801 000	-0.000 223
(2,28)	3.481 996	-0.000 099	(7,19)	3.973 157	-0.000 262
(2,30)	3.670 226	-0.000 124	(7,25)	4.776 479	-0.000 583
(2,33)	4.022 772	-0.000 194	(8,0)	3.361 814	-0.000 166
(3,0)	2.486 624	-0.000 045	(8,8)	3.522 082	-0.000 188
(3,11)	2.686 333	-0.000 053	(8,16)	3.996 314	-0.000 282
(3,12)	2.721 870	-0.000 054	(8,18)	4.182 442	-0.000 333
(3,13)	2.760 207	-0.000 056	(8,20)	4.411 462	-0.000 412
(3,14)	2.801 348	-0.000 058	(8,24)	5.110 488	-0.000 818
(3,25)	3.463 117	-0.000 112	(9,0)	3.580 773	-0.000 211
(3,31)	4.096 677	-0.000 234	(9,22)	5.240 791	-0.000 911

H_2^+ continued

(v,N)	$\langle R\rangle_{\mathrm{non-ad}}/a_0$	$\langle \Delta R\rangle_{\mathrm{non-ad}}/a_0$	(v,N)	$\langle R\rangle_{\mathrm{non-ad}}/a_0$	$\langle \Delta R\rangle_{\mathrm{non-ad}}/a_0$
(10,0)	3.823 507	-0.000 270	(14,0)	5.242 768	-0.000 886
(10,1)	3.829 052	-0.000 271	(14,1)	5.254 737	-0.000 893
(10,2)	3.840 160	-0.000 274	(14,2)	5.278 878	-0.000 909
(10,3)	3.856 870	-0.000 277	(14,3)	5.315 610	-0.000 932
(10,4)	3.879 242	-0.000 282	(14,4)	5.365 608	-0.000 965
(10,5)	3.907 365	-0.000 289	(14,5)	5.429 863	-0.001 009
(10,6)	3.940 364	-0.000 297	(14,7)	5.607 350	-0.001 141
(10,12)	4.283 227	-0.000 393	(14,9)	5.867 896	-0.001 365
(10,16)	4.688 851	-0.000 553	(14,12)	6.524 493	-0.002 151
(10,20)	5.396 382	-0.001 029	(14,13)	6.884 186	-0.002 785
(11,0)	4.097 166	-0.000 351	(15,0)	5.834 398	-0.001 316
(11,1)	4.103 559	-0.000 352	(15,1)	5.850 972	-0.001 330
(11,2)	4.116 378	-0.000 356	(15,2)	5.884 541	-0.001 359
(11,3)	4.135 693	-0.000 361	(15,3)	5.935 996	-0.001 404
(11,7)	4.280 936	-0.000 406	(15,4)	6.006 796	-0.001 470
(11,11)	4.551 555	-0.000 504	(15,5)	6.099 156	-0.001 559
(11,13)	4.748 948	-0.000 591	(15,7)	6.363 356	-0.001 846
(11,15)	5.006 251	-0.000 730	(15,9)	6.782 020	-0.002 414
(11,19)	5.879 008	-0.001 523	(15,11)	7.516 485	-0.003 946
(12,0)	4.412 279	-0.000 464	(16,0)	6.664 038	-0.002 140
(12,1)	4.419 850	-0.000 467	(16,1)	6.689 900	-0.002 172
(12,2)	4.435 052	-0.000 472	(16,2)	6.742 708	-0.002 240
(12,3)	4.458 009	-0.000 481	(16,3)	6.824 814	-0.002 351
(12,5)	4.528 054	-0.000 507	(16,4)	6.940 262	-0.002 514
(12,6)	4.575 813	-0.000 526	(16,5)	7.095 656	-0.002 753
(12,7)	4.632 714	-0.000 550	(16,6)	7.301 928	-0.003 107
(12,8)	4.699 455	-0.000 579	(16,7)	7.578 364	-0.003 660
(12,10)	4.866 478	-0.000 659	(16,8)	7.963 660	-0.004 627
(12,12)	5.088 885	-0.000 783	(16,9)	8.560 789	-0.006 910
(12,16)	5.821 640	-0.001 391	(17,0)	8.014 527	-0.004 206
(12,17)	6.126 303	-0.001 781	(17,1)	8.066 007	-0.004 319
(13,0)	4.785 144	-0.000 630	(17,2)	8.173 407	-0.004 566
(13,1)	4.794 435	-0.000 634	(17,3)	8.347 128	-0.004 997
(13,2)	4.813 122	-0.000 643	(17,4)	8.607 923	-0.005 730
(13,3)	4.841 429	-0.000 657	(17,5)	8.999 589	-0.007 069
(13,4)	4.879 707	-0.000 675	(17,6)	9.639 539	-0.010 227
(13,5)	4.928 467	-0.000 700	(18,0)	11.174 728	-0.013 755
(13,6)	4.988 418	-0.000 732	(18,1)	11.382 683	-0.014 870
(13,8)	5.146 110	-0.000 822	(18,2)	11.869 715	-0.017 846
(13,10)	5.365 606	-0.000 966	(18,3)	12.909 287	-0.026 680
(13,12)	5.672 167	-0.001 210	(19,0)	25.243 3	-0.082 6
(13,14)	6.123 413	-0.001 690	(19,1)	30.457	-0.173
(13,15)	6.448 016	-0.002 165			

Table 5.2: D_2^+: non-adiabatic bond lengths and non-adiabatic corrections (non-adiabatic − partitioned).

(v, N)	$\langle R\rangle_{\mathrm{non-ad}}/a_0$	$\langle \Delta R\rangle_{\mathrm{non-ad}}/a_0$	(v, N)	$\langle R\rangle_{\mathrm{non-ad}}/a_0$	$\langle \Delta R\rangle_{\mathrm{non-ad}}/a_0$
(0,0)	2.044 070	-0.000 002	(6,36)	3.767 489	-0.000 087
(0,8)	2.092 042	-0.000 002	(6,37)	3.839 877	-0.000 094
(0,16)	2.220 789	-0.000 003	(6,38)	3.917 068	-0.000 103
(0,24)	2.421 988	-0.000 006	(6,39)	3.999 823	-0.000 112
(0,32)	2.691 249	-0.000 010	(6,40)	4.089 133	-0.000 124
(0,40)	3.035 017	-0.000 017	(6,42)	4.293 268	-0.000 158
(0,48)	3.484 038	-0.000 032	(7,0)	2.770 454	-0.000 038
(0,50)	3.622 374	-0.000 038	(7,30)	3.571 232	-0.000 076
(1,0)	2.138 662	-0.000 006	(7,36)	3.972 405	-0.000 115
(1,49)	3.747 789	-0.000 054	(7,37)	4.055 516	-0.000 125
(2,0)	2.235 803	-0.000 010	(7,41)	4.470 493	-0.000 201
(2,20)	2.522 485	-0.000 014	(8,0)	2.890 104	-0.000 046
(2,45)	3.643 772	-0.000 054	(8,6)	2.927 919	-0.000 047
(2,46)	3.718 026	-0.000 059	(8,8)	2.954 825	-0.000 048
(2,48)	3.882 013	-0.000 073	(8,16)	3.133 160	-0.000 055
(3,0)	2.335 753	-0.000 015	(8,24)	3.429 791	-0.000 071
(3,40)	3.488 458	-0.000 050	(8,27)	3.576 903	-0.000 082
(3,42)	3.619 458	-0.000 058	(8,28)	3.631 242	-0.000 086
(3,43)	3.690 447	-0.000 063	(8,32)	3.881 370	-0.000 109
(3,44)	3.765 808	-0.000 069	(8,39)	4.531 241	-0.000 219
(3,45)	3.846 266	-0.000 077	(9,0)	3.015 346	-0.000 054
(3,47)	4.026 676	-0.000 097	(9,25)	3.642 912	-0.000 092
(4,0)	2.438 813	-0.000 020	(9,26)	3.696 566	-0.000 096
(4,8)	2.493 312	-0.000 021	(9,34)	4.268 707	-0.000 169
(4,16)	2.640 941	-0.000 024	(9,38)	4.732 413	-0.000 277
(4,24)	2.876 785	-0.000 029	(10,0)	3.146 993	-0.000 064
(4,32)	3.206 457	-0.000 041	(10,20)	3.574 209	-0.000 091
(4,40)	3.666 627	-0.000 067	(10,22)	3.665 537	-0.000 099
(4,41)	3.738 275	-0.000 073	(10,24)	3.768 155	-0.000 108
(4,42)	3.814 463	-0.000 080	(10,27)	3.946 990	-0.000 127
(4,43)	3.895 938	-0.000 088	(10,30)	4.164 060	-0.000 157
(4,44)	3.983 684	-0.000 098	(10,36)	4.802 407	-0.000 299
(5,0)	2.545 333	-0.000 025	(11,0)	3.286 033	-0.000 076
(5,39)	3.787 872	-0.000 084	(11,21)	3.795 359	-0.000 116
(5,44)	4.238 039	-0.000 143	(11,25)	4.023 703	-0.000 142
(6,0)	2.655 720	-0.000 031	(11,27)	4.162 520	-0.000 161
(6,20)	2.993 446	-0.000 041	(11,29)	4.323 076	-0.000 187
(6,32)	3.515 722	-0.000 067	(11,35)	5.036 358	-0.000 380

D_2^+ continued

(v, N)	$\langle R\rangle_{\mathrm{non-ad}}/a_0$	$\langle \Delta R\rangle_{\mathrm{non-ad}}/a_0$	(v, N)	$\langle R\rangle_{\mathrm{non-ad}}/a_0$	$\langle \Delta R\rangle_{\mathrm{non-ad}}/a_0$
(12,0)	3.433 676	-0.000 090	(17,0)	4.370 504	-0.000 224
(12,4)	3.456 597	-0.000 092	(17,2)	4.381 621	-0.000 226
(12,8)	3.516 404	-0.000 096	(17,3)	4.392 780	-0.000 228
(12,12)	3.613 968	-0.000 104	(17,5)	4.426 517	-0.000 234
(12,16)	3.751 662	-0.000 116	(17,8)	4.506 867	-0.000 249
(12,22)	4.046 764	-0.000 150	(17,10)	4.581 760	-0.000 264
(12,24)	4.175 062	-0.000 168	(17,13)	4.730 416	-0.000 296
(12,25)	4.246 410	-0.000 179	(17,25)	6.196 021	-0.000 945
(12,26)	4.323 312	-0.000 192	(18,0)	4.621 439	-0.000 277
(12,27)	4.406 516	-0.000 207	(18,1)	4.625 683	-0.000 277
(12,28)	4.496 973	-0.000 225	(18,2)	4.634 191	-0.000 279
(12,32)	4.963 616	-0.000 351	(18,3)	4.647 006	-0.000 282
(13,0)	3.591 425	-0.000 107	(18,6)	4.712 072	-0.000 296
(13,23)	4.339 895	-0.000 199	(18,11)	4.918 747	-0.000 345
(13,25)	4.499 401	-0.000 230	(18,14)	5.115 482	-0.000 401
(13,29)	4.920 438	-0.000 336	(18,17)	5.388 833	-0.000 492
(13,32)	5.402 569	-0.000 530	(18,20)	5.781 321	-0.000 661
(14,0)	3.761 169	-0.000 127	(18,23)	6.411 306	-0.001 076
(14,20)	4.374 878	-0.000 210	(19,0)	4.907 936	-0.000 347
(14,21)	4.444 934	-0.000 223	(19,1)	4.912 905	-0.000 348
(14,22)	4.520 952	-0.000 238	(19,2)	4.922 875	-0.000 350
(14,26)	4.903 400	-0.000 332	(19,3)	4.937 911	-0.000 354
(14,30)	5.511 496	-0.000 574	(19,10)	5.199 127	-0.000 428
(15,0)	3.945 326	-0.000 152	(19,15)	5.608 335	-0.000 575
(15,2)	3.954 192	-0.000 153	(19,17)	5.858 110	-0.000 688
(15,3)	3.963 075	-0.000 154	(19,21)	6.675 631	-0.001 255
(15,5)	3.989 841	-0.000 158	(20,0)	5.241 898	-0.000 443
(15,18)	4.494 798	-0.000 237	(20,2)	5.259 877	-0.000 448
(15,23)	4.911 922	-0.000 336	(20,4)	5.302 422	-0.000 462
(15,28)	5.636 943	-0.000 627	(20,6)	5.371 062	-0.000 484
(16,0)	4.417 041	-0.000 184	(20,8)	5.468 520	-0.000 518
(16,2)	4.156 900	-0.000 185	(20,10)	5.599 264	-0.000 567
(16,3)	4.166 786	-0.000 187	(20,11)	5.679 237	-0.000 600
(16,5)	4.196 618	-0.000 191	(20,14)	5.994 764	-0.000 745
(16,8)	4.267 316	-0.000 202	(20,16)	6.294 309	-0.000 914
(16,12)	4.414 102	-0.000 227	(20,19)	7.008 460	-0.001 514
(16,16)	4.632 092	-0.000 270	(21,0)	5.641 803	-0.000 582
(16,20)	4.947 467	-0.000 348	(21,3)	5.686 892	-0.000 599
(16,24)	5.426 241	-0.000 514	(21,5)	5.756 485	-0.000 627
(16,27)	6.017 431	-0.000 847	(21,7)	5.861 562	-0.000 672

D_2^+ continued

(v,N)	$\langle R\rangle_{\mathrm{non-ad}}/a_0$	$\langle \Delta R\rangle_{\mathrm{non-ad}}/a_0$	(v,N)	$\langle R\rangle_{\mathrm{non-ad}}/a_0$	$\langle \Delta R\rangle_{\mathrm{non-ad}}/a_0$
(21,10)	6.100 317	-0.000 785	(24,2)	7.780 776	-0.001 887
(21,13)	6.477 381	-0.001 004	(24,4)	7.946 155	-0.002 059
(21,17)	7.443 184	-0.001 922	(24,6)	8.240 050	-0.002 405
(22,0)	5.241 898	-0.000 793	(24,7)	8.455 327	-0.002 698
(22,2)	6.167 827	-0.000 807	(24,8)	8.738 595	-0.003 146
(22,4)	6.238 169	-0.000 843	(24,10)	9.715 917	-0.005 659
(22,6)	6.354 223	-0.000 905	(25,0)	9.250 802	-0.003 542
(22,15)	8.045 022	-0.002 654	(25,2)	9.390 110	-0.003 775
(23,0)	6.788 598	-0.001 144	(25,4)	9.759 933	-0.004 480
(23,3)	6.872 549	-0.001 200	(25,7)	11.328 181	-0.009 875
(23,5)	7.005 945	-0.001 295	(26,0)	12.735 308	-0.009 900
(23,7)	7.217 385	-0.001 462	(26,2)	13.265 901	-0.011 539
(23,9)	7.537 630	-0.001 759	(26,4)	15.245 067	-0.022 483
(23,10)	7.757 717	-0.001 998	(27,0)	22.916 403	-0.033 319
(23,12)	8.414 624	-0.002 978	(27,1)	24.183 268	-0.040 453
(24,0)	7.714 110	-0.001 822	(27,2)	29.012 459	-0.099 853

Table 5.3: HD^+: non-adiabatic bond lengths and non-adiabatic corrections (non-adiabatic − transformed).

(v,N)	$\langle R\rangle_{\mathrm{non-ad}}/a_0$	$\langle \Delta R\rangle_{\mathrm{non-ad}}/a_0$	(v,N)	$\langle R\rangle_{\mathrm{non-ad}}/a_0$	$\langle \Delta R\rangle_{\mathrm{non-ad}}/a_0$
(0,0)	2.054 803	-0.000 004	(6,6)	2.880 173	-0.000 065
(0,8)	2.126 609	-0.000 004	(6,8)	2.919 321	-0.000 067
(0,16)	2.316 940	-0.000 008	(6,15)	3.137 080	-0.000 080
(0,24)	2.612 547	-0.000 014	(6,16)	3.178 658	-0.000 083
(0,30)	2.904 014	-0.000 022	(6,18)	3.270 190	-0.000 089
(0,32)	3.016 574	-0.000 026	(6,20)	3.373 626	-0.000 098
(0,40)	3.579 16	-0.000 06	(6,22)	3.490 272	-0.000 109
(1,0)	2.171 318	-0.000 011	(6,24)	3.622 136	-0.000 124
(1,30)	3.065 654	-0.000 036	(6,33)	4.556 199	-0.000 336
(1,31)	3.125 417	-0.000 038	(7,0)	2.975 361	-0.000 077
(1,32)	3.187 845	-0.000 042	(7,15)	3.310 260	-0.000 101
(1,35)	3.393 737	-0.000 054	(7,17)	3.403 508	-0.000 109
(1,36)	3.469 779	-0.000 059	(7,19)	3.510 224	-0.000 120
(1,40)	3.828 361	-0.000 095	(7,21)	3.631 824	-0.000 134
(2,0)	2.291 782	-0.000 019	(7,24)	3.847 951	-0.000 164
(2,4)	2.313 492	-0.000 020	(7,26)	4.021 021	-0.000 195
(2,6)	2.337 182	-0.000 020	(7,28)	4.226 471	-0.000 240
(2,8)	2.369 189	-0.000 021	(7,31)	4.633 273	-0.000 371
(2,38)	3.890 280	-0.000 117	(8,0)	3.134 902	-0.000 095
(3,0)	2.416 706	-0.000 028	(8,8)	3.242 727	-0.000 103
(3,28)	3.295 118	-0.000 066	(8,14)	3.451 074	-0.000 122
(3,37)	4.067 332	-0.000 162	(8,16)	3.546 715	-0.000 133
(4,0)	2.546 701	-0.000 038	(8,18)	3.657 214	-0.000 146
(4,8)	2.631 330	-0.000 041	(8,20)	3.784 572	-0.000 164
(4,16)	2.860 154	-0.000 049	(8,22)	3.931 909	-0.000 187
(4,20)	3.027 648	-0.000 057	(8,24)	4.104 186	-0.000 221
(4,24)	3.234 203	-0.000 070	(8,26)	4.309 703	-0.000 270
(4,25)	3.292 813	-0.000 074	(8,27)	4.429 208	-0.000 304
(4,32)	3.812 470	-0.000 129	(8,30)	4.898 319	-0.000 498
(4,35)	4.131 975	-0.000 188	(9,0)	3.305 393	-0.000 117
(5,0)	2.682 507	-0.000 049	(9,15)	3.701 654	-0.000 161
(5,11)	2.844 879	-0.000 056	(9,19)	3.950 716	-0.000 200
(5,14)	2.939 413	-0.000 061	(9,21)	4.108 018	-0.000 229
(5,17)	3.055 459	-0.000 067	(9,22)	4.197 201	-0.000 251
(5,18)	3.099 087	-0.000 069	(9,23)	4.294 849	-0.000 274
(5,20)	3.194 180	-0.000 076	(9,25)	4.522 223	-0.000 341
(5,23)	3.358 191	-0.000 088	(9,28)	4.992 186	-0.000 544
(5,26)	3.552 539	-0.000 107	(10,0)	3.489 073	-0.000 143
(5,28)	3.703 389	-0.000 124	(10,2)	3.499 654	-0.000 145
(5,34)	4.331 525	-0.000 251	(10,4)	3.524 382	-0.000 147
(6,0)	2.825 024	-0.000 062	(10,6)	3.563 374	-0.000 152
(6,4)	2.851 343	-0.000 064	(10,8)	3.616 872	-0.000 158

HD^+ continued

(v,N)	$\langle R\rangle_{\rm non-ad}/a_0$	$\langle\Delta R\rangle_{\rm non-ad}/a_0$	(v,N)	$\langle R\rangle_{\rm non-ad}/a_0$	$\langle\Delta R\rangle_{\rm non-ad}/a_0$
(10,14)	3.870 685	-0.000 196	(16,15)	6.592 800	-0.001 624
(10,16)	3.990 839	-0.000 216	(16,16)	6.943 544	-0.001 879
(10,18)	4.133 105	-0.000 245	(17,0)	5.611 218	-0.000 852
(10,20)	4.302 488	-0.000 285	(17,1)	5.622 210	-0.000 858
(10,22)	4.507 312	-0.000 343	(17,2)	5.644 376	-0.000 870
(10,24)	4.762 527	-0.000 435	(17,3)	5.678 086	-0.000 890
(10,26)	5.098 880	-0.000 599	(17,4)	5.723 936	-0.000 917
(11,0)	3.688 871	-0.000 177	(17,5)	5.782 788	-0.000 952
(11,3)	3.712 227	-0.000 180	(17,6)	5.855 847	-0.000 999
(11,5)	3.747 431	-0.000 185	(17,7)	5.944 780	-0.001 057
(11,7)	3.798 696	-0.000 193	(17,8)	6.051 894	-0.001 131
(11,10)	3.907 089	-0.000 211	(17,9)	6.180 442	-0.001 225
(11,13)	4.056 889	-0.000 238	(17,10)	6.335 135	-0.001 343
(11,20)	4.627 276	-0.000 389	(17,11)	6.523 102	-0.001 493
(11,25)	5.442 656	-0.000 815	(17,12)	6.755 851	-0.001 670
(12,0)	3.908 691	-0.000 220	(17,13)	7.053 959	-0.001 796
(12,2)	3.921 739	-0.000 222	(17,14)	7.461 617	-0.001 350
(12,4)	3.952 336	-0.000 228	(18,0)	6.227 343	-0.001 231
(12,6)	4.000 882	-0.000 237	(18,2)	6.273 792	-0.001 263
(12,8)	4.068 117	-0.000 250	(18,4)	6.386 776	-0.001 344
(12,16)	4.563 095	-0.000 375	(18,6)	6.579 367	-0.001 481
(12,23)	5.589 463	-0.000 905	(18,7)	6.713 424	-0.001 571
(13,0)	4.153 883	-0.000 277	(18,8)	6.880 131	-0.001 661
(13,3)	4.183 637	-0.000 284	(18,9)	7.089 141	-0.001 705
(13,5)	4.228 770	-0.000 294	(18,10)	7.356 929	-0.001 520
(13,7)	4.295 134	-0.000 309	(18,11)	7.715 746	-0.000 420
(13,15)	4.823 072	-0.000 472	(19,0)	7.098 863	-0.001 630
(13,21)	5.765 579	-0.001 020	(19,2)	7.712 759	-0.001 611
(14,0)	4.432 010	-0.000 354	(19,4)	7.357 593	-0.001 459
(14,2)	4.449 263	-0.000 359	(19,6)	7.692 743	-0.000 567
(14,4)	4.489 935	-0.000 370	(19,7)	7.945 539	0.000 896
(14,6)	4.555 110	-0.000 389	(19,8)	8.292 134	0.004 147
(14,8)	4.646 763	-0.000 417	(19,9)	8.814 074	0.008 533
(14,19)	5.980 515	-0.001 170	(20,0)	8.549 765	0.007 213
(14,20)	6.281 042	-0.001 477	(20,1)	8.600 817	0.007 878
(15,0)	4.754 204	-0.000 461	(20,2)	8.707 600	0.009 242
(15,3)	4.795 583	-0.000 475	(20,3)	8.881 359	0.011 198
(15,5)	4.859 019	-0.000 498	(20,4)	9.145 798	0.012 673
(15,7)	4.953 852	-0.000 534	(20,5)	9.557 298	0.007 515
(15,10)	5.165 308	-0.000 624	(20,6)	10.320 015	-0.047 758
(15,17)	6.248 575	-0.001 370	(21,0)	12.950 4	-0.310 9
(15,18)	6.567 867	-0.001 696	(21,1)	13.272 296	-0.366 0
(16,0)	5.137 716	-0.000 616	(21,2)	14.019 779	-0.509 9
(16,2)	5.163 213	-0.000 627	(21,3)	15.621 901	-0.971 0
(16,4)	5.223 892	-0.000 654	(22,0)	28.603	-2.351
(16,6)	5.322 897	-0.000 701	(22,1)	34.727 840	-6.560
(16,8)	5.466 165	-0.000 775			

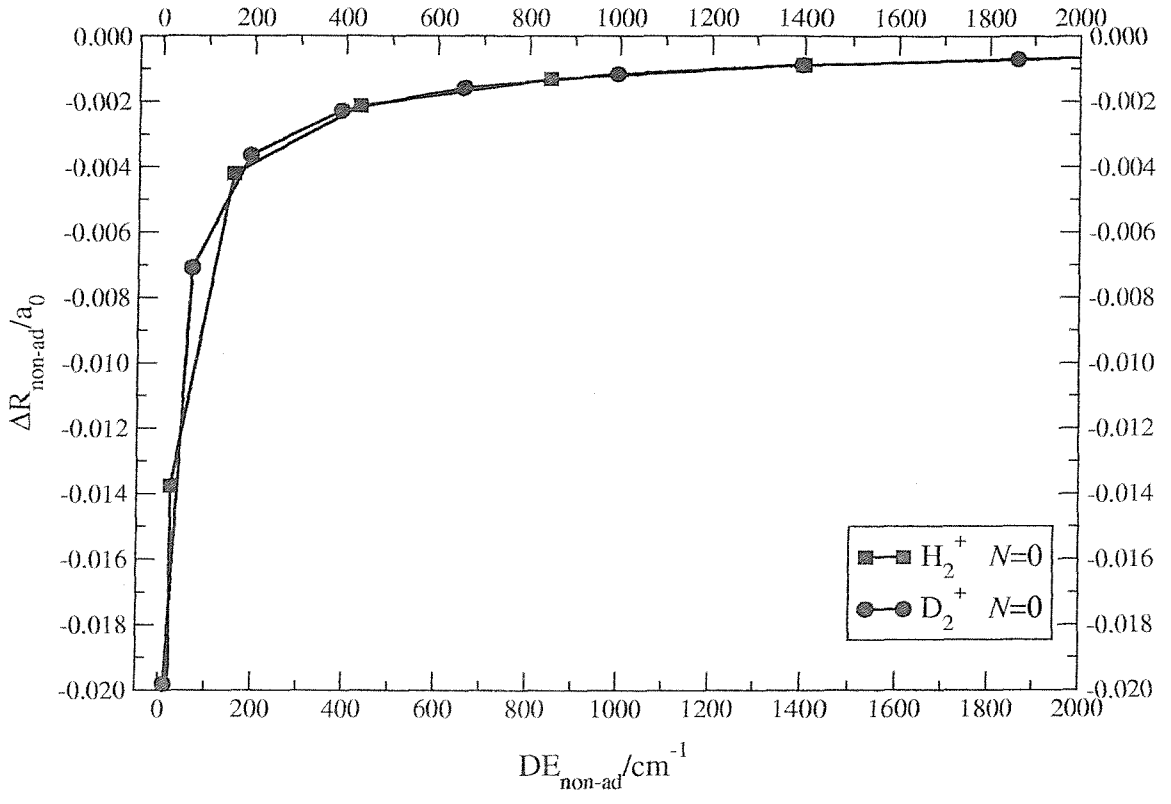

Figure 5.11: Non-adiabatic corrections (non-adiabatic − partitioned) for H_2^+ and D_2^+ to the bond length for N=0 against dissociation energies; a scaling factor of 2 to D_2^+ is applied.

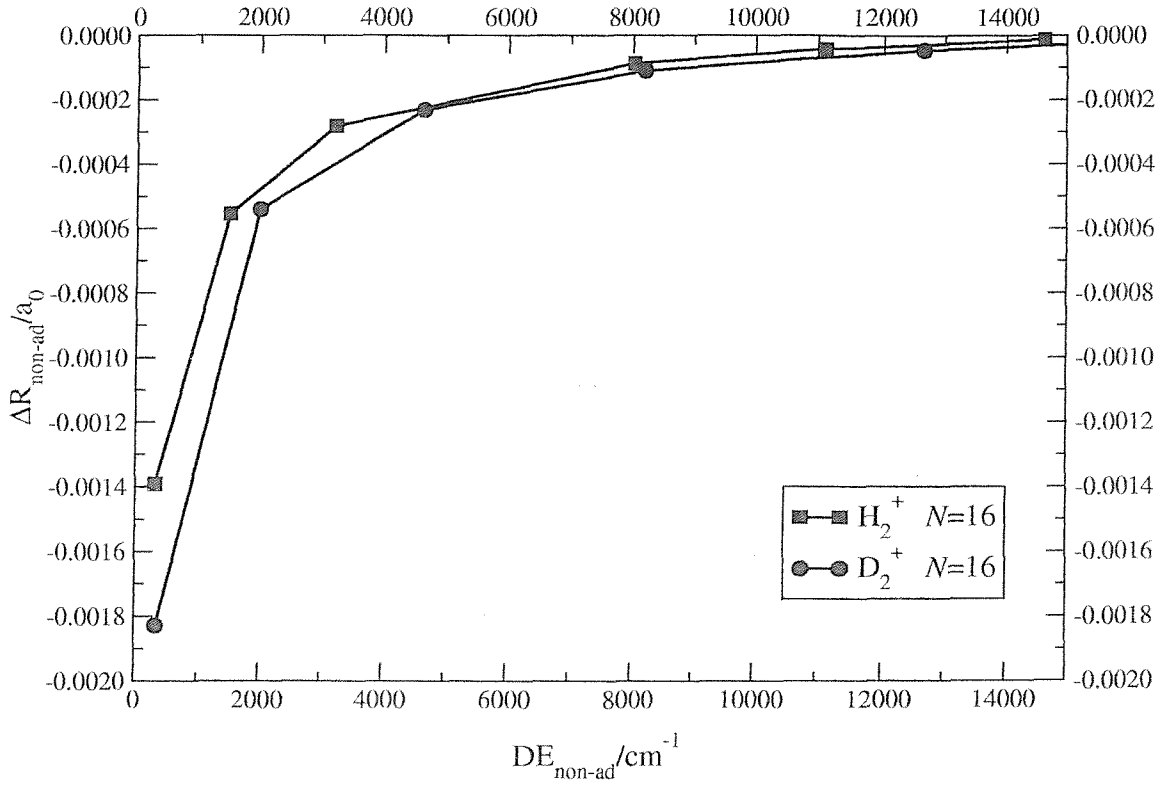

Figure 5.12: Non-adiabatic corrections (non-adiabatic − partitioned) for H_2^+ and D_2^+ to the bond length for N=16 against dissociation energies; a scaling factor of 2 to D_2^+ is applied.

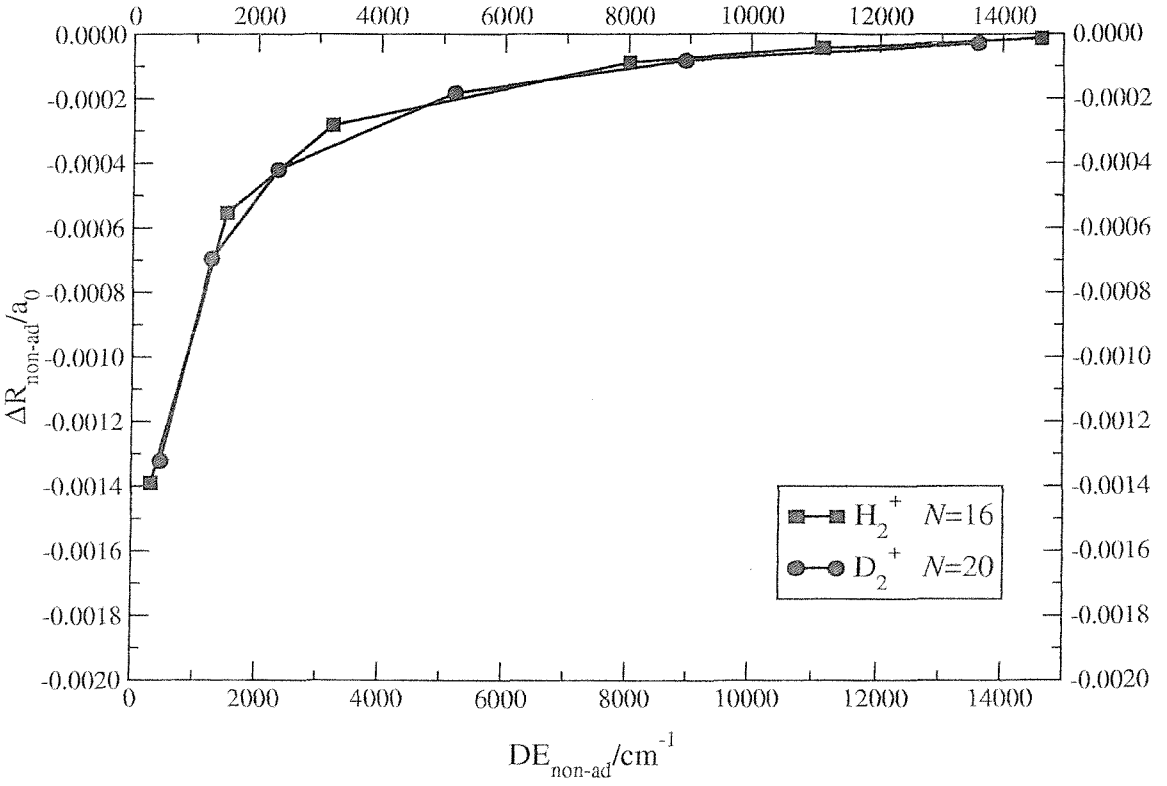

Figure 5.13: Non-adiabatic corrections (non-adiabatic − partitioned) for H_2^+ and D_2^+ to the bond length for N=16 and N=20 respectively against dissociation energies; a scaling factor of 2 to D_2^+ is applied.

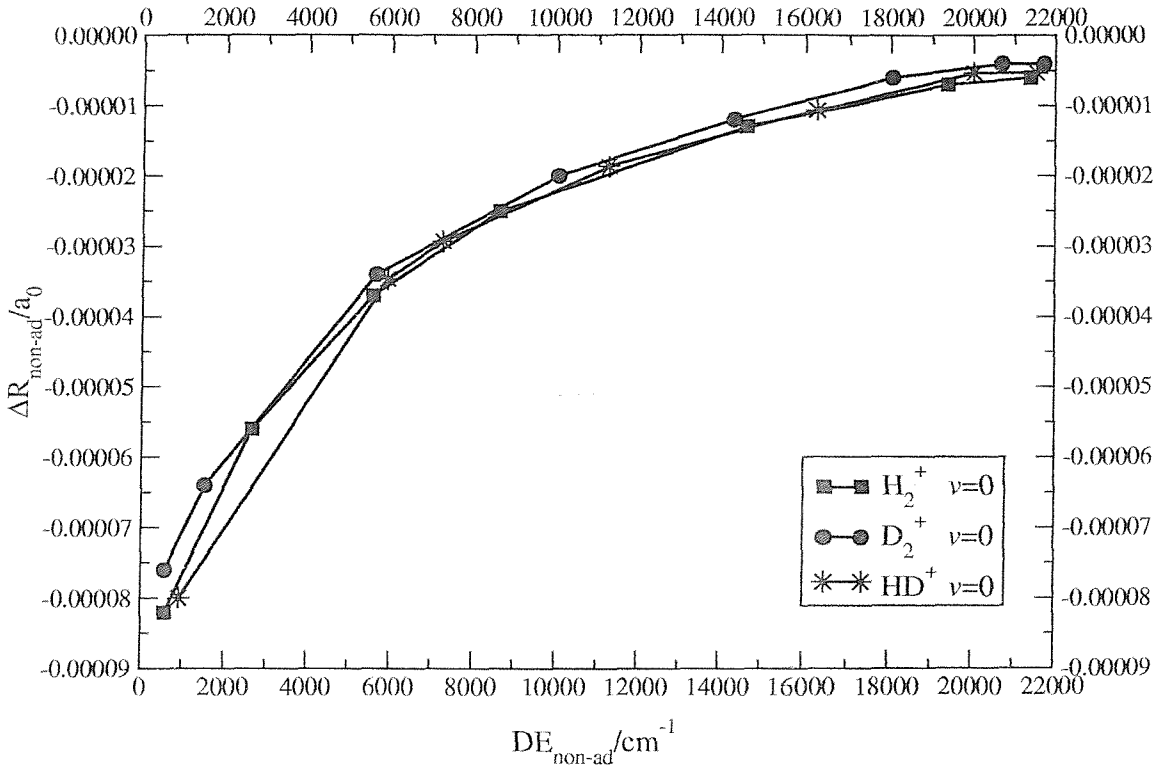

Figure 5.14: Non-adiabatic corrections (non-adiabatic − partitioned) for H_2^+ and D_2^+ and for HD^+ (non-adiabatic − transformed) to the bond length for v=0 against dissociation energies; a scaling factor of 2 to D_2^+ and of 4/3 to HD^+ is applied.

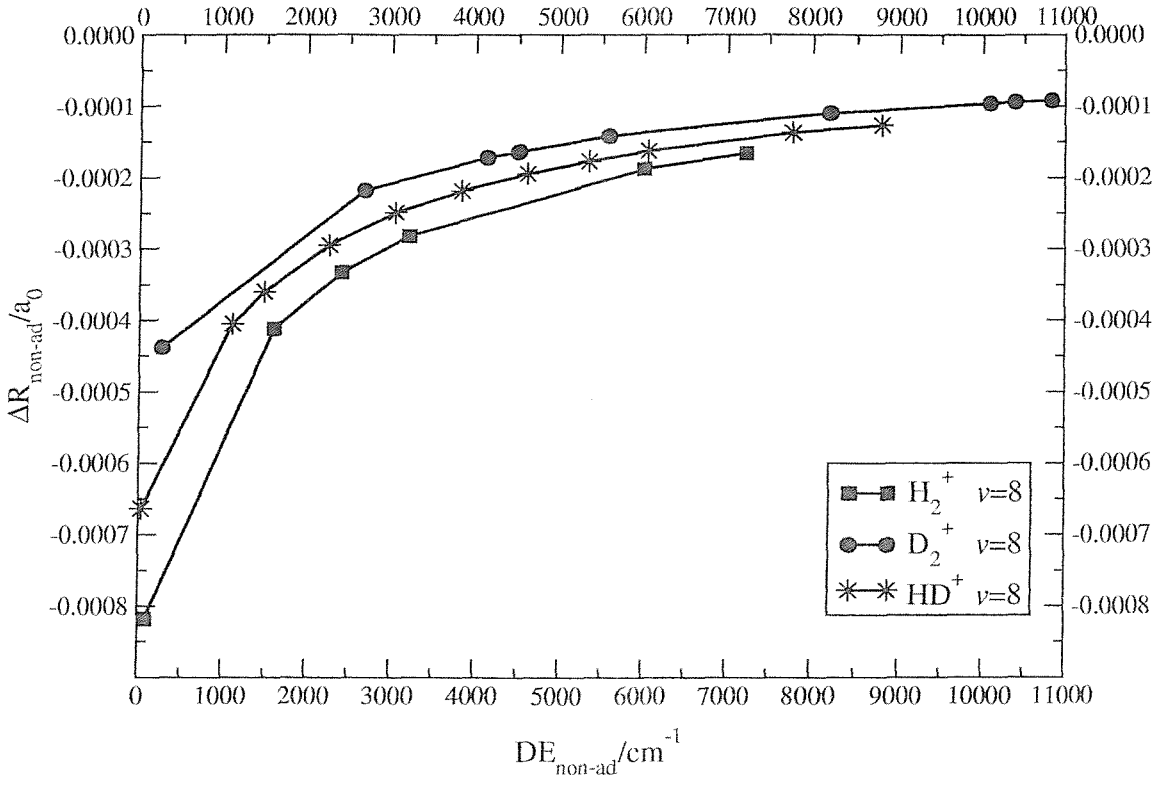

Figure 5.15: Non-adiabatic corrections (non-adiabatic – partitioned) for H_2^+ and D_2^+ and for HD^+ (non-adiabatic – transformed) to the bond length for v=8 against dissociation energies; a scaling factor of 2 to D_2^+ and of 4/3 to HD^+ is applied.

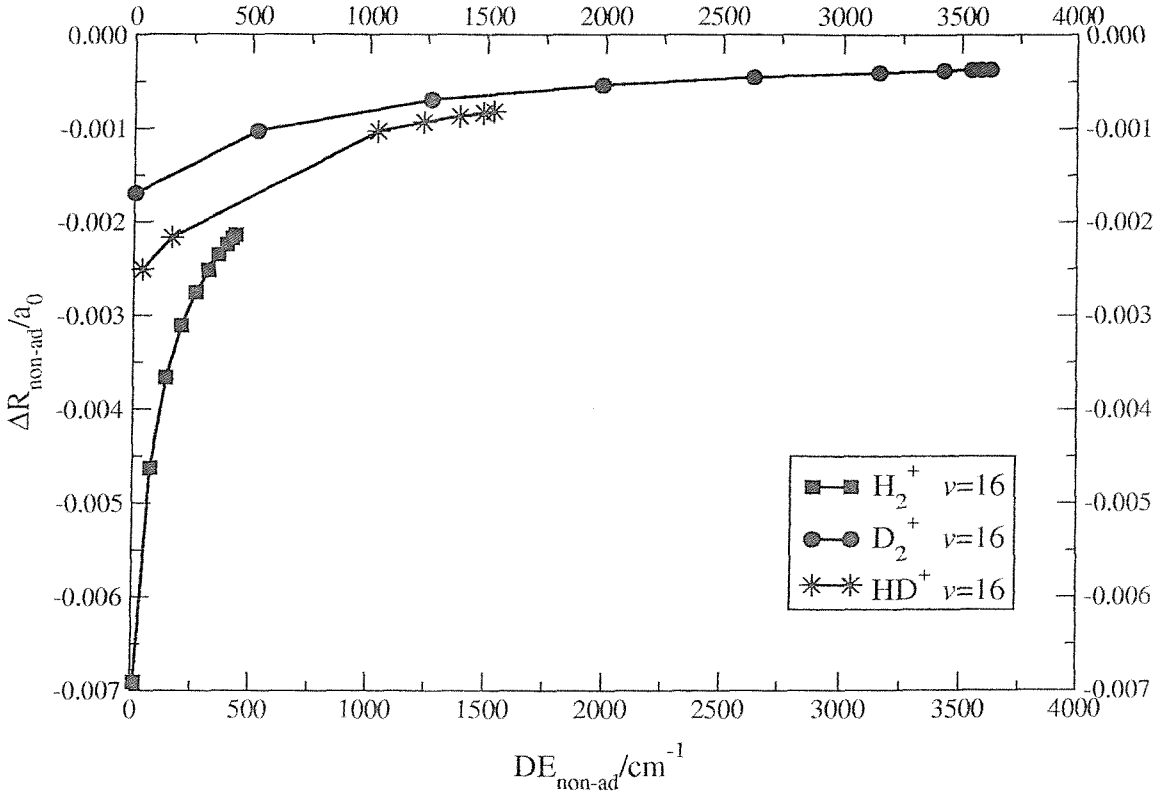

Figure 5.16: Non-adiabatic corrections (non-adiabatic − partitioned) for H_2^+ and D_2^+ and for HD^+ (non-adiabatic − transformed) to the bond length for v=16 against dissociation energies; a scaling factor of 2 to D_2^+ and of 4/3 to HD^+ is applied.

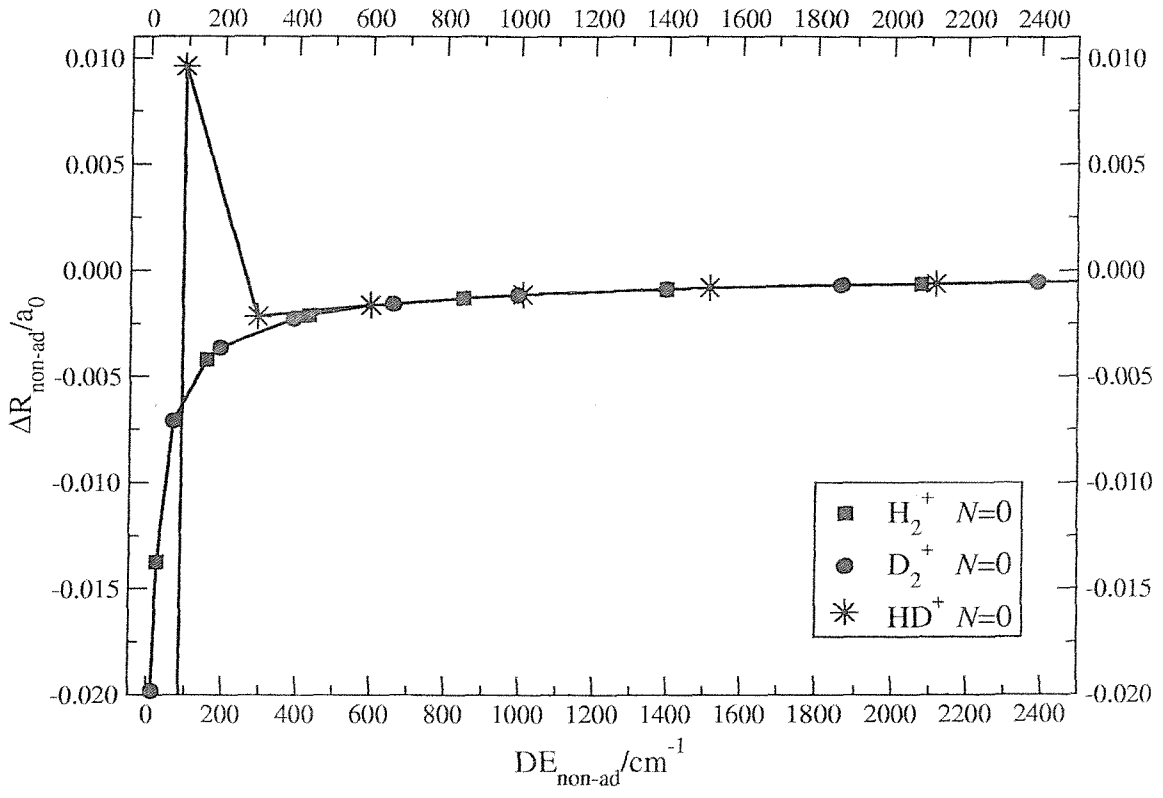

Figure 5.17: Non-adiabatic corrections (non-adiabatic − partitioned) for H_2^+ and D_2^+ and for HD^+ (non-adiabatic − transformed) to the bond length for N=0 against dissociation energies; a scaling factor of 2 to D_2^+ and of 4/3 to HD^+ is applied.

(v,N)	$\langle R\rangle_{\mathrm{non-ad}}/a_0$	$\langle \Delta R\rangle_{\mathrm{non-ad}}/a_0$
(17,12)	6.755 851	−0.001 670
(17,13)	7.053 956	−0.001 796
(17,14)	7.461 617	−0.001 350
(18,8)	6.880 131	−0.001 661
(18,9)	7.089 141	−0.001 705
(18,10)	7.356 929	−0.001 520
(18,11)	7.715 746	−0.000 420
(19,0)	7.098 863	−0.001 630
(19,1)	7.123 172	−0.001 626
(19,2)	7.172 759	−0.001 611
(19,3)	7.249 711	−0.001 568
(19,4)	7.357 593	−0.001 459
(19,5)	7.502 150	−0.001 194
(19,6)	7.692 743	−0.000 567
(19,7)	7.945 539	0.000 896
(19,8)	8.292 134	0.004 147
(19,9)	8.814 074	0.008 533
(20,0)	8.549 765	0.007 213
(20,1)	8.600 817	0.007 878
(20,2)	8.707 600	0.009 242
(20,3)	8.881 359	0.011 198
(20,4)	9.145 798	0.012 673
(20,5)	9.557 298	0.007 515
(20,6)	10.320 015	−0.047 758
(21,0)	12.950 4	−0.310 9
(21,1)	13.272 3	−0.366 0
(21,2)	14.019 8	−0.509 9
(21,3)	15.621 9	−0.971 0
(22,0)	28.603	−2.351
(22,1)	34.728	−6.560

Table 5.4: HD^+: selection from the results reported in table 5.3 of non-adiabatic bond lengths and non-adiabatic corrections (non-adiabatic − intermediate transformed adiabatic) for vibration-rotational levels of the ground electronic state. In general non-adiabatic corrections to the bond length are negative and increase in magnitude with the approach of dissociation. In this table the levels that do not follow this trend are reported.

5.4 Conclusions

It was reported previously [37] that the non-adiabatic correction to the bond length of HD^+ v=20, N=0 was anomalous. Further levels were found for HD^+ where the non-adiabatic corrections are anomalous, in that they do not lie on smooth curves predicted from the corrections for H_2^+ [32]. As explained in chapter 4, the anomaly occurs in the range of bond lengths where the g/u symmetry breaking correction arises.

In general corrections to the bond length are negative and increase in magnitude with v for given N or with N for given v. However this pattern is disrupted to the extent that for some levels the correction is positive. These levels have dissociation energies between 99.0 and 10.0 cm^{-1} and bond lengths between 7.9 and 9.6 a_0. If levels for which the corrections are negative but decrease in magnitude are included, then the dissociation energy range widens considerably to 270 cm^{-1} at the upper end, while the lower limit of the bond length range decreases to 7.4 a_0.

As noted in the previous chapter, it can be argued that the non-adiabatic corrections increase the dissociation energies for all the levels and, as a consequence, reduce the bond lengths as reported in this chapter.

Chapter 6

Results: non-adiabatic dissociation energies and non-adiabatic bond lengths for HT^+ and DT^+

6.1 Introduction

The content of the present chapter goes beyond the original aim of the project. Since Frolov [39, 40] recently published dissociation energies and other properties for the (v=0, N=0) level of the ground electronic states of T_2^+, HT^+ and DT^+, the idea to compare his results with those that can be obtained with the numerical approaches used in this work, arose. For this reason, non-adiabatic dissociation energies and non-adiabatic bond lengths are presented with the respective non-adiabatic corrections, for all the rotationless levels of the ground electronic states of HT^+ and DT^+. The procedure used is the same as that used for HD^+ and which is explained in detail in chapters 2 and 3.

The main objective is to confirm that the observed anomalous behaviour in the lighter isotopomer HD^+ (see chapters 4 and 5) also occured for HT^+ and DT^+. According to the reduced masses of the molecules, the anomaly might be expected to be larger for HT^+ than for HD^+, but smaller for DT^+.

The masses used for the nuclei are consistent with those used by Frolov. Even though Frolov referred to the masses reported in [41], the masses he used were m_p=1836.152701 m_e, m_d=3670.483014 m_e and m_t=5496.921580 m_e [35], the same as those used throughout this work.

6.2 Non-adiabatic dissociation energies for HT^+ and DT^+

The non-adiabatic dissociation energies and the non-adiabatic corrections to the dissociation energy for the three-body systems HT^+ and DT^+, which contain proton, deuterium and tritium nuclei, are here reported for all the rotationless levels of these heteronuclear diatomic molecules; that is the levels studied are $v = 0 - 23$, $N = 0$ for HT^+ and $v = 0 - 30$, $N = 0$ for DT^+.

A comparison with Frolov's available results [39, 40] is made for the level v=0, N=0 both with the variational and the scattering/transformed Hamiltonian approaches. The agreement between Frolov's results and these obtained with the calculation methods used in this work, is shown in table 6.1 for the (0,0) level of the ground electronic states of T_2^+, HT^+ and DT^+.

Cation	Frolov [39,40]	This work/variational	This work/scattering
T_2^+	-0.599 506 910 111 541 45	-0.599 506 910 112	-0.599 506 910 113
HT^+	-0.598 176 134 669 765 7	-0.598 176 134 669 7	-0.598 176 134 671 0
DT^+	-0.599 130 662 855 061 64	-0.599 130 662 855 0	-0.599 130 662 856 0

Table 6.1: Comparison between Frolov's results [39,40] and those obtained with the calculation methods used in this work for the non-adiabatic dissociation energy (in E_h) of the (0,0) level of the ground electronic states of T_2^+, HT^+ and DT^+.

Starting from these encouraging results, non-adiabatic dissociation energies for all the rotationless levels are calculated through the scattering/transformed Hamiltonian method; all the results are reported in table 6.2.

As for HD^+ in chapter 4, the behaviour of the non-adiabatic corrections to the dissociation energy for HT^+ and DT^+ is plotted against the vibrational quantum numbers in figure 6.1; in figure 6.2 the complete behaviour over the whole range of the dissociation energies is reported, while in figure 6.3 the particular of the anomaly is shown in the range of 0-800 cm^{-1}, that is for levels close to dissociation. Due to the ratio between the reduced masses of these two isotopomers of tritium, a scaling factor of 5/3 to DT^+ is applied.

HT^+	DE_{non-ad}/cm^{-1}	$\Delta DE_{non-ad}/cm^{-1}$	DT^+	DE_{non-ad}/cm^{-1}	$\Delta DE_{non-ad}/cm^{-1}$
(0,0)	21 567.130 68	0.059 51	(0,0)	21 776.625 40	0.029 40
(1,0)	19 757.930 95	0.170 35	(1,0)	20 331.243 26	0.085 07
(2,0)	18 034.448 22	0.273 16	(2,0)	18 939.994 18	0.137 56
(3,0)	16 394.247 37	0.368 26	(3,0)	17 601.610 58	0.186 97
(4,0)	14 835.190 96	0.455 82	(4,0)	16 314.943 45	0.233 39
(5,0)	13 355.431 10	0.535 94	(5,0)	15 078.959 25	0.276 88
(6,0)	11 953.404 04	0.608 62	(6,0)	13 892.737 46	0.317 46
(7,0)	10 627.827 72	0.673 69	(7,0)	12 755.468 96	0.355 14
(8,0)	9 377.702 38	0.730 90	(8,0)	11 666.454 96	0.389 88
(9,0)	8 202.314 23	0.779 82	(9,0)	10 625.106 82	0.421 64
(10,0)	7 101.242 55	0.819 88	(10,0)	9 630.946 46	0.450 19
(11,0)	6 074.370 57	0.850 32	(11,0)	8 683.607 64	0.475 82
(12,0)	5 121.900 54	0.870 17	(12,0)	7 782.838 07	0.497 94
(13,0)	4 244.373 63	0.878 27	(13,0)	6 928.502 38	0.516 50
(14,0)	3 442.695 32	0.873 16	(14,0)	6 120.586 06	0.531 23
(15,0)	2 718.167 26	0.853 20	(15,0)	5 359.200 56	0.541 83
(16,0)	2 072.526 10	0.816 45	(16,0)	4 644.589 48	0.547 94
(17,0)	1 507.989 66	0.760 77	(17,0)	3 977.136 19	0.549 16
(18,0)	1 027.307 99	0.684 02	(18,0)	3 357.372 85	0.544 99
(19,0)	633.809 48	0.585 24	(19,0)	2 785.991 21	0.534 92
(20,0)	331.408 98	0.474 27	(20,0)	2 263.854 95	0.513 00
(21,0)	124.521 46	0.515 44	(21,0)	1 792.013 94	0.494 51
(22,0)	19.606 85	1.181 20	(22,0)	1 371.719 37	0.462 77
(23,0)	1.739 41	0.257 56	(23,0)	1 004.438 50	0.422 33
			(24,0)	691.863 52	0.372 41
			(25,0)	435.899 86	0.312 39
			(26,0)	238.586 79	0.243 00
			(27,0)	101.777 11	0.187 46
			(28,0)	25.877 12	0.571 56
			(29,0)	4.491 47	1.071 68
			(30,0)	0.164 21	0.009 19

Table 6.2: HT^+ and DT^+: non-adiabatic dissociation energies and non-adiabatic corrections (non-adiabatic − intermediate transformed adiabatic) for the rotationless levels of the ground electronic states.

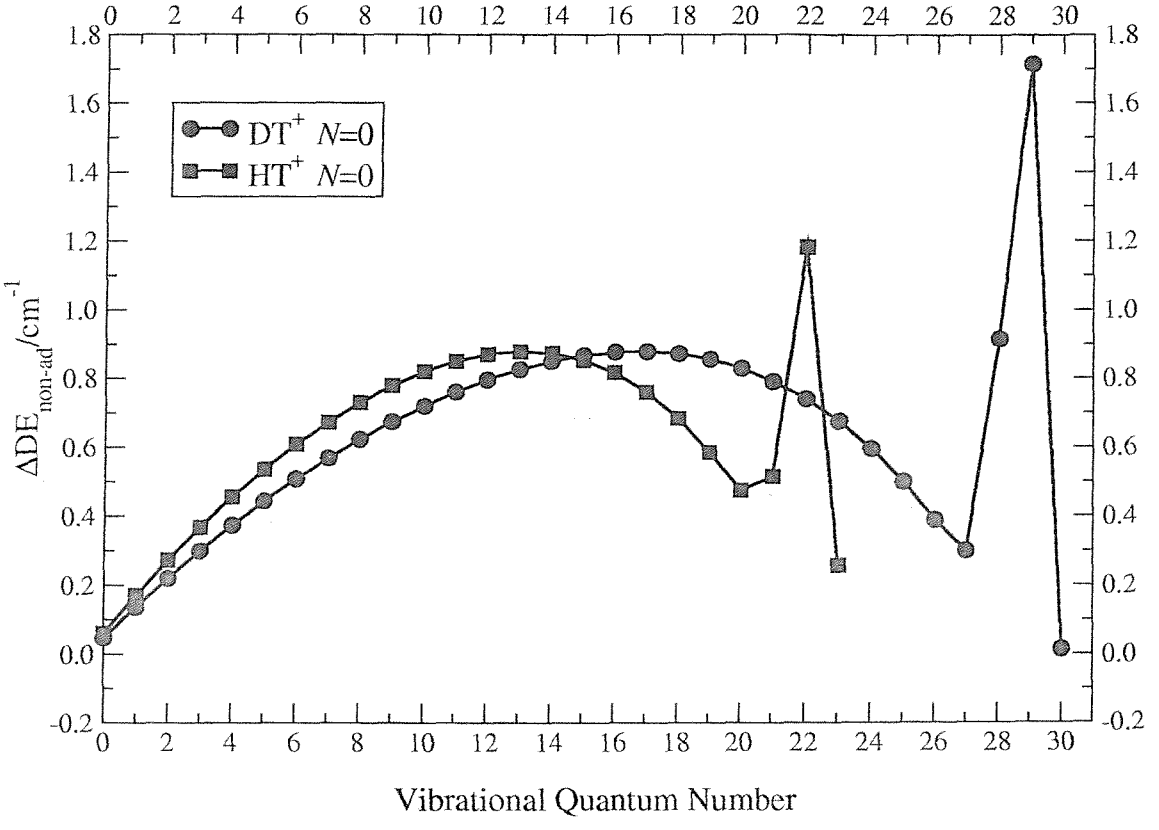

Figure 6.1: Non-adiabatic corrections (non-adiabatic − intermediate transformed hamiltonian) for HT^+ and DT^+ to the dissociation energy for $N = 0$ levels plotted against the vibrational quantum numbers; a scaling factor of 5/3 to DT^+ is applied.

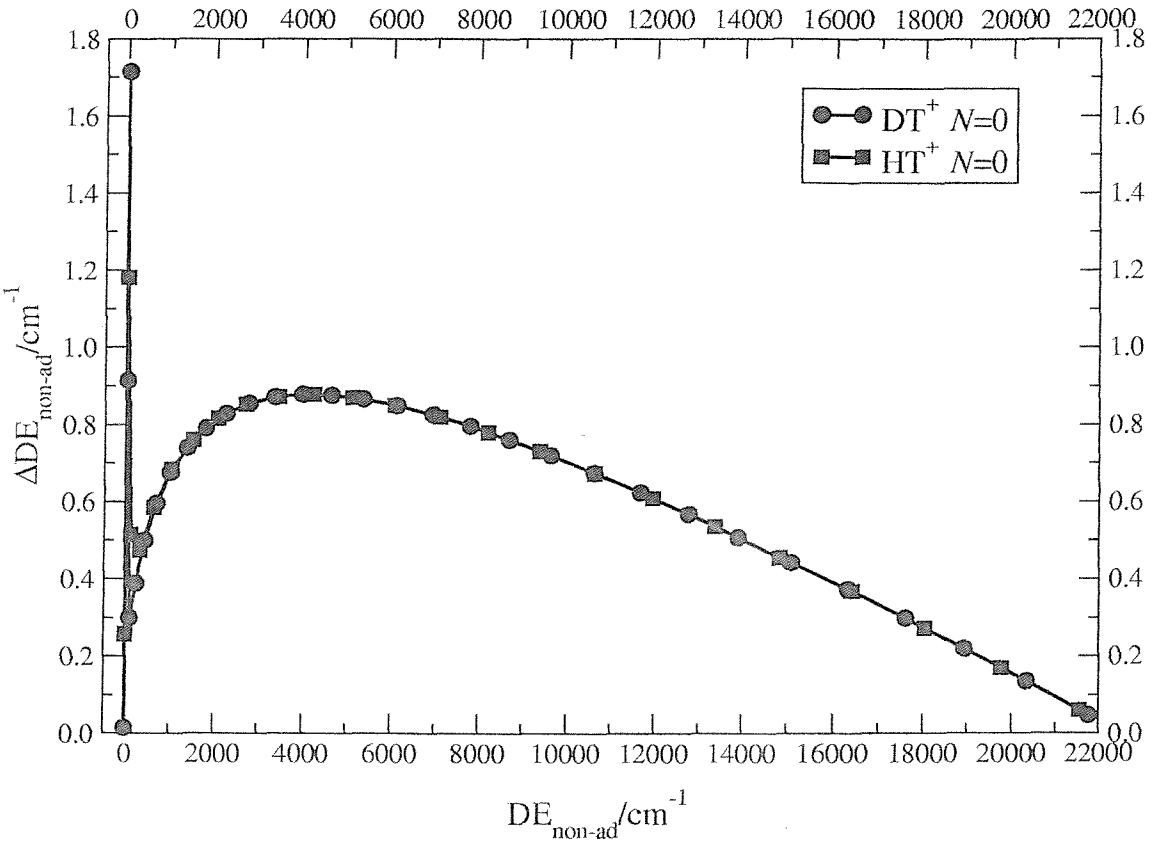

Figure 6.2: Non-adiabatic corrections (non-adiabatic − intermediate transformed hamiltonian) for HT^+ and DT^+ to the dissociation energy for $N = 0$ levels plotted against the non-adiabatic dissociation energies; a scaling factor of 5/3 to DT^+ is applied.

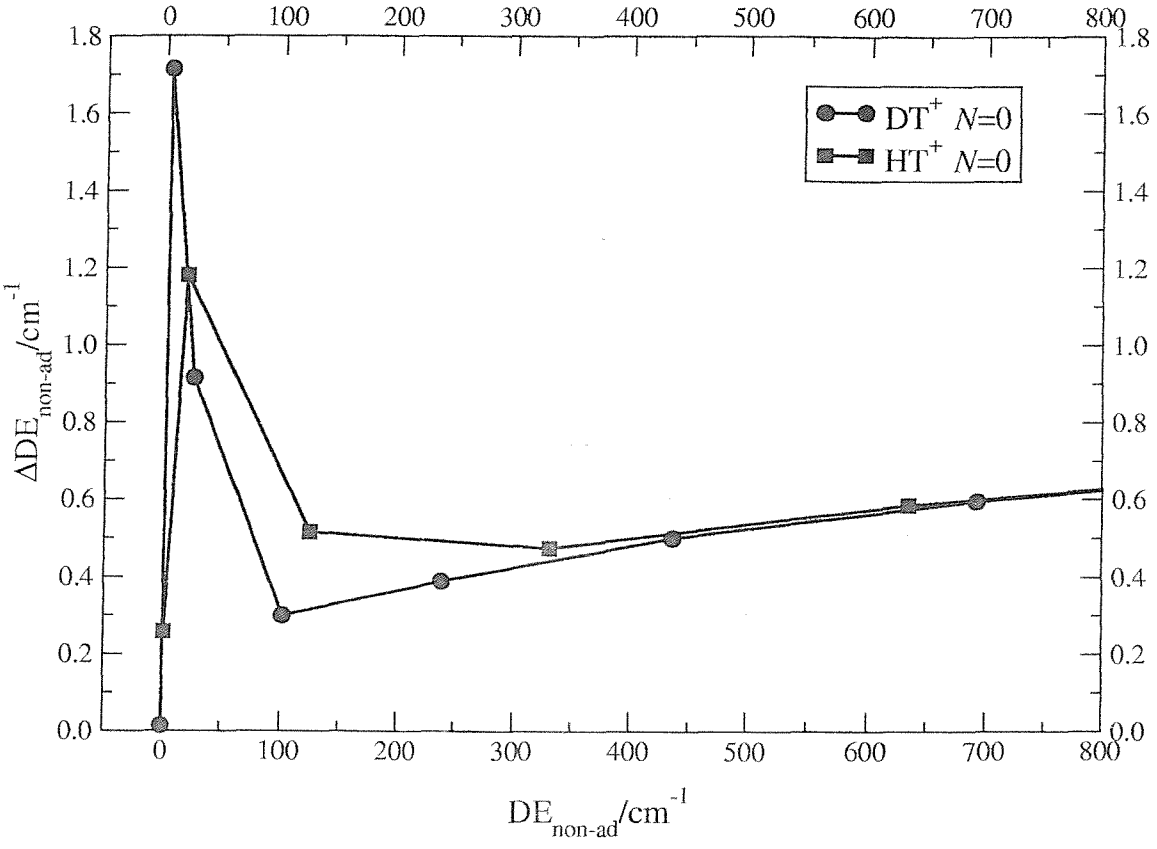

Figure 6.3: Details of the non-adiabatic corrections (non-adiabatic − intermediate transformed hamiltonian) in the range 0-800 cm^{-1} (levels close to dissociation) for HT^+ and DT^+ to the dissociation energy for $N = 0$ levels plotted against non-adiabatic dissociation energies; a scaling factor of 5/3 to DT^+ is applied.

6.3 Non-adiabatic bond lengths for HT^+ and DT^+

The non-adiabatic bond lengths and the non-adiabatic corrections to the bond length are also computed for the rotationless levels of HT^+ and DT^+.

The behaviour of the non-adiabatic corrections to the bond length against non-adiabatic dissociation energies is plotted in figure 6.4 for levels close to dissociation and all the results are reported in table 6.3.

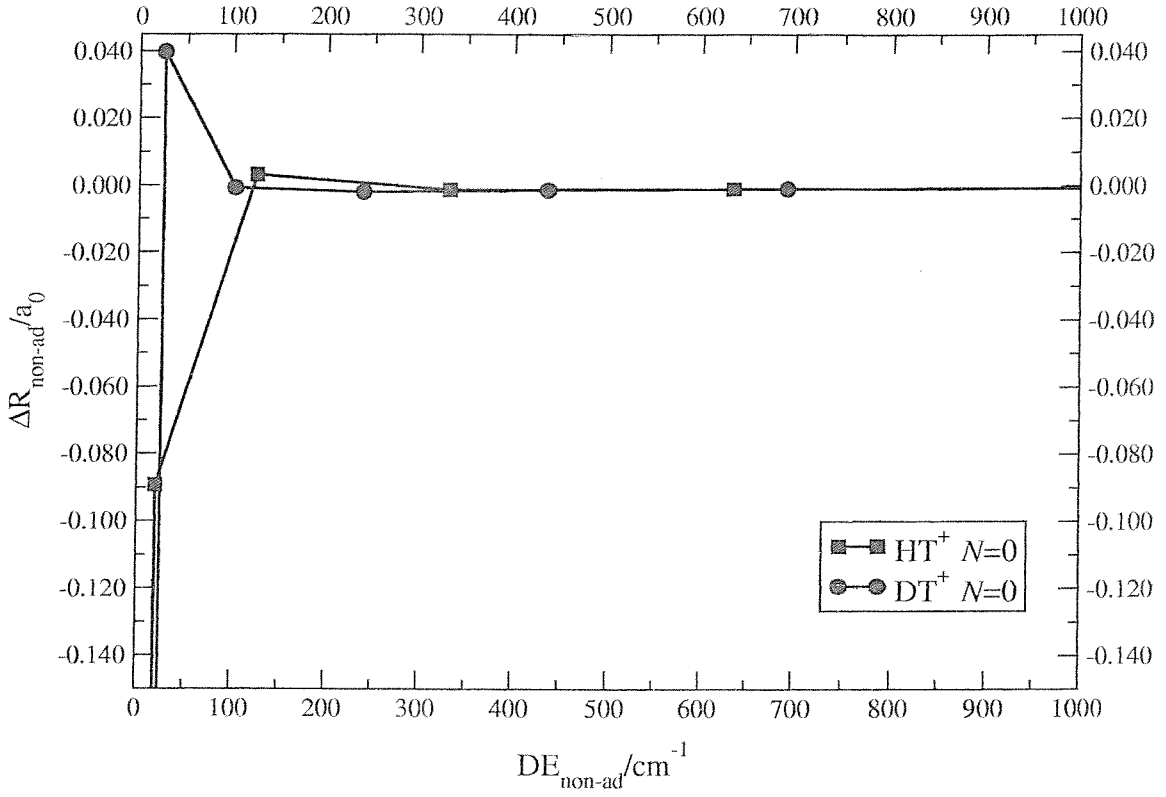

Figure 6.4: Non-adiabatic corrections (non-adiabatic − intermediate transformed hamiltonian) for HT^+ and DT^+ to the bond length for $N = 0$ levels close to dissociation plotted against non-adiabatic dissociation energies; a scaling factor of 5/3 to DT^+ is applied.

HT^+	$\langle R\rangle_{non-ad}/a_0$	$\langle \Delta R\rangle_{non-ad}/a_0$	DT^+	$\langle R\rangle_{non-ad}/a_0$	$\langle \Delta R\rangle_{non-ad}/a_0$
(0,0)	2.051 457	-0.000 003	(0,0)	2.039 939	-0.000 002
(1,0)	2.161 124	-0.000 010	(1,0)	2.126 124	-0.000 004
(2,0)	2.274 267	-0.000 017	(2,0)	2.214 406	-0.000 008
(3,0)	2.391 306	-0.000 023	(3,0)	2.304 981	-0.000 011
(4,0)	2.512 736	-0.000 031	(4,0)	2.398 069	-0.000 014
(5,0)	2.639 150	-0.000 041	(5,0)	2.493 921	-0.000 019
(6,0)	2.771 262	-0.000 051	(6,0)	2.592 829	-0.000 023
(7,0)	2.909 935	-0.000 063	(7,0)	2.695 127	-0.000 028
(8,0)	3.056 230	-0.000 076	(8,0)	2.801 205	-0.000 033
(9,0)	3.211 458	-0.000 093	(9,0)	2.911 519	-0.000 039
(10,0)	3.377 268	-0.000 112	(10,0)	3.026 603	-0.000 047
(11,0)	3.555 759	-0.000 137	(11,0)	3.147 094	-0.000 054
(12,0)	3.749 652	-0.000 168	(12,0)	3.273 748	-0.000 063
(13,0)	3.962 548	-0.000 206	(13,0)	3.407 478	-0.000 073
(14,0)	4.199 326	-0.000 257	(14,0)	3.549 394	-0.000 085
(15,0)	4.466 800	-0.000 325	(15,0)	3.700 863	-0.000 100
(16,0)	4.774 850	-0.000 416	(16,0)	3.863 587	-0.000 117
(17,0)	5.138 492	-0.000 547	(17,0)	4.039 717	-0.000 139
(18,0)	5.582 051	-0.000 742	(18,0)	4.232 024	-0.000 165
(19,0)	6.148 591	-0.001 039	(19,0)	4.444 139	-0.000 199
(20,0)	6.925 362	-0.001 339	(20,0)	4.680 948	-0.000 242
(21,0)	8.138 887	0.003 156	(21,0)	4.949 212	-0.000 299
(22,0)	11.111 55	-0.089 23	(22,0)	5.258 638	-0.000 374
(23,0)	19.757 66	-1.068 83	(23,0)	5.623 810	-0.000 479
			(24,0)	6.068 012	-0.000 632
			(25,0)	6.631 607	-0.000 872
			(26,0)	7.393 454	-0.001 255
			(27,0)	8.539 543	-0.000 476
			(28,0)	10.704 323	0.024 855
			(29,0)	15.794 60	-1.224 15
			(30,0)	26.535 2	-10.330 9

Table 6.3: HT^+ and DT^+: non-adiabatic bond lengths and non-adiabatic corrections (non-adiabatic − intermediate transformed adiabatic) for the rotationless levels of the ground electronic states.

6.4 Conclusions

In this chapter a study of the rotationless levels of the ground electronic state of HT^+ and DT^+ is reported. In particular the non-adiabatic corrections to the dissociation energy and to the bond length are studied; new results concerning these properties of these two diatomic species containing a nucleus of tritium are reported.

As expected from the results obtained for the heteronuclear molecule HD^+ (see chapters 4 and 5), HT^+ and DT^+ show similar anomalies for high vibrational levels. Near the dissociation limit, the dissociation energy corrections are expected to reduce in magnitude as v increases, but out of line are the levels $v = 21, N = 0$ and $v = 28, N = 0$ for HT^+ and DT^+ respectively; consistent with this observation, while in general corrections to the bond length are negative and increase in magnitude with v for given N or with N for given v, this pattern is not followed for the mentioned levels whose dissociation energies lie between 125.0 and 20 cm^{-1} for HT^+ and 26.0 and 4.5 cm^{-1} for DT^+. As expected from considerations concerning the reduced masses of the molecules, the anomaly is confirmed to be larger for HT^+ than for HD^+, but smaller for DT^+. In the case of HD^+ the range of the anomaly for the rotationless levels lies between 94.1 and 10.2 cm^{-1}, so for HT^+ the range is wider and shifted to higher values of the dissociation energy while for DT^+ the range is more narrow and shifted to lower dissociation energies.

In the case of the non-adiabatic bond lengths, the anomalies for the rotationless levels lie between 9.5 ans 13.0 a_0 for HD^+, 8.1 and 11.1 a_0 for HT^+ and 10.7 and 15.8 a_0 for DT^+.

Chapter 7

Results: non-adiabatic dipole polarizability for H_2^+, D_2^+ and HD^+

7.1 Introduction

In this chapter fully non-adiabatic calculations are reported of the electric dipole polarizabilities for the N=0 and N=1 levels of the ground electronic states of H_2^+ for $v \leq 16$, D_2^+ for $v \leq 24$ and HD^+ for $v \leq 20$.

During the last decade experiments and theoretical calculations have been developed for the determination of accurate results in particular for $H_2^+(0,0)$ and $D_2^+(0,0)$. While earlier theoretical calculations (see for example [42–44]) agreed with experiments, recently with the increase in experimental accuracy, the agreement with theory has been removed [45].

While experimental results on HD^+ are still missing, theoretical results are reported in this chapter. After a review about previous experimental and theoretical works, the theory concerning non-adiabatic calculations of the electric dipole polarizability is explained and new non-adiabatic results reported and commented [46].

7.2 The dipole polarizability: a brief review of previous studies

Analysis of microwave spectra of Rydberg states of the hydrogen molecular cations has provided experimental values of molecular properties and in particular Lundeen *et al.* have determined electric dipole polarizabilities [45, 47–49]. An early determination of this property for $H_2^+(0,1)$ [47] was followed by more precise values for $H_2^+(0,0)$ and $D_2^+(0,0)$ [48, 49], and yet more recently by even better results for these (0,0) levels [45].

Earlier theoretical calculations [50] using a clamped nuclei approximation did not agree with experiment for $H_2^+(0,0)$ and it was emphasized by Lundeen that, in particular, non-adiabatic effects needed to be accounted for in *ab initio* calculations. Fully non-adiabatic calculations, that were not inconsistent with experiment at the time, used a finite element method [42], a localized variational method [43] and a variational method [44]. A quasi-non-adiabatic treatment [51], in which the breakdown of the Born-Oppenheimer approximation due to vibration is accounted for, but in which rotation is averaged classically, also gave agreement with experiment, although in retrospect [52] this agreement was shown to be due to neglect of third-order effects, involving the coupling of electronic and rotational angular momenta, compensating for the use of classical rotational averaging; that is when quantum mechanical averaging of rotation is employed, agreement with experiment was only achieved when third-order effects were included [52], the importance of this being realised also by Taylor *et al.* [44]. Further support for the current theoretical result comes from recent work on two-photon transition probabilities [53].

However, the recent experimental results for $H_2^+(0,0)$ [45] have removed the agreement with theory, although the less precise determination for $D_2^+(0,0)$ is still consistent. An estimate of the relativistic effects for $H_2^+(0,0)$ [54] could only explain about one fifth of the remaining discrepancy. Another possibility is that fourth-order effects may contribute, although there was no evidence for them in a calculation for the $H_2^+(0,1)$ level [55], where these were implicitly included.

The electric dipole polarizability of the heteronuclear hydrogen molecular cation HD^+

poses new problems, since electronic g/u symmetry breaking due to the mass asymmetry removes the simplification that the electric dipole moment operator only connects states of opposite g/u parity. In particular HD^+ has a significant permanent electric dipole moment even in the Born-Oppenheimer approximation [56]. Bhatia and Drachman [57] appear to be the only authors to have attempted a calculation. They employed their localized variational method to determine accurate wavefunctions for excited states as well as the ground state, and used these in conventional second-order perturbation theory.

7.3 Theory

7.3.1 The transformed electric field perturbation operator

As already seen in the case of the non-adiabatic bond lengths (see chapter 5), properties may be extracted from accurate energies determined with the Hamiltonian for the molecule perturbed with an appropriate operator (see section 3.4).

The dipole polarizability arises when an external electric field is applied and this mixes different electronic states. The additional term in the most general case of the Hamiltonian of HD^+ is

$$H' = \lambda \boldsymbol{n} \cdot \left[\frac{(m_2 - m_1)}{2(m_2 + m_1 + 1)} \boldsymbol{R} + \frac{(m_2 + m_2 + 2)}{(m_2 + m_p + 1)} \boldsymbol{r}_{\mathrm{g}} \right] \tag{7.1}$$

where the perturbation parameter λ is the magnitude of the electric field and $\boldsymbol{n}$ is the unit vector in its direction; $\boldsymbol{R}$ is the internuclear separation and $\boldsymbol{r}_{\mathrm{g}}$ is the position of the electron relative to the geometric centre of the nuclei. Note that the first term in equation (7.1) vanishes for the homonuclear species H_2^+ and D_2^+. The perturbation changes the energy E_0 for a level to

$$E = E_0 - \mu\lambda - \frac{1}{2}\alpha\lambda^2 - \frac{1}{6}\beta\lambda^3 - \frac{1}{24}\gamma\lambda^4 + \mathcal{O}(\lambda^5). \tag{7.2}$$

From equation (7.2), if the dipole moment μ and the first hyperpolarizability β vanish,

then linear regression of $(E - E_0)/\lambda^2$ on λ^2 gives a determination of the electric dipole polarizability as the intercept, together with an estimate of the second hyperpolarizability γ; this is the situation for both H_2^+ and D_2^+ and also for HD^+, if molecular rotation is averaged quantum mechanically, as will be explained. As in the case of the bond lengths, the values of the parameter λ are chosen so that the correlation coefficient determined in the linear regression is very close to ± 1; the standard deviations obtained give an indication of how many figures are justified in the results.

The same calculation methods used to study the non-adiabatic bond lengths are applied in the case of the dipole polarizability. If the variational method is used, the perturbation operator is as given in equation (7.1). On the other hand, if a transformed Hamiltonian is used, the perturbation must undergo the same transformation; as already explained, the transformation is introduced in two stages, the first relevant only to the heteronuclear molecule HD^+, dealing with the mass asymmetry.

For H_2^+ and D_2^+ the transformation of operators including (7.1), is straightforward since only the second part of the transformation is relevant. Even for HD^+ the molecular properties considered up until now (*i.e.* bond lengths) have not presented any difficulty, since they only involve internal coordinates, namely functions of the bond length and the expectation value of r_Z, the component of the electron position along the internuclear axis.

In the case of the dipole polarizability, things change since now the external electric field defines a space-fixed axis, so that perturbation (7.1) implicity contains angular coordinates. The first part of the transformation, which is only relevant to HD^+, involves derivatives with respect to these angular coordinates in addition to the internal coordinates. If the electric field is along the Z space-fixed axis, then perturbation operator (7.1) may be abbreviated to

$$H' = -\lambda(AR_Z + Br_Z) \tag{7.3}$$

where

$$A = \frac{-(m_2 - m_1)}{2(m_2 + m_1 + 1)}, \tag{7.4}$$

$$B = \frac{(m_2 + m_1 + 2)}{(m_2 + m_1 + 1)} \tag{7.5}$$

and

$$\mu_Z = AR_Z + Br_Z \tag{7.6}$$

is the Z-component of the electric dipole moment of the molecule. After the intermediate transformation, the new expression for the perturbed term of the Hamiltonian is

$$H'_{\rm int} = -\lambda\left[(AR_Z + Br_Z)\cosh\frac{\omega}{2} + 2(Ar_Z + \frac{1}{4}BR_Z)\sinh\frac{\omega}{2}\right] = -\lambda\mu'_Z. \tag{7.7}$$

The hyperbolic functions may now be expressed in terms of the effective nuclear charges Z_1 and Z_2 through equations (2.109) and (2.110) which lead to

$$\cosh\frac{\omega}{2} = \frac{1}{2}(Z_1 + Z_2) \tag{7.8}$$

and

$$\sinh\frac{\omega}{2} = \frac{1}{2}(Z_2 - Z_1). \tag{7.9}$$

The second part of the transformation results only in the introduction of the multiplicative factor $\rho^{-1/2}$ [23], so that finally the transformed perturbation for HD^+ is

$$H'_{\rm t} = -\lambda\rho^{-1/2}\left[\frac{1}{2}(Z_1 + Z_2)(AR_Z + Br_Z) + (Z_2 - Z_1)(Ar_Z + \frac{1}{4}BR_Z)\right] = -\lambda\mu''_Z \tag{7.10}$$

where

$$\rho = 1 + \frac{1}{(4\mu_{\rm eff} + 1)}(\xi^2 + \eta^2 - 1) \tag{7.11}$$

and

$$\frac{1}{\mu_{\rm eff}} = \frac{1}{\mu_{\rm a}}(p^2 - 1)^{1/2} - 2 \approx \frac{1}{\mu}, \tag{7.12}$$

with p as indicated in (2.100).

7.3.2 Matrix elements

For determining matrix elements, the coordinates R, ξ, η, θ and χ may be reintroduced

$$R_Z = R\cos\theta, \tag{7.13}$$

$$r_Z = \frac{1}{2}R\{\xi\eta\cos\theta - \sqrt{(\xi^2-1)(1-\eta^2)}\sin\theta\cos\chi\}. \tag{7.14}$$

All the matrix elements needed may be evaluated analytically, provided that $\rho^{-1/2}$ in equation (7.10) is expanded as a power series in $1/\mu$ and $1/\mu_a$.

As emphasized in [52], when third- and higher-order contributions to the polarizability are included and the relevant matrix elements arise from different parts of the total Hamiltonian, it is most important to use a consistent policy for the angular functions involved. In particular, care must be taken to use the correct relative signs of the matrix elements arising from the electric field perturbation and the term in the unperturbed Hamiltonian that couples rotational and electronic angular momenta. Here the matrix elements of [4,6], which were taken from [12], are used for the zeroth-order Hamiltonian. The angular parts of these matrix elements are determined using the definitions and relationships of Kolos and Wolniewicz [58], and accordingly for consistency they are also used here for the perturbation.

The angular matrix elements depend on Λ, N and M. Λ is the electronic angular momentum quantum number and takes on the value 0 for Σ states and ±1 for Π states; Δ and other states with $\Lambda > 1$ are ignored. N is the total angular momentum quantum number, while M refers to its projection along the space fixed Z axis and is a good quantum number. In this work only levels with $N = 0$, 1 are studied, so the only values of M needed are 0, ±1. The relevant matrix elements are given below; note that $N = 0$ is only possible for Σ ($\Lambda = 0$) states.

For $M = 0$,

$$\langle \Lambda = 0, N = 0|\cos\theta|\Lambda = 0, N = 1\rangle = -\frac{1}{\sqrt{3}}, \tag{7.15}$$

$$\langle \Lambda = 0, N = 1|\cos\theta|\Lambda = 0, N = 2\rangle = -\frac{2}{\sqrt{15}}, \tag{7.16}$$

$$\langle \Lambda = \pm1, N = 1|\cos\theta|\Lambda = \pm1, N = 2\rangle = -\frac{1}{\sqrt{5}}, \tag{7.17}$$

$$\langle \Lambda = 0, N = 0| - \sin\theta\cos\chi|\Lambda = \pm 1, N = 1\rangle = \mp\frac{1}{\sqrt{6}}, \tag{7.18}$$

$$\langle \Lambda = 0, N = 1| - \sin\theta\cos\chi|\Lambda = \pm 1, N = 2\rangle = \mp\frac{1}{\sqrt{10}}, \tag{7.19}$$

$$\langle \Lambda = 0, N = 2| - \sin\theta\cos\chi|\Lambda = \pm 1, N = 1\rangle = \pm\frac{1}{\sqrt{30}}, \tag{7.20}$$

while for $M = \pm 1$,

$$\langle \Lambda = 0, N = 1|\cos\theta|\Lambda = 0, N = 2\rangle = -\frac{1}{\sqrt{5}}, \tag{7.21}$$

$$\langle \Lambda = \pm 1, N = 1|\cos\theta|\Lambda = \pm 1, N = 2\rangle = -\frac{\sqrt{3}}{2\sqrt{5}}, \tag{7.22}$$

$$\langle \Lambda = 0, N = 1| - \sin\theta\cos\chi|\Lambda = \pm 1, N = 2\rangle = \mp\frac{\sqrt{3}}{2\sqrt{10}}, \tag{7.23}$$

$$\langle \Lambda = 0, N = 2| - \sin\theta\cos\chi|\Lambda = \pm 1, N = 1\rangle = \pm\frac{1}{2\sqrt{10}}. \tag{7.24}$$

Finally for $M = +1$,

$$\langle \Lambda = \pm 1, N = 1|\cos\theta|\Lambda = \pm 1, N = 1\rangle = \pm\frac{1}{2}, \tag{7.25}$$

$$\langle \Lambda = \pm 1, N = 2|\cos\theta|\Lambda = \pm 1, N = 2\rangle = \pm\frac{1}{6}, \tag{7.26}$$

$$\langle \Lambda = 0, N = 1| - \sin\theta\cos\chi|\Lambda = \pm 1, N = 1\rangle = \mp\frac{1}{2\sqrt{2}}, \tag{7.27}$$

$$\langle \Lambda = 0, N = 2| - \sin\theta\cos\chi|\Lambda = \pm 1, N = 2\rangle = \mp\frac{1}{2\sqrt{6}}. \tag{7.28}$$

For $M = -1$ the right hand sides of the last three matrix elements should be multiplied by -1. In an electric field the energy depends only on $|M|$, so that separate calculations are not needed for $M = +1$ and $M = -1$, although they provide an indication of computational rounding errors.

7.3.3 Quasi-non-adiabatic calculations

Although quasi-non-adiabatic calculations have now been superseded for H_2^+ and D_2^+, it is nevertheless instructive to report results for HD^+, particularly as it will be seen that quasi-non-adiabatic and fully non-adiabatic results are dramatically different. When classical averaging of rotation is used, as in the quasi-non-adiabatic treatment, the dipole polarizability is given in terms of the parallel and perpendicular components by

$$\alpha = \frac{1}{3}(\alpha_{\|} + 2\alpha_{\perp}) \tag{7.29}$$

where, according to the second-order term of a perturbation theory

$$\alpha_{\|} = -\frac{2}{3}\sum_{\Sigma_u^+} \frac{|\langle \Sigma_g^+, N=0|\mu_z|\Sigma_u^+, N=0\rangle|^2}{E(\Sigma_g^+, N=0) - E(\Sigma_u^+, N=0)} \tag{7.30}$$

and

$$\alpha_{\perp} = -\frac{2}{3}\sum_{\Pi_u} \frac{|\langle \Sigma_g^+, N=0|\mu_x|\Pi_u, N=0\rangle|^2}{E(\Sigma_g^+, N=0) - E(\Pi_u, N=0)}. \tag{7.31}$$

In equations (7.30) and (7.31) μ_z and μ_x are the components of the electric dipole moment in the molecule-fixed frame system, the factor -2 arises from the definition of polarizability and the 1/3 is from the rotational averaging. The parallel component is found by assuming the electric field lies along the internuclear space-fixed axis Z, while for the perpendicular component the field is perpendicular to the axis. In these calculations the coupling between levels does not depend on the rotational quantum numbers N and M, even to the extent that for $\alpha_{\perp}$ of (0,0) levels coupling to Π states with $N = 0$ is implicit, even though $N = 0$ is not allowed for Π states.

Note that for HD^+ the determination of $\alpha_{\|}$ is less precise, since the electric dipole moment along the internuclear axis is non-zero, so that in using equation (7.2) allowance must be made by regressing $(E - E_0)/\lambda$ on λ and extracting $\alpha_{\|}$ as a slope. This does not apply to $\alpha_{\perp}$, which may be determined as an intercept, just as for both components in the homonuclear ions and for α in fully non-adiabatic calculations.

7.3.4 Fully non-adiabatic calculations

In a fully non-adiabatic calculation the rotation is averaged quantum mechanically, so that even though the mass asymmetry in HD^+ is responsible for a charge asymmetry, the expectation values of the electric dipole moment and the first hyperpolarizability vanish and, just as for the homonuclear ions, regression of $(E - E_0)/\lambda^2$ on λ^2 gives the polarizability α from the intercept and the second hyperpolarizability γ from the slope.

Equations formally similar to (7.30) and (7.31) for a quasi-non-adiabatic approximation can be written in the case of a second-order fully non-adiabatic approach as

$$\alpha_{\parallel} = -\frac{2}{3}\sum_{\Sigma_u^+} \frac{|\langle \Sigma_g^+, N=0|\mu_Z|\Sigma_u^+, N=1\rangle|^2}{E(\Sigma_g^+, N=0) - E(\Sigma_u^+, N=1)} \tag{7.32}$$

and

$$\alpha_{\perp} = -\frac{2}{3}\sum_{\Pi_u} \frac{|\langle \Sigma_g^+, N=0|\mu_Z|\Pi_u, N=1\rangle|^2}{E(\Sigma_g^+, N=0) - E(\Pi_u, N=1)}. \tag{7.33}$$

In (7.32) and (7.33) μ_Z is the component of the electric dipole moment in the space-fixed frame system (see equation (7.6)). The other difference with respect to the equations for the quasi-non-adiabatic approximation is that now the averaging is between $N = 0$ and $N = 1$ levels. This makes the denominator larger and the contribution to the dipole polarizability smaller in both the components.

For homonuclear ions in the absence of an electric field the total angular momentum N is a good quantum number and in the absence of nuclear spin states may be labelled g or u. Coupling of rotational and electronic angular momenta occurs between Σ and Π states for levels of the same $N \geq 1$ and the same g/u electronic parity. An electric field mixes states with N differing by 1 and also mixes g and u electronic states, so that in studying a g state of an homonuclear ion only u basis functions with N differing by 1 need to be considered and this is illustrated in figures 7.1, 7.2 and 7.3.

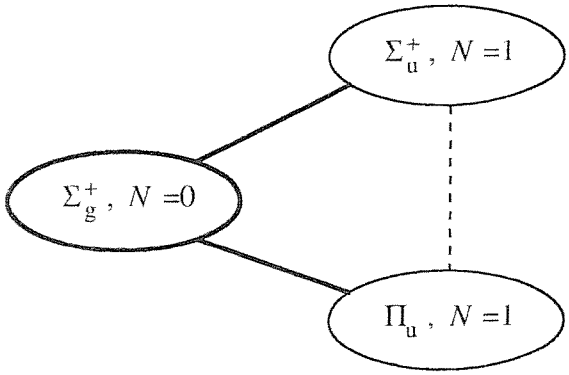

Figure 7.1: The relevant couplings in calculations of the dipole polarizability of the (0,0) ($M = 0$) level of the ground electronic states of H_2^+ and D_2^+: thick lines indicate the major, second-order contributions; the dashed lines represent the interaction of electronic and rotational angular momenta.

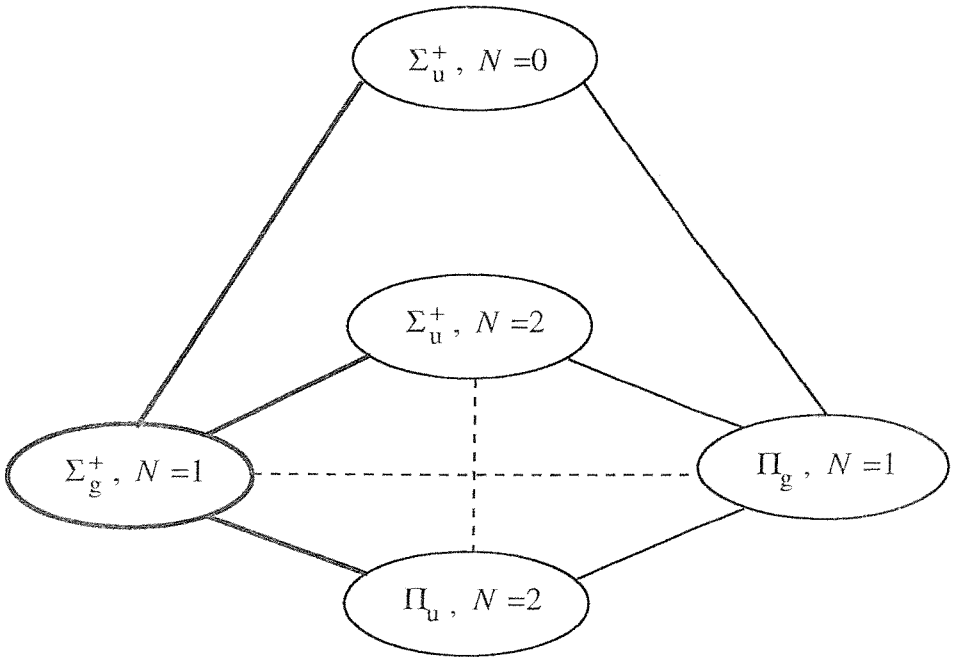

Figure 7.2: The relevant couplings in calculations of the dipole polarizability the (0,1) ($M = 0$) level of the ground electronic states of H_2^+ and D_2^+: full lines represent the electric field perturbation; thick lines indicate the major, second-order contributions; thinner lines are for couplings involved third- and higher-order interactions; the dashed lines represent the interaction of electronic and rotational angular momenta.

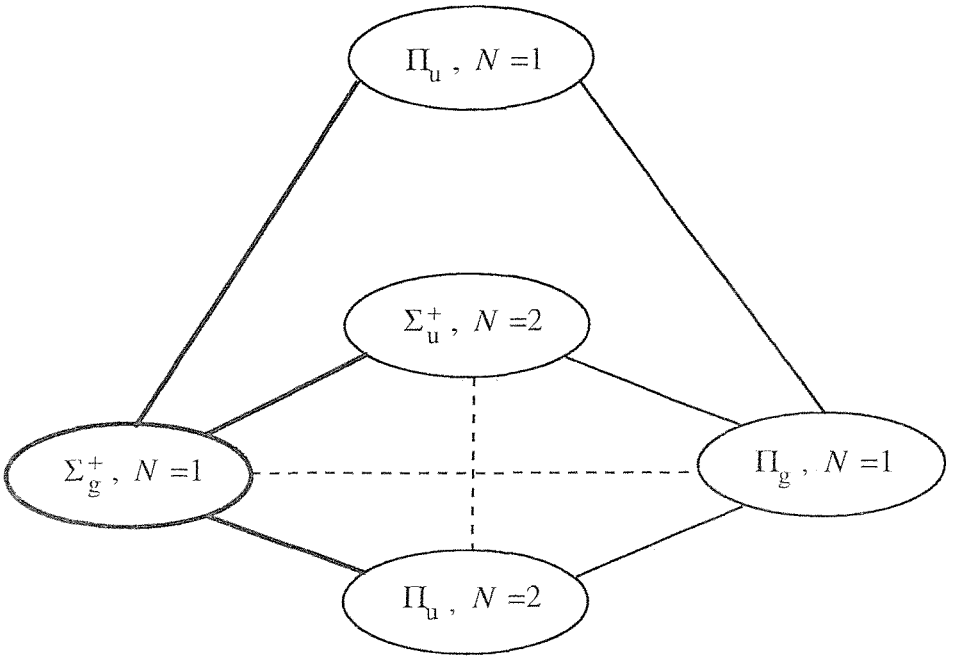

Figure 7.3: The relevant couplings in calculations of the dipole polarizability of the (0,1) ($M = \pm 1$) level of the ground electronic states of H_2^+ and D_2^+: full lines represent the electric field perturbation; thick lines indicate the major, second-order contributions; thinner lines are for couplings involved third- and higher-order interactions; the dashed lines represent the interaction of electronic and rotational angular momenta.

However, for HD^+ the mass asymmetry removes the electronic g/u symmetry and mixing of g and u functions with the same N occurs, so that more basis functions are needed. The modified diagram for HD^+ for $M = \pm 1$ is given in figure 7.4. The other diagrams for HD^+ are not reported since they are the same as the ones in figures 7.1 and 7.2 where now the g/u characterization has to be removed. It has been found that higher-order contributions involving these interactions are significant [52, 55].

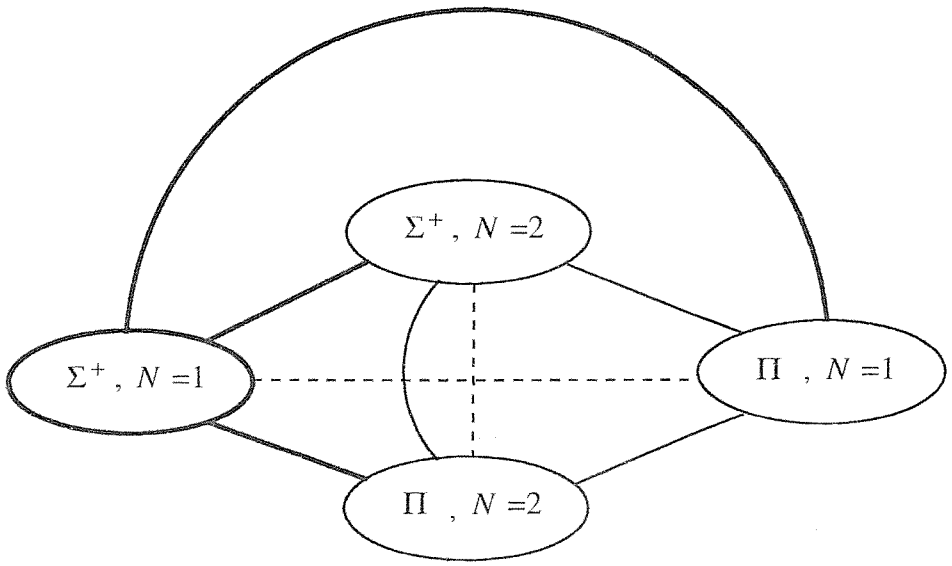

Figure 7.4: The relevant couplings in calculations of the dipole polarizability the (0,1) ($M = \pm 1$) level of the ground electronic state of HD^+: full lines represent the electric field perturbation; thick lines indicate the major, second-order contributions; thinner lines are for couplings involved third- and higher-order interactions; the dashed lines represent the interaction of electronic and rotational angular momenta.

As reported, figure 7.1 describes the situation for the (0,0) level for the ground electronic of the homonuclear molecules; in the case of HD^+, the electric field couples this level with $N = 1$ levels of Σ and Π states and the nearest level is now (0,1) of the ground electronic state itself, so that this interaction dominates [57]. As will be reported, this explains the dramatically different polarizability of HD^+ compared with H_2^+ and D_2^+, for which the nearest interacting level is the (0,1) level of the first excited electronic Σ_u^+ state.

Figure 7.2 seen without the g/u labels illustrates the interactions for the (0,1) level of the ground electronic state of HD^+, for which averaging over $M = 0$ and $M = \pm 1$ is necessary.

For $M = 0$, the $N = 1$ level interacts with Σ^+, $N = 0$ levels and with Σ^+ and Π, $N = 2$ levels as well as there being mixing with Π, $N = 1$ levels. There is competition between the coupling with the Σ^+ ground electronic state (0,0) and (0,2) levels. As might be expected from a consideration of the energy separation involved, the $N = 0$ contribution dominates and the polarizability is negative, as will be seen from the results.

As already mentioned, figure 7.4 differs most from the corresponding figure 7.3 for the homonuclear ions in that it does not have separate Π_g and Π_u states indicated. In addition, an electric field interaction is included between Σ^+, $N = 2$ and Π, $N = 2$; for H_2^+, Π_g, $N = 2$ basis functions are not involved. For $M = \pm 1$ there are no $N = 0$ levels with which to interact so, since (0,1) is the lowest level with $M = \pm 1$, the polarizability is positive.

Note that figure 7.1 is embedded in figure 7.2 so that the latter is also appropriate for the (0,0) level of the ion, but includes higher-order interactions. In particular this provides another opportunity to determine whether these could be responsible for the remaining discrepancy between theory and experiment for the (0,0) level of H_2^+.

7.4 Results

The variational method and the transformed Hamiltonian/scattering method give the same results to at least the figures quoted in this work, so they will not be given separately. In the case of the variational method the parameters used were taken from [6] and care was taken that enough Σ and Π functions were used. For the scattering method the parameters were as used in [4] and it was confirmed that enough basis functions were included, that integration was taken out far enough and that the intervals used for R were small enough. The fact that the results from these two quite different methods agree is reassuring.

The calculations involve diagonalization of large matrices in the variational method or the diagonalization and inversion of smaller matrices many times in the scattering method. Comparing results for $M = +1$ and $M = -1$ calculations indicates that rounding errors do not affect the results to the precision quoted. Accordingly only joint results for $|M|$ are given.

Care has to be taken in choosing appropriate values of the perturbation parameter λ by monitoring the relative error in α and the correlation coefficient obtained in the linear regression. In particular, the second hyperpolarizability γ for $N = 0$ levels of the ions has major contributions from the $N = 2$ basis functions (see figure 7.2) and this can affect the precision of the calculated dipole polarizabilities unless smaller λ are used than those that are satisfactory in calculations ignoring $N = 2$ (see figure 7.1).

Table 7.1 reports the quasi-non-adiabatic calculations for HD^+ (0,0). For comparison, the results for H_2^+ and D_2^+ are also given; these results are taken from [51] but multiplied by the homonuclear equivalent of B^2, where B is defined by equation (7.5); namely they are multiplied by $(1+\epsilon)^2$ with

$$\epsilon = \frac{1}{2m+1}. \tag{7.34}$$

Not surprisingly the value for $\alpha_\perp$ lies between those of H_2^+ and D_2^+. This is not true for $\alpha_\parallel$ or for the rotational average $\alpha = \frac{1}{3}(\alpha_\parallel + 2\alpha_\perp)$. Neither are determined as well as for $\alpha_\perp$ because of the non-zero electric dipole moment of HD^+, which is also given in table 7.1 and is in agreement with that previously reported in [37].

Cation	$\alpha_\parallel/e^2a_0^2E_h^{-1}$	$\alpha_\perp/e^2a_0^2E_h^{-1}$	$\alpha = \frac{1}{3}(\alpha_\parallel + 2\alpha_\perp)$	μ/ea_0
H_2^+	5.830 354	1.837 295	3.168 315	-
HD^+	6.012	1.825 695	3.221	−0.342 755
D_2^+	5.590 746	1.812 294	3.071 778	-

Table 7.1: Quasi-non-adiabatic polarizabilities (in units of $4\pi\epsilon_0 a_0^3$ or $e^2a_0^2E_h^{-1}$) for the (0,0) levels of the ground electronic states of H_2^+, D_2^+ [51] and HD^+; the electric dipole moment (in ea_0) of HD^+ is also given. The uncertainties are 1 in the last digit quoted.

It is expected that any comparison with experiment will involve the (0,0) or (0,1) levels. In addition, the only previous fully non-adiabatic calculation of the polarizability for HD^+ is for the (0,0) level [57]. For HD^+ (0,0) the polarizability is calculated to be 395.306 $e^2a_0^2E_h^{-1}$, in good agreement with the 395.289 $e^2a_0^2E_h^{-1}$ from the localized variational method of Bhatia

and Drachman [57]. As argued in section 7.3.4 the result for HD^+ (0,1) $M = 0$ is negative (-229.986 $e^2a_0^2E_h^{-1}$), while that for $|M| = 1$ is positive (120.979 $e^2a_0^2E_h^{-1}$), giving a rotational average of 3.991 $e^2a_0^2E_h^{-1}$. These results are included in tables 7.2 and 7.3.

The second hyperpolarizabilities are also determined in these calculations, but the results are only good to two significant figures. For HD^+ (0,0), (0,1) $M = 0$ and $|M| = 1$ they are -3.3×10^9, -3.3×10^9 and -2.1×10^8 $e^4a_0^4E_h^{-1}$, respectively.

As already emphasized, the great advantage of the transformed Hamiltonian/scattering method is that it is not limited to low vibrational levels, although many more basis functions are needed for the calculation of polarizabilities than for properties that do not involve the mixing of different N. Accordingly, table 7.2 presents the polarizabilities for many $N = 0$ levels of H_2^+, D_2^+ and HD^+; these results include the higher-order contributions from $N = 2$ basis functions (figures 7.2, 7.3 for the homonuclear species and 7.4 for HD^+). Also included in table 7.2 are the Hilico *et al.* [53] published values for $v \leq 10$, $N = 0$ levels of H_2^+ and D_2^+; although $N = 2$ basis functions were not included, these were given to ten significant figures, but the results reported here are not as optimistic and only six figures are quoted. For these levels the results found in this work are consistent with theirs. Not surprisingly, plots of polarizability against dissociation energies for H_2^+ and D_2^+ levels are coincident, as illustrated in figure 7.5. It has to be noted that the scaling factor due to the different reduced masses of the cations is not applied here since a comparison between non-adiabatic values of the property is made; the scaling factor has to be applied when non-adiabatic corrections to the property of interest are studied.

Table 7.3 reports polarizabilities for $N = 1$, $M = 0$ and $|M| = 1$ levels, together with their averages. Again, higher levels are not included due to the number of basis functions needed to study levels so close to dissociation and involving the indicated couplings between levels of different N. Since the basis functions used are for $N = 0$, 1 and 2, there are no higher-order contributions included from basis functions with N differing by 2 from the $N = 1$ levels of interest. Again, the polarizability for a D_2^+ level could be predicted from a plot of polarizability against dissociation energy for H_2^+ (see figure 7.6).

$(v,0)$	H_2^+	H_2^+ [53]	D_2^+	D_2^+ [53]	HD^+
0	3.168 726	3.168 725 803	3.071 989	3.071 988 696	395.306
1	3.897 56	3.897 563 360	3.553 03	3.553 025 791	462.65
2	4.821 50	4.821 500 365	4.119 58	4.119 581 678	540.69
3	6.009 33	6.009 327 479	4.791 29	4.791 282 711	631.4
4	7.560 46	7.560 453 090	5.593 32	5.593 314 877	737.3
5	9.621 78	9.621 773 445	6.558 32	6.558 318 701	861.7
6	12.416 0	12.415 999 87	7.729 06	7.729 054 615	1008.
7	16.291 0	16.290 999 14	9.162 21	9.162 209 589	1184.
8	21.809 5	21.809 472 78	10.933 9	10.933 925 39	1394.
9	29.920 3	29.920 326 97	13.148 0	13.147 976 83	1651.
10	42.306 3	42.306 328 65	15.948 1	15.948 120 78	1698.
11	62.142 6	-	19.537 2	-	2367.
12	95.908 0	-	24.207 3	-	2880.
13	158.242	-	30.389 2	-	3558.
14	287.145	-	38.735 5	-	4488.
15	603.100	-	50.266 6	-	5822.
16	1 630.58	-	66.637 7	-	7860.
17	-	-	90.654 3	-	11 28.
18	-	-	127.331	-	17 950.
19	-	-	186.239	-	35 20.
20			287.227	-	126 40.
21			476.191	-	-
22			876.264	-	-
23			1 897.62	-	
24			5 471.28	-	

Table 7.2: Non-adiabatic polarizabilities (in units of $4\pi\epsilon_0 a_0^3$ or $e^2 a_0^2 E_h^{-1}$) for rotationless levels of the ground electronic states of H_2^+, D_2^+ and HD^+. For comparison the results from [53] are included. The highest levels, $v = 17 - 19$, $v = 25 - 27$ and $v = 21 - 22$, for H_2^+, D_2^+ and HD^+, respectively, are not included due to the number of basis functions needed to study levels so close to dissociation and involving the indicated couplings between levels of different N.

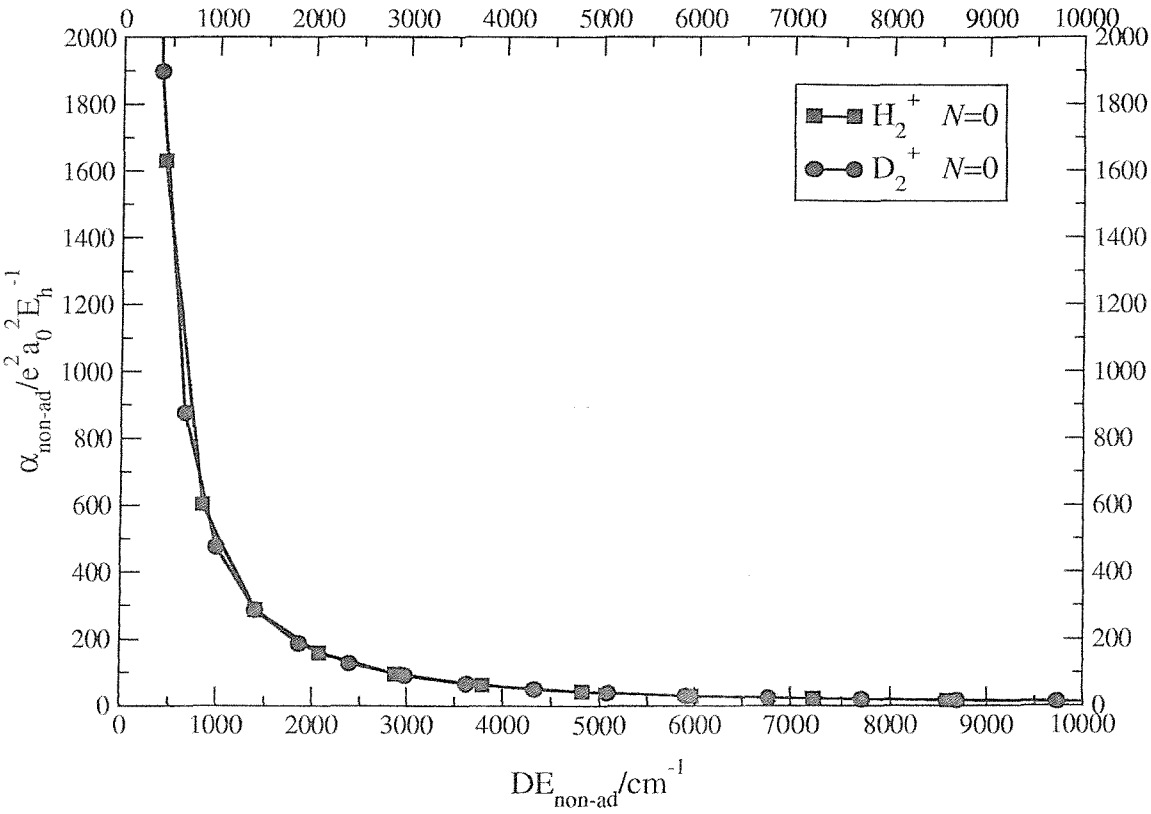

Figure 7.5: Non-adiabatic dipole polarizability versus non-adiabatic dissociation energies for H_2^+ and D_2^+, for $N = 0$, $M = 0$.

		H_2^+			D_2^+			HD^+	
$(v,1)$	M=0	$M = \|1\|$	Average	M=0	$M = \|1\|$	Average	M=0	$M = \|1\|$	Average
0	4.249 47	2.642 72	3.178 30	4.087 19	2.571 29	3.076 59	−229.986	120.979	3.991
1	5.435 71	3.147 30	3.910 10	4.862 95	2.906 40	3.558 58	−268.90	141.50	4.70
2	6.971 51	3.771 38	4.838 09	5.791 12	3.293 92	4.126 32	−313.87	165.29	5.57
3	8.982 16	4.556 24	6.031 55	6.907 34	3.745 59	4.799 51	−366.00	192.95	6.63
4	11.648 6	5.561 66	7.590 6	8.257 28	4.276 48	5.603 41	−426.66	225.26	7.95
5	15.238 4	6.876 08	9.663 5	9.900 15	4.906 13	6.570 80	−497.57	263.22	9.62
6	20.157 0	8.633 79	12.474 9	11.913 5	5.660 18	7.744 6	−580.99	308.11	11.74
7	27.037 3	11.044 7	16.375 6	14.399 9	6.572 65	9.181 7	−679.82	361.66	14.50
8	36.907 2	14.438 9	21.928 3	17.497 6	7.689 26	10.958 7	−737.96	426.19	18.14
9	51.495 6	19.423 0	30.113 9	21.394 5	9.072 39	13.179 8	−940.72	504.94	23.05
10	73.877 5	26.985 7	42.616 3	26.351 1	10.808 5	15.989 4	−1 115.5	602.48	29.8
11	109.864	39.067 7	62.666	32.734 9	13.019 7	19.591 4	−1 332.8	725.55	39.4
12	171.340	59.615 3	96.857	41.075 5	15.881 9	24.279 8	−1 608.3	884.41	53.5
13	285.257	97.571 3	160.133	52.153 8	19.654 8	30.487 8	−1 965.8	1 095.4	75.0
14	521.919	176.238	291.465	67.153 8	24.732 1	38.872 7	−2 444.0	1 386.1	109.4
15	1 105.99	369.927	615.28	87.927 2	31.729 7	50.462 2	−3 108.3	1 806.4	168.2
16	3 029.40	1 005.36	1 680.04	117.480	41.647 5	66.925	−4 079.1	2 455.8	277.5
17	-	-	-	160.913	56.181 8	91.092	−5 602.4	3 561.9	507.1
18	-	-	-	227.352	78.367 7	128.029	−8 270.8	5 765.9	1 087.0
19	-	-	-	334.243	114.005	187.148	−14 046	11 671	3 099
20				517.842	175.142	289.375	−39 022	45 104	17 062
21				862.217	289.694	480.535	-	-	-
22				1 593.85	532.774	886.47	-	-	-
23				3 472.18	1 155.72	1 927.87			
24				10 116.6	3 350.76	5 606.0			

Table 7.3: Non-adiabatic polarizabilities (in units of $4\pi\epsilon_0 a_0^3$ or $e^2 a_0^2 E_h^{-1}$) for N=1 levels of the ground electronic states of H_2^+, D_2^+ and HD^+.

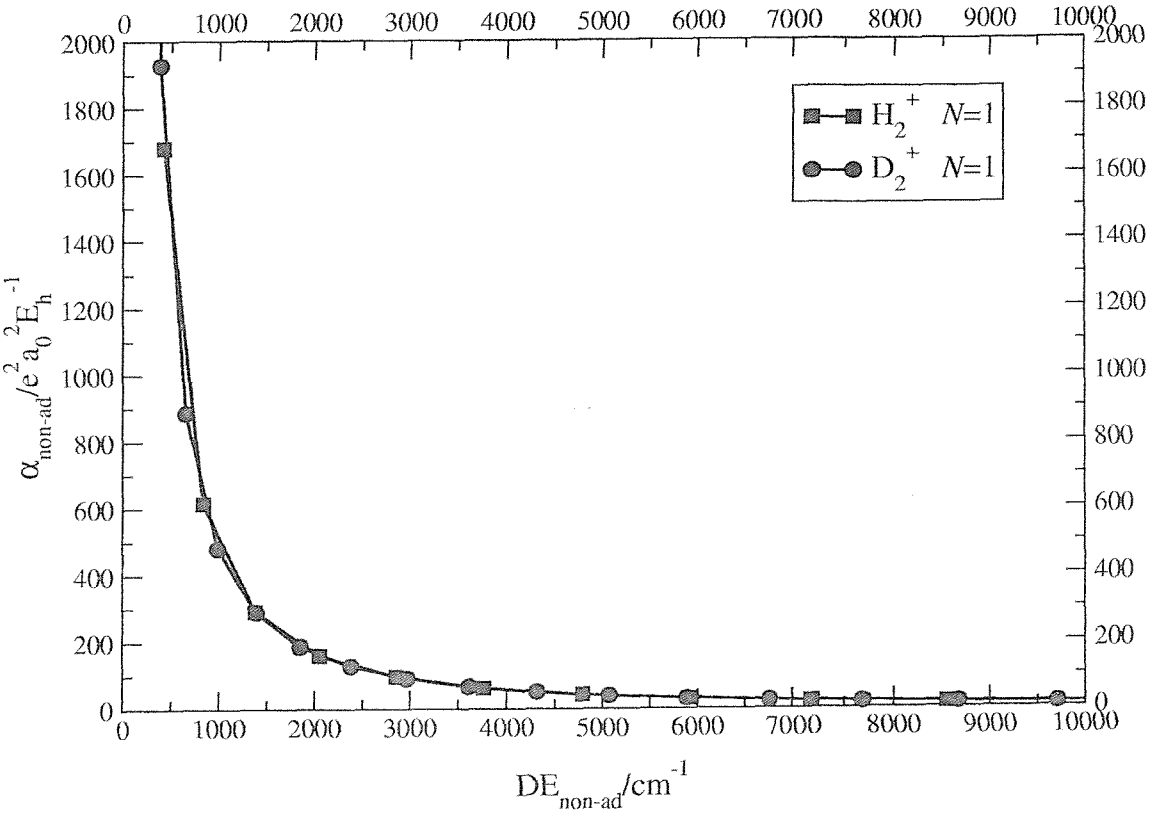

Figure 7.6: Non-adiabatic dipole polarizability versus non-adiabatic dissociation energies for H_2^+ and D_2^+, for $N = 1$, averaged value between $M = 0$ and $|M| = 1$.

There are at least three fully non-adiabatic calculations that agree to $1 \times 10^{-6}\ e^2a_0^2E_h^{-1}$ that the H_2^+ (0,0) polarizability is $3.168\,726\ e^2a_0^2E_h^{-1}$ [44,52,53]. The fact that there is still a discrepancy between these and the experimental value of $3.167\,96(15)\ e^2a_0^2E_h^{-1}$ [45] suggests that the theoreticians are not calculating the quantity that is observed experimentally. Korobov [54] has shown that relativistic effects can only account for about 20% of the difference.

Previous calculations have not accounted for the contribution of $N = 2$ levels through fourth- and higher-order corrections. The program used for the HD^+ (0,1) $M = 0$ calculation includes $N = 0$, 1 and 2 basis functions, so that by targeting $N = 0$ the higher-order corrections are accounted for. The result is unchanged at $3.168\,726\ e^2a_0^2E_h^{-1}$ suggesting that these corrections only affect at most the sixth decimal place. The difference between theory and experiment is not resolved. The influence of Δ electronic states has yet to be considered, but is unlikely to be significant since the largest contribution is presumably fourth-order involving Π, $N = 1$ and Δ, $N = 2$.

Another possible source of any discrepancy is hyperfine effects. However the H_2^+ (0,0) level is unaffected by the dominant Fermi contact interaction, as is the nearest interacting level (Σ_u^+ (0,1)), since they are both in *para* nuclear spin states. H_2^+ (0,1) is *ortho*, but a back-of-the-envelope calculation of the likely effect on $\alpha_{||}$, based only on the change in energy separation between Σ_g^+ (0,1) and the nearest interacting levels, Σ_u^+ (0,0) and (0,2), suggests that this would only affect the sixth decimal place. This is in the context that a similar rough estimate of the influence of relativistic effects for H_2^+ (0,0) (as calculated by Korobov [54]) underestimates by a factor of three while, if radiative effects are included as well, the combined contribution to the discrepancy is even less.

To conclude, it has to be noted that the second-order hyperpolarizability for H_2^+ (0,0) is $1.14 \times 10^4\ e^4a_0^4E_h^{-1}$.

7.5 Conclusions

In this chapter new results for the dipole polarizability of the hydrogen molecular cation and its isotopomers are reported. Many levels are studied, although levels close to dissociation will require more effort. Also, if needed, it should be possible to add an extra significant figure to the results given here. Only levels with $N = 0$ and 1 are considered, since for a given N, the $(N+1)$ values of $|M|$ must be considered separately, but again other N could be studied if necessary.

HD^+ is of particular interest here since only one previous calculation of its polarizability was reported; the presence of an asymmetric charge distribution provides novelty. The result obtained for (0,0) is close to the only previous one.

The opportunity was taken to revisit H_2^+ (0,0), but including higher-order contributions than previous studies has not removed the difference between experiment and theory.

Finally it should be noted that the values of the perturbation parameter used, may be relevant to experiment. For H_2^+ and D_2^+ they correspond to electric fields of up to $2 \times 10^{-3}\ E_h e^{-1} a_0^{-1}$ (1×10^9 V m^{-1}), while for HD^+ the corresponding fields are up to $4 \times 10^{-5}\ E_h e^{-1} a_0^{-1}$ (2×10^7 V m^{-1}).

Chapter 8

Results: relativistic correction for H_2^+

8.1 Introduction

In this chapter results concerning the relativistic corrections for the ground electronic state of the hydrogen molecular cation H_2^+ are reported. While fully relativistic calculations for atoms are common, relativistic corrections for molecules are still estimated from non-relativistic wavefunctions using perturbation theory. Since high-resolution spectra data are available, relativistic effects are very important for light species such as H_2^+, even though in order to have an agreement between experimental and theoretical results to 0.001 cm^{-1} or better, the radiative correction should also be included.

In the past, tables of the corrections to the potential for the ground state of H_2^+ as a function of internuclear distance have been published [59] and these have been used to calculate relativistic corrections for H_2^+, D_2^+ and HD^+. However, those results extended only to R=10.0 a_0 while Carrington and coworkers investigated the very highest vibrational levels of all the three molecules [60–62], levels for which bond lengths greater than 10.0 a_0 make significant contributions. More recently Kennedy and coworkers [63] extended the evaluation of the relativistic correction to far beyond R=10.0 a_0. They too treated the nuclei as being fixed, thus assuming that the small non-adiabatic effects did not significantly influence the relativistic corrections.

In this work the relativistic correction is treated at a non-adiabatic level and the results reported are obtained, as for the other properties, through the variational and the scattering

methods. However, as is explained below, analytic evaluation of some of the matrix elements is not possible and numerical integration (see section 3.5) is used to achieve the reported results.

8.2 Theory: the Dirac Hamiltonian

In considering relativistic corrections it would be desirable to write down an Hamiltonian for the two protons and one electron and separate off the overall translation. Unfortunately this is not possible relativistically. In addition, the corrections are dominated by the electron motion, so attention is to be confined to the electron in the presence of two nuclei. For this reason the Dirac Hamiltonian has to be considered

$$H_{\mathrm{D}} = \beta mc^2 + c\boldsymbol{\alpha}\cdot\boldsymbol{\pi} - e\phi = \beta mc^2 + c\boldsymbol{\alpha}\cdot\boldsymbol{\pi} - \frac{e^2}{4\pi\epsilon_0}\left(\frac{1}{r_{1\mathrm{e}}} + \frac{1}{r_{2\mathrm{e}}}\right) \tag{8.1}$$

where

$$\boldsymbol{\pi} = \boldsymbol{p} + e\boldsymbol{A} \tag{8.2}$$

is the mechanical momentum, ϕ is the scalar potential and β and $\boldsymbol{\alpha}$ are the Dirac operators which can be seen as operators representing a new degree of freedom intrinsic to the electron. Specifically, in equation (8.2) $\boldsymbol{p}$ is the canonical momentum and $\boldsymbol{A}$ is the vector potential. All the other symbols have their usual meaning. Explicitly, the Dirac operators can be written in the following forms, known as the *standard representation*

$$\beta = \alpha_0 = \begin{pmatrix} 1 & 0 & 0 & 0 \\ 0 & 1 & 0 & 0 \\ 0 & 0 & -1 & 0 \\ 0 & 0 & 0 & -1 \end{pmatrix} \tag{8.3}$$

$$\alpha_x = \begin{pmatrix} 0 & 0 & 0 & 1 \\ 0 & 0 & 1 & 0 \\ 0 & 1 & 0 & 0 \\ 1 & 0 & 0 & 0 \end{pmatrix} \tag{8.4}$$

$$\alpha_y = \begin{pmatrix} 0 & 0 & 0 & -i \\ 0 & 0 & i & 0 \\ 0 & -i & 0 & 0 \\ i & 0 & 0 & 0 \end{pmatrix} \tag{8.5}$$

$$\alpha_z = \begin{pmatrix} 0 & 0 & 1 & 0 \\ 0 & 0 & 0 & -1 \\ 1 & 0 & 0 & 0 \\ 0 & -1 & 0 & 0 \end{pmatrix}. \tag{8.6}$$

It is convenient to rewrite equation (8.1) in dimensionless coordinates in which lengths are measured in a_0 and indroducing α, the fine structure constant

$$H_{\rm D} = mc^2\Big[\beta + \alpha\boldsymbol{\alpha}\cdot\boldsymbol{\pi} - \alpha^2\Big(\frac{1}{r_{1e}} + \frac{1}{r_{2e}}\Big)\Big] \tag{8.7}$$

with

$$\alpha = \frac{e^2}{2h\epsilon_0 c} = 7.29735 \times 10^{-3}. \tag{8.8}$$

The form of equation (8.7) arises from considerations concerning the decoupling between its positive and negative solutions, as is explained later. With any decoupling method, the Hamiltonian is obtained as a power series (see later) which converges for electrons moving with velocities much less than the speed of light. Since the largest term in the Dirac Hamiltonian (8.7) is mc^2, it is appropriate to estimate the magnitude of the other terms, relative to this one.

In the first Bohr orbit, the electron's speed is

$$v = \frac{e^2}{2\epsilon_0 h} = c\alpha \tag{8.9}$$

so now α and v/c are comparable expansion parameters; in addition, the radius of the first Bohr orbit is

$$a_0 = \frac{4\pi\epsilon_0\hbar^2}{me^2}. \tag{8.10}$$

So, classically

$$c\boldsymbol{\alpha}\cdot\boldsymbol{\pi} \sim cmv = mc^2\alpha \tag{8.11}$$

and

$$e\phi \sim \frac{e^2}{4\pi\epsilon_0 a_0} = mc^2\alpha^2 \tag{8.12}$$

from which equation (8.7) arises.

The Dirac equation is the proper relativistic quantum mechanical equation for the electron. However, as it is a four-component equation, it involves four-by-four matrices and the wavefunction is a four-component vector. This is its main difference from non-relativistic equations, whose wavefunctions have two components corresponding to the two possible orientations of the electron's spin.

Besides, the Dirac equation has two negative energy components which are coupled to the positive energy components. Since just positive energies have to be considered, the necessity to decouple the positive and the negative energy components arises, to obtain a two-component equation for the positive energy solutions which is similar to the non-relativistic equations and can be used in the same way. The Dirac equation is, in this way, reduced to a non-relativistic form.

The method used to obtain the non-relativistic form of the Dirac equation that is used to achieve the results reported in this work, is the Foldy-Wouthuysen transformation (see for example [64]). The starting point is to express the Hamiltonian as a power series in α

$$H_{\mathrm{D}} = mc^2 + mc^2\alpha^2\Big(\frac{1}{2}\Theta^2 + \epsilon\Big) + \mathcal{O}(mc^2\alpha^4), \tag{8.13}$$

where

$$\Theta = \boldsymbol{\sigma}\cdot\boldsymbol{p} \tag{8.14}$$

and

$$\epsilon = -\Big(\frac{1}{r_{1\mathrm{e}}} + \frac{1}{r_{2\mathrm{e}}}\Big) \tag{8.15}$$

the components of $\boldsymbol{\sigma}$ being the Pauli spin matrices; note that $\Theta^2 = p^2$. The first term of equation (8.13) is the electron rest energy and is omitted in the rest of this work; the term of order $mc^2\alpha^2$ corresponds to the non-relativistic energy; the relativistic corrections that are of interest are the expectation values of the $mc^2\alpha^4$ terms. Higher order corrections become increasingly divergent and would present technical problems far beyond the scope of this work.

Briefly, the Foldy-Wouthuysen transformation consists in performing a series of unitary transformations by which the coupling terms between the positive and the negative solutions

are progressively eliminated to obtain the resulting non-relativistic Hamiltonian which is hermitian. Following the choice of transformation in [65], the result for the correction is

$$H_{\rm rel} = mc^2\alpha^4\Big\{ -\frac{1}{8}\Theta^4 - \frac{1}{8}\Big[\Theta\big[\Theta,\epsilon\big]\Big]\Big\} + \mathcal{O}(mc^2\alpha^6). \tag{8.16}$$

Substitution of (8.14) gives

$$H_{\rm rel} = mc^2\alpha^4\Big\{ -\frac{1}{8}p^4 + \frac{\pi}{2}\Big[\delta(\boldsymbol{r}_{1\rm e}) + \delta(\boldsymbol{r}_{2\rm e})\Big] + \frac{1}{4}\boldsymbol{\sigma}\cdot\Big(\frac{r_{1\rm e}}{\boldsymbol{r}_{1\rm e}^3} + \frac{r_{2\rm e}}{\boldsymbol{r}_{2\rm e}^3}\Big)\times\boldsymbol{p}\Big\}. \tag{8.17}$$

The spin-orbit coupling term makes no contribution to Σ molecular states so that the final form of the relativistic contribution to the non-relativistic Dirac equation used throughout this chapter is

$$H_{\rm rel} = mc^2\alpha^4\Big\{ -\frac{1}{8}p^4 + \frac{\pi}{2}\Big[\delta(\boldsymbol{r}_{1\rm e}) + \delta(\boldsymbol{r}_{2\rm e})\Big]\Big\}. \tag{8.18}$$

8.3 Theory: expectation values and numerical approaches

8.3.1 Introduction

In order to study the relativistic correction, the expectation value of operator (8.18) has to be considered; namely the expectation values of the fourth power of the canonical momentum $\boldsymbol{p}$ and of the electron density at the nuclei $\delta(\boldsymbol{r}_{n\rm e})$ have to be studied. This section is dedicated to these topics.

As already done for all the other properties that have been reported in this work, a preliminary comparison between the results obtained with the variational and the scattering methods is made. As explained in the next section, the expectation values of the electron density at the nuclei are computed through analytic integration. In section 8.3.3 the approach adopted to study the expectation value of p^4 is reported; due to the presence of singularities in the expression for this operator, the results are achieved through numerical integration (see 3.5) since singular integrands appear.

8.3.2 Electron density at the nuclei

The explicit expressions of the electron density at the nuclei in equation (8.18) are the following, according to the nucleus they refer to; namely for nucleus 1 ($\xi = 1, \eta = -1$)

$$\delta(\boldsymbol{r}_{1e}) = \frac{4\delta(\xi-1)\delta(\eta+1)}{\pi R^3(\xi^2-\eta^2)} \tag{8.19}$$

and for nucleus 2 ($\xi = 1, \eta = 1$)

$$\delta(\boldsymbol{r}_{2e}) = \frac{4\delta(\xi-1)\delta(\eta-1)}{\pi R^3(\xi^2-\eta^2)}. \tag{8.20}$$

Within the variational method (see section 3.2 for the details) the matrix elements of this property are computed between the basis functions

$$\Psi_i(\xi,\eta,R) = e^{-\frac{\alpha(\xi-1)}{2}}(\xi^2-1)^{\frac{|\Lambda|}{2}}\mathcal{L}_{m_i}^{(|\Lambda|)}[\alpha(\xi-1)]\mathcal{P}_{n_i}^{(|\Lambda|)}(\eta)\frac{1}{R}\psi_{k_i}(R) \tag{8.21}$$

using the volume element

$$d\tau = \frac{R^5}{8}(\xi^2-\eta^2)d\xi d\eta dR. \tag{8.22}$$

Operators (8.19) and (8.20) do not depend upon any angular variable, so just matrix elements between basis functions with same Λ, N, M have to be taken into account. In addition only Σ basis functions are non-zero on the molecular axis, so that matrix elements involving $\Pi, \Delta, \ldots$ vanish. Only $\Sigma - \Sigma$ matrix elements then need to be considered. The matrix elements for the electron density at nucleus 1 are then

$$\langle i|\delta(\boldsymbol{r}_{1e})|j\rangle = \frac{1}{2\pi}(-1)^{n_i+n_j}\int_0^\infty \psi_{k_i}(R)\psi_{k_j}(R)dR \tag{8.23}$$

and at nucleus 2

$$\langle i|\delta(\boldsymbol{r}_{2e})|j\rangle = \frac{1}{2\pi}\int_0^\infty \psi_{k_i}(R)\psi_{k_j}(R)dR. \tag{8.24}$$

On the other hand, if the scattering and the transformed Hamiltonian approaches are to be used, the operator has to be transformed; the transformation leads to the equation (see page 32 to page 34)

$$\delta_t(\boldsymbol{r}_{ne}) = \rho^{\frac{3}{2}}Z_n^3\delta(\boldsymbol{r}_{ne}) \tag{8.25}$$

where in the particular case of the choices $\xi = 1$ and $\eta = \pm 1$

$$\rho = 1 + \kappa \tag{8.26}$$

with

$$\kappa = \frac{1}{4\mu_{\text{eff}} + 1} \tag{8.27}$$

as already indicated (see for example equation (7.11)). Equation (8.26) leads to the final expression to be used within the scattering method for the electron density at the nucleus n

$$\delta_{\text{t}}(\boldsymbol{r}_{\text{ne}}) = (1 + \kappa)^{\frac{3}{2}} Z_{\text{n}}^3 \delta(\boldsymbol{r}_{\text{ne}}). \tag{8.28}$$

Within this method, the matrix elements of this property are computed between the basis functions

$$\Psi_i(\xi, \eta; R) = e^{-\frac{\alpha(\xi-1)}{2}} (\xi^2 - 1)^{\frac{|\Lambda|}{2}} \mathcal{L}_{m_i}^{(|\Lambda|)}[\alpha(\xi - 1)] \mathcal{P}_{n_i}^{(|\Lambda|)}(\eta) \tag{8.29}$$

using the volume element

$$d\tau = \frac{1}{8}(\xi^2 - \eta^2) d\xi d\eta dR. \tag{8.30}$$

It has to be noted that in equation (8.28) Z_{n} has the meaning of an effective nuclear charge which is equal to 1 for H_2^+ and D_2^+ but for HD^+ is 0.999 931 987 for the proton and 1.000 068 018 for the deuteron, these values arising from equations (2.109) and (2.110).

8.3.3 The expectation value of p^4

The general form of the second-power of the canonical momentum is given by

$$p^2 = -\frac{4}{R^2} X_\Lambda \tag{8.31}$$

where the operator X_Λ is defined in equation (2.59).

Explicitly, for $\Sigma - \Sigma$ couplings it leads to

$$p^2_{\Sigma-\Sigma} = -\frac{4}{R^2(\xi^2 - \eta^2)} \left[\frac{\partial}{\partial \xi} (\xi^2 - 1) \frac{\partial}{\partial \xi} + \frac{\partial}{\partial \eta} (1 - \eta^2) \frac{\partial}{\partial \eta} \right] \tag{8.32}$$

and for $\Pi - \Pi$ to

$$p^2_{\Pi-\Pi} = -\frac{4}{R^2(\xi^2-\eta^2)}\Big[\frac{\partial}{\partial\xi}(\xi^2-1)\frac{\partial}{\partial\xi} + \frac{\partial}{\partial\eta}(1-\eta^2)\frac{\partial}{\partial\eta} - \frac{\xi^2-\eta^2}{(\xi^2-1)(1-\eta^2)}\Big]. \tag{8.33}$$

Since this operator is hermitian, the study of $\langle p^4\rangle$ can be reduced to $\langle p^2\Psi|p^2\Psi\rangle$ where Ψ is given by a linear combination of appropriate basis functions.

Variational approach

Once the p^2 operator is applied to Σ and Π basis functions within the variational method, the following expressions arise respectively

$$(p^2\Psi_i)_\Sigma = -\frac{4}{R^2}\frac{e^{-\frac{\alpha_\Sigma(\xi-1)}{2}}}{(\xi^2-\eta^2)}\Big\{\Big[\frac{\alpha_\Sigma^2}{4}(\xi^2-1) - \alpha_\Sigma(m_i+1)\xi + m_i(1-\alpha_\Sigma) - n_i(n_i+1)\Big]$$

$$\cdot\mathcal{L}_{m_i}[\alpha_\Sigma(\xi-1)] - m_i\mathcal{L}_{m_i-1}[\alpha_\Sigma(\xi-1)\Big\}\mathcal{P}_{n_i}(\eta), \tag{8.34}$$

where the convention $\mathcal{L}^0_{m_i}(x) = \mathcal{L}_{m_i}(x)$ is used, and

$$(p^2\Psi_i)_\Pi = -\frac{4}{R^2}\frac{e^{-\frac{\alpha_\Pi(\xi-1)}{2}}}{(\xi^2-\eta^2)}(\xi^2-1)^{\frac{1}{2}}\Big\{\Big[\frac{\alpha_\Pi^2}{4}(\xi^2-1) - 2\alpha_\Pi\xi - m_i\alpha_\Pi(\xi+1) + 2(m_i+1) - n_i(n_1+1)\Big]$$

$$\cdot\mathcal{L}^{(1)}_{m_i}[\alpha_\Pi(\xi-1)] - 2(m_i+1)\mathcal{L}^{(1)}_{m_i-1}[\alpha_\Pi(\xi-1)]\Big\}\mathcal{P}^{(1)}_{n_i}(\eta). \tag{8.35}$$

Note that here the variational parameters α_Σ and α_Π do not depend upon R and all the symbols used have their usual meaning.

The transformation of p^4 and the scattering approach

When the expectation value of p^4 has to be studied with the scattering method and the transformed Hamiltonian theory, the operator has to be transformed; since

$$e^{iS}p^4e^{-iS} = (e^{iS}p^2e^{-iS})(e^{iS}p^2e^{-iS}), \tag{8.36}$$

the transformed expression for p^2 can be used

$$p_t^2 = [1 + \kappa(\xi^2 + \eta^2 - 1)]p^2 - \frac{8\kappa}{R^2}(2Y + 3) - \frac{4\kappa}{R^2}(2Y + 3)\frac{\partial}{\partial R}R + \mathcal{O}(\kappa^2) \tag{8.37}$$

where all symbols have their usual meaning and

$$Y = \frac{1}{\xi^2 - \eta^2}\Big[\xi(\xi^2 - 1)\frac{\partial}{\partial \xi} + \eta(1 - \eta^2)\frac{\partial}{\partial \eta}\Big]. \tag{8.38}$$

It has to be noted that $\frac{\partial}{\partial R}R$ could be replaced by $(R\frac{\partial}{\partial R} + 1)$; the choice for leaving this term as it is, depends on the fact that the scattering method cannot cope with any term involving a dependence on R and the form of the vibrational part of the basis functions used in the variational method (see below).

The terms involving $\partial/\partial R$ have to be estimated in some other way, as will be explained in the next paragraphs. For this reason, in the scattering method, the following expectation values involving part of the operator (8.37) can be computed

$$\langle \rho p^2 - \frac{8\kappa}{R^2}(2Y + 3)|\rho p^2 - \frac{8\kappa}{R^2}(2Y + 3)\rangle. \tag{8.39}$$

Tests on the contribution of terms in κ^2 confirmed that these terms are negligible.

Correction for $\partial/\partial R$ with the variational method

The term that cannot be studied with the scattering method in equation (8.37)

$$-\frac{4\kappa}{R^2}(2Y + 3)\frac{\partial}{\partial R}R \tag{8.40}$$

can be treated with the variational method through

$$\langle p^2|\frac{4}{R^2}(2Y + 3)\frac{\partial}{\partial R}R\rangle \tag{8.41}$$

since the basis functions (8.21) involve $\frac{1}{R}\psi_{k_i}(R)$. Note that to obtain the final contribution to p^4 arising from the $\frac{\partial}{\partial R}R$ term, the results of (8.41) have to be multiplied by (2κ).

However, since the variational method is not expected to be satisfactory for high vibrational levels, another method has to be adopted; this alternative approach is described in the next paragraph.

Once the $(2Y+3)$ term of (8.41) is applied to Σ and Π basis functions within the variational method, the following expressions arise respectively

$$[(2Y+3)\Psi_i]_\Sigma = \frac{e^{-\frac{\alpha_\Sigma(\xi-1)}{2}}}{(\xi^2-\eta^2)}\Big\{\Big[\xi(\xi+1)[2m_i-\alpha_\Sigma(\xi-1)]+3(\xi^2-\eta^2)-2n_i\eta^2\Big]$$

$$\cdot\mathcal{L}_{m_i}[\alpha_\Sigma(\xi-1)]\mathcal{P}_{n_i}(\eta)-2m_i\xi(\xi+1)\mathcal{L}_{m_{i-1}}[\alpha_\Sigma(\xi-1)]\mathcal{P}_{n_i}(\eta)+2n_i\eta\mathcal{L}_{m_i}[\alpha_\Sigma(\xi-1)]\mathcal{P}_{n_{i-1}}(\eta)\Big\}$$

$$+2n_i\eta\mathcal{L}_{m_i}[\alpha_\Sigma(\xi-1)]\mathcal{P}_{n_{i-1}}(\eta)\Big\}\frac{1}{R}\psi_i(R), \tag{8.42}$$

$$[(2Y+3)\Psi_i]_\Pi = \frac{e^{-\frac{\alpha_\Pi(\xi-1)}{2}}}{(\xi^2-\eta^2)}\Big\{(\xi^2-1)^{\frac{1}{2}}\Big[\Big(-\alpha_\Pi^2+3\alpha(\xi^2-\eta^2)+2(n_i+1)\eta^2\Big)$$

$$\cdot\mathcal{L}^{(1)}_{m_i}[\alpha_\Pi(\xi-1)]\mathcal{P}^{(1)}_{n_i}(\eta)-2n_i\eta\mathcal{L}^{(1)}_{m_i}[\alpha_\Pi(\xi-1)]\mathcal{P}^{(1)}_{n_{i+1}}(\eta)\Big]$$

$$+(\xi^2-1)^{-\frac{1}{2}}\Big[\Big(2\alpha_\Pi m_i(\xi+1)+2\alpha\xi\Big)\mathcal{L}^{(1)}_{m_i}[\alpha_\Pi(\xi-1)]\mathcal{P}^{(1)}_{n_i}(\eta)$$

$$-2\alpha_\Pi(m_i+1)(\xi+1)\mathcal{L}^{(1)}_{m_{i-1}}[\alpha_\Pi(\xi-1)]\mathcal{P}^{(1)}_{n_i}(\eta)\Big]\Big\}\frac{1}{R}\psi_i(R) \tag{8.43}$$

while the term dependent on R becomes

$$\frac{\partial}{\partial R}R\frac{1}{R}\psi_{k_i}(R)=\Big[\Big(k_i+\frac{\beta+1}{2}\Big)\frac{1}{R}-\frac{\epsilon_{k_i}\beta}{2}\Big]\psi_{k_i}(R)-(k_i+\beta)\frac{1}{R}\psi_{k_i-1}(R). \tag{8.44}$$

It has to be remembered here that the $\psi_{k_i}(R)$ basis functions are defined as

$$\psi_{k_i}(R)=\frac{1}{R}e^{-\frac{y}{2}}y^{\frac{\beta+1}{2}}\mathcal{L}^{(\beta)}_{k_i}(y) \tag{8.45}$$

where $\mathcal{L}^{(\beta)}_{k_i}(y)$ are associated Laguerre polynomials. Here

$$y=\epsilon_{k_i}R\delta \tag{8.46}$$

where

$$\epsilon_{k_i} = \frac{4\gamma}{2k_i + \beta + 1}, \tag{8.47}$$

$$\beta = 2\sqrt{\gamma + N(N+1) + \frac{1}{4}} \tag{8.48}$$

and

$$\gamma = \frac{k\mu}{\delta^2}; \tag{8.49}$$

as usual μ is the reduced mass of the nuclei. In the above equations k and $\delta = 1/R_e$ are taken to be non-linear parameters. From equation (8.44) new matrix elements to be evaluated arise

$$\int_0^\infty \psi_{k_i} \frac{1}{R} \psi_{k_j} R^5 dR, \tag{8.50}$$

$$\int_0^\infty \psi_{k_{i-1}} \frac{1}{R} \psi_{k_{j-1}} R^5 dR \tag{8.51}$$

but, as with other vibrational integrals, analytic formulae can be derived.

Another approach to study the correction for $\partial/\partial R$

As asserted before, the variational method is not expected to be satisfactory for high vibrational quantum numbers and another method to study the corrections arising from the $\partial/\partial R$ term has to be used. Namely it consists in determining the corrections as a function of R and then averaging over R using the LEVEL program [7].

However, this approach does not allow for mixing of Σ and Π states, so the results for high levels (with $N \neq 0$) will present some discrepancies. Nevertheless, this method has the advantage of producing corrections for all the (v, N) levels in just a few runs of the LEVEL program.

The basis functions are now

$$\Psi(\xi, \eta, R) = \psi(\xi, \eta; R)\chi(R) \tag{8.52}$$

with

$$\psi(\xi,\eta;R)=\sum_i c_i(R)\phi_i(\xi,\eta;R). \tag{8.53}$$

For the correction as a function of R, the method described in [23] is used. Note that, in addition to using a transformed Hamiltonian, the volume element is changed to remove the first derivative term in $\partial/\partial R$; this must be allowed for since the extra term involves $\partial/\partial R$. So now

$$-\frac{4\kappa}{R^2}(2Y+3)\frac{\partial}{\partial R}R=-\frac{4\kappa}{R^2}(2Y+3)\Big(1+R\frac{\partial}{\partial R}\Big); \tag{8.54}$$

and, since the volume element changes from

$$d\tau\propto R^5dR \quad \text{to} \quad d\tau\propto dR$$

and the eigenfunctions from

$$\psi \quad \text{to} \quad R^{-5/2}\psi,$$

the term to study is now

$$-\frac{4\kappa}{R^2}(2Y+3)\Big(-\frac{3}{2}+R\frac{\partial}{\partial R}\Big). \tag{8.55}$$

It is convenient to note at this stage that p_t^2 could be partitioned differently; in fact, it could be separated into a part that can be calculated with the scattering program and a part that has to be estimated in other ways. Namely the alternative partition would be

$$p_t^2=\rho p^2-\frac{8\kappa}{R^2}(2Y+3)+a\frac{4\kappa}{R^2}(2Y+3)-\frac{4\kappa}{R^2}(2Y+3)\Big(\frac{\partial}{\partial R}R+a\Big). \tag{8.56}$$

Chosing $a=3/2$ would give the extra term as

$$-\frac{4\kappa}{R^2}(2Y+3)R\frac{\partial}{\partial R},$$

while $a\sim 1$ would minimize the magnitude of the correction. However, tests show that the calculated corrections do not differ significantly for different partitions and the original partition is kept.

Functions $\phi_i(\xi,\eta;R)$ of equation (8.53) have the usual form being

$$\phi_i(\xi,\eta;R) = e^{-\frac{\alpha_\Sigma(\xi-1)}{2}}\mathcal{L}_{m_i}[\alpha_\Sigma(\xi-1)]\mathcal{P}_{n_i}(\eta) \tag{8.57}$$

where the dependence on R is contained in the parameter α_Σ; unlike the variational method, this parameter has been optimized at different bond lengths and is input. The expectation values of the extra term to be computed are then

$$\langle\psi_i(\xi,\eta;R)\chi(R)|\mathcal{K}\Big(-\frac{3}{2}+R\frac{\partial}{\partial R}\Big)|\psi_j(\xi,\eta;R)\chi(R)\rangle \tag{8.58}$$

where

$$\mathcal{K} = -p^2\frac{4\kappa}{R^2}(2Y+3); \tag{8.59}$$

namely

$$\langle\chi(R)|\Big\{-\frac{3}{2}\sum_{i,j}c_i(R)c_j(R)\langle\phi_i\mathcal{K}\phi_j\rangle+\sum_{i,j}c_i(R)\frac{\partial c_j(R)}{\partial R}R\langle\phi_i\mathcal{K}\phi_j\rangle$$

$$+\sum_{i,j}c_i(R)c_j(R)R\langle\phi_i\mathcal{K}\frac{\partial\phi_j}{\partial R}\rangle+\sum_{i,j}c_i(R)c_j(R)R\langle\phi_i\mathcal{K}\phi_j\rangle\frac{\partial}{\partial R}|\chi(R)\rangle. \tag{8.60}$$

The $\chi(R)$ functions and the expectation values of (8.60) for each vibration-rotational level are determined using the LEVEL program. The electronic parts of (8.60) involve

$$\frac{\partial c_i(R)}{\partial R} \quad \text{and} \quad \frac{\partial\phi_i(R)}{\partial R}$$

and they are dealt with using the approach reported in [24]. For the partial derivative of $\phi_i(\xi,\eta;R)$ basis functions with respect to R

$$\frac{\partial\phi_i(R)}{\partial R} = \frac{\partial\phi_i(\alpha_\Sigma)}{\partial\alpha_\Sigma}\frac{\partial\alpha_\Sigma}{\partial R} \tag{8.61}$$

where $\partial\alpha_\Sigma/\partial R$ is calculated from input α_Σ. In [24] it was not recognized that the functions $\phi_i(\xi,\eta;R)$ can be taken to be independent of R, namely α_Σ can be considered constant; the dependence of these functions on R then resides entirely in the $c_i(R)$ coefficients. In this case the $\partial c_i(R)/\partial R$ are significantly different, but the two approaches

$$\frac{\partial\alpha_\Sigma}{\partial R} = 0 \quad \text{and} \quad \frac{\partial\alpha_\Sigma}{\partial R} \neq 0$$

give results that do not differ until the seventh significant figure.

If

$$\frac{\partial \alpha_\Sigma}{\partial R} \neq 0$$

then $\frac{\partial \phi_i(R)}{\partial \alpha_\Sigma}$ is needed at each bond length

$$\frac{\partial \phi_i(R)}{\partial R} = e^{-\frac{\alpha_\Sigma(\xi-1)}{2}}\Big[-\frac{1}{2}(\xi-1)\mathcal{L}_{m_i}[\alpha_\Sigma(\xi-1)] + \frac{m_i}{\alpha_\Sigma}\Big(\mathcal{L}_{m_i}[\alpha_\Sigma(\xi-1)]$$

$$-\mathcal{L}_{m_{i-1}}[\alpha_\Sigma(\xi-1)]\Big)\Big]\mathcal{P}_{n_i}(\eta)\frac{\partial \alpha_\Sigma}{\partial R} \tag{8.62}$$

and

$$(2Y+3)\frac{\partial \phi_i(R)}{\partial R} = \frac{\partial \alpha_\Sigma}{\partial R}\frac{e^{-\alpha_\Sigma(\xi-1)/2}}{\xi^2-\eta^2}\Bigg\{\mathcal{L}_{m_i}[\alpha_\Sigma(\xi-1)]\mathcal{P}_{n_i}(\eta)\Big[\frac{\alpha_\Sigma}{2}\xi^4 - \Big(\frac{\alpha_\Sigma}{2}+2m_i+1\Big)\xi^3$$

$$+\Big(-\frac{\alpha_\Sigma}{2}+\frac{2m_i^2}{\alpha_\Sigma}\Big)\xi^2+\Big(\frac{\alpha_\Sigma}{2}+2m_i+1+\frac{2m_i^2}{\alpha_\Sigma}\Big)\xi+n_i\eta^2\Big(\xi-1-\frac{2m_i}{\alpha_\Sigma}\Big)+3(\xi^2-\eta^2)\Big(-\frac{1}{2}\xi+\frac{1}{2}+\frac{m_i}{\alpha_\Sigma}\Big)\Big]$$

$$+\mathcal{L}_{m_{i-1}}[\alpha_\Sigma(\xi-1)]\mathcal{P}_{n_i}(\eta)\Big[2m_i\xi^3 - \frac{2m_i}{\alpha_\Sigma}(2m_i-1)\xi^2 - 2m_i\Big(\frac{2m_i-1}{\alpha_\Sigma}+1\Big)+\frac{2m_i}{\alpha_\Sigma}n_i\eta^2$$

$$-\frac{3m_i}{\alpha_\Sigma}(\xi^2-\eta^2)\Big] + \mathcal{L}_{m_{i-2}}[\alpha_\Sigma(\xi-1)]\mathcal{P}_{n_i}(\eta)\Big[2\xi(\xi+1)\frac{m_i}{\alpha_\Sigma}(m_i-1)\Big]$$

$$+\mathcal{L}_{m_i}[\alpha_\Sigma(\xi-1)]\mathcal{P}_{n_{i-1}}(\eta)\Big[n_i\eta\Big(\frac{2m_i}{\alpha_\Sigma}-\xi+1\Big)\Big] + \mathcal{L}_{m_{i-1}}[\alpha_\Sigma(\xi-1)]\mathcal{P}_{n_{i-1}}(\eta)\Big[-\frac{2m_i}{\alpha_\Sigma}n_i\eta\Big]\Bigg\}. \tag{8.63}$$

To summarize, the expectation values of the following quantities are calculated with the LEVEL program

$$\frac{\partial \alpha_\Sigma}{\partial R}\sum_{i,j} c_i(R)c_j(R)R\langle\phi_i\mathcal{K}\frac{\partial \phi_i}{\partial \alpha_\Sigma}\rangle; \tag{8.64}$$

$$\sum_{i,j} c_i(R)c_j(R)R\frac{\partial c_j}{\partial R}\langle\phi_i\mathcal{K}\phi_j\rangle; \tag{8.65}$$

$$-\frac{3}{2}\sum_{i,j} c_i(R)c_j(R)\langle\phi_i\mathcal{K}\phi_j\rangle; \tag{8.66}$$

while a slightly modified version of LEVEL, using a 5-point formula for $\partial\chi/\partial R$ is used for the expectation values of

$$\sum_{i,j} c_i(R)c_j(R)\langle\phi_i|\mathcal{K}|\phi_j\rangle R\frac{\partial}{\partial R}. \tag{8.67}$$

8.4 Results

Before describing the complete results that are obtained with the methods described in the previous sections, it is convenient to show the agreement between the different approaches in studying the expectation values of the operator p^4.

For this purpose two levels of H_2^+ are chosen, (0,0) as a starting point and (2,25); this second level is expected to represent an appropriate test both for the variational and the scattering methods since for $v = 2$ the former gives reliable results and $N = 25$ may be a good test for using the latter, which does not include some $\Sigma - \Pi$ contribution, to study the vibration-rotational levels of interest, in principle, all of them.

In tables 8.1 and 8.2 the results for $\langle p^4\rangle$ in units of $a_0^{-4}\hbar^4$ for these two levels are reported respectively; the method used, the main and the $\partial/\partial R$ contributions to $\langle p^4\rangle$, the total result for $\langle p^4\rangle$ and its value divided by 8 are indicated. This last result is the one of interest in computing the relativistic corrections.

As explained in the previous section, for high rotational quantum numbers the descrepancy between the two approaches is more pronounced since the averaging over R using the LEVEL program cannot deal with the $\Sigma-\Pi$ mixing. However, when the numerical factor $1/8$ is introduced, the difference becomes less significant. In addition it has to be noted that the detailed results from the variational method suggest that the total Π contribution to the expectation value of $p^4/8$ for the level (2,25) is 0.000024.

Optimistically for rotationless and low N levels the agreement is reliable to the sixth decimal place, while for high N levels the accuracy decreases to the fifth significant figure.

The complete results for the $\partial/\partial R$ contribution obtained with the LEVEL program is reported in table 8.3. These results have to be multiplied by (2κ) to obtained the right

contributions that have to be added to the main part of the expectation value of $\langle p^4 \rangle$ computed with the scattering method.

Method	Main contr.	$\partial/\partial R$ contr.	Total $\langle p^4 \rangle / a_0^{-4}\hbar^4$	$(\langle p^4 \rangle/8)/a_0^{-4}\hbar^4$
Variational	-	-	6.285 660	0.785 708
Scattering + Variational	6.284 852	0.000 816	6.285 668	0.785 709
Scattering + LEVEL	6.284 852	0.000 804	6.285 656	0.785 707

Table 8.1: $\langle p^4 \rangle$ in units of $a_0^{-4}\hbar^4$ for H_2^+ (0,0): comparison between all the numerical methods that are approached and tested in this study. The main contribution is obtained with a full scattering approach, the $\partial/\partial R$ contribution both through the variational method and the LEVEL program. Note that the $\partial/\partial R$ contributions include the factor (2κ).

Method	Main contr.	$\partial/\partial R$ contr.	Total $\langle p^4 \rangle / a_0^{-4}\hbar^4$	$(\langle p^4 \rangle/8)/a_0^{-4}\hbar^4$
Variational	-	-	4.807 958	0.600 995
Scattering + Variational	4.807 945	0.000 300	4.807 945	0.600 993
Scattering + LEVEL	4.807 945	0.000 274	4.807 919	0.600 990

Table 8.2: $\langle p^4 \rangle$ in units of $a_0^{-4}\hbar^4$ for H_2^+ (2,25): comparison between all the numerical methods that are approached and tested in this study. The main contribution is obtained with a full scattering approach, the $\partial/\partial R$ contribution both through the variational method and the LEVEL program. Note that the $\partial/\partial R$ contributions include the factor (2κ).

Table 8.3: H_2^+: total $\partial/\partial R$ contributions to $\langle p^4 \rangle$ in units of $a_0^{-4}\hbar^4$ computed with the LEVEL program; these results have to be multiplied by the numerical factor (2κ) and be added to the results for $\langle p^4 \rangle$ obtained with the scattering method. Just bounds levels are included.

v/N	0	1	2	3	4	5	6	7	8	9
0	1.476	1.470	1.459	1.443	1.421	1.395	1.364	1.330	1.292	1.252
1	1.410	1.404	1.393	1.377	1.356	1.330	1.301	1.268	1.231	1.192
2	1.344	1.338	1.328	1.312	1.292	1.267	1.238	1.206	1.171	1.133
3	1.278	1.273	1.262	1.247	1.228	1.204	1.176	1.145	1.111	1.075
4	1.212	1.207	1.197	1.183	1.164	1.140	1.114	1.084	1.051	1.016
5	1.147	1.142	1.132	1.118	1.100	1.077	1.051	1.023	0.991	0.957
6	1.081	1.076	1.067	1.053	1.035	1.014	0.989	0.961	0.931	0.898
7	1.014	1.010	1.001	0.988	0.970	0.950	0.926	0.899	0.870	0.838
8	0.947	0.942	0.934	0.921	0.905	0.885	0.862	0.836	0.808	0.778
9	0.878	0.874	0.866	0.854	0.838	0.819	0.796	0.772	0.744	0.716
10	0.808	0.804	0.796	0.784	0.769	0.751	0.729	0.705	0.679	0.651
11	0.736	0.732	0.724	0.713	0.698	0.681	0.660	0.637	0.612	0.585
12	0.661	0.657	0.649	0.639	0.625	0.607	0.588	0.565	0.541	0.515
13	0.582	0.578	0.571	0.561	0.547	0.531	0.511	0.490	0.466	0.440
14	0.499	0.495	0.488	0.478	0.465	0.449	0.430	0.408	0.385	0.359
15	0.410	0.406	0.400	0.389	0.376	0.360	0.341	0.319	0.295	0.268
16	0.313	0.309	0.303	0.292	0.279	0.262	0.241	0.218	0.190	0.156
17	0.206	0.202	0.194	0.183	0.168	0.148	0.123			
18	0.088	0.084	0.075	0.061						
19	0.015	0.011								
v/N	10	11	12	13	14	15	16	17	18	19
0	1.210	1.166	1.121	1.075	1.029	0.983	0.937	0.892	0.847	0.804
1	1.152	1.109	1.066	1.021	0.977	0.932	0.888	0.845	0.802	0.761
2	1.094	1.053	1.011	0.968	0.925	0.883	0.840	0.798	0.757	0.717
3	1.037	0.997	0.956	0.915	0.874	0.833	0.792	0.752	0.712	0.674
4	0.979	0.941	0.902	0.863	0.823	0.783	0.744	0.705	0.667	0.630
5	0.922	0.885	0.848	0.810	0.771	0.733	0.695	0.658	0.621	0.585
6	0.864	0.829	0.793	0.756	0.719	0.682	0.646	0.610	0.574	0.540
7	0.806	0.772	0.737	0.701	0.666	0.630	0.595	0.561	0.526	0.493
8	0.746	0.713	0.680	0.646	0.612	0.577	0.543	0.509	0.476	0.443
9	0.685	0.654	0.621	0.588	0.555	0.522	0.489	0.456	0.423	0.391
10	0.622	0.592	0.560	0.528	0.496	0.464	0.431	0.399	0.366	0.333
11	0.556	0.527	0.496	0.465	0.433	0.401	0.369	0.335	0.301	0.266
12	0.487	0.458	0.428	0.397	0.365	0.332	0.298	0.262		
13	0.413	0.384	0.354	0.322	0.288	0.252				
14	0.331	0.301	0.269	0.233						
15	0.237	0.203								

continued

v/N	20	21	22	23	24	25	26	27
0	0.762	0.721	0.682	0.644	0.608	0.573	0.539	0.507
1	0.720	0.681	0.643	0.607	0.571	0.538	0.505	0.475
2	0.678	0.641	0.604	0.569	0.535	0.503	0.471	0.441
3	0.636	0.600	0.565	0.531	0.498	0.467	0.436	0.407
4	0.594	0.559	0.525	0.492	0.460	0.430	0.400	0.372
5	0.551	0.517	0.484	0.452	0.421	0.391	0.362	0.334
6	0.506	0.473	0.441	0.410	0.380	0.350	0.321	0.292
7	0.460	0.428	0.396	0.365	0.335	0.305		
8	0.411	0.379	0.348	0.316	0.284			
9	0.358	0.326	0.293					
10	0.299							
v/N	28	29	30	31	32	33	34	35
0	0.476	0.447	0.419	0.393	0.367	0.343	0.320	0.298
1	0.445	0.417	0.390	0.364	0.339	0.316	0.293	
2	0.413	0.385	0.359	0.334	0.309	0.286		
3	0.380	0.353	0.327	0.301				
4	0.344	0.318	0.291					
5	0.306							

The complete results for the relativistic corrections for the ground electronic state of H_2^+ for all the vibrational levels for $N = 0, 1, 5$ and $N = 25$ are reported in table 8.4. As usual just bound levels are considered.

In figures 8.1, 8.4 and 8.6 the comparison between these results and Kennedy's reported in [2] are plotted against non-adiabatic dissociation energies for the rotational levels $N = 0, N = 5$ and $N = 25$ respectively. Detailed plots in the range of 0-3000 cm^{-1} are reported in figures 8.2, 8.3 and 8.5, for $N = 0, 1$ and $N = 5$ respectively.

The difference between the results for the relativistic corrections obtained by Kennedy through an adiabatic approach and the non-adiabatic method of this work is roughly constant over all the vibrational levels; for the rotationless levels this difference (non-adiabatic − adiabatic) goes from a maximum of 0.0067 cm^{-1} for $v = 0$ to a minimum of 0.0062 cm^{-1} for $6 \leq v \leq 14$. Similar values can be recognised for the other rotational levels that are reported, namely $N = 1$ and $N = 5$. The difference seems to decrease for high rotational levels being for $N = 25$ between 0.0058 and 0.0060 cm^{-1}.

In [63] the results for the relativistic correction were reported as a function of R, before averaging over R. When the variational program is modified to calculate $\langle p^4 \rangle$, $\langle \delta(r_{1e}) \rangle$ and $\langle H_{rel} \rangle$ as a functions of R, there is agreement to as many significant figures as Kennedy quoted, up to $R = 10$ a_0. Thereafter more and more electronic basis functions are needed for convergence to agreement; Kennedy's method works better at large R and is able to approach the atomic limit.

For $N = 0$ only $v = 17, 18, 19$ levels sample $R > 10$ a_0 and there is no evidence that convergence is not achieved. However, $v = 19$ results should be treated with caution since it is only for the very highest vibrational levels that the transitions have been observed and there is no evidence that Kennedy's relativistic corrections to transition frequencies are not reliable [60–63].

To investigate the origin of the discrepancy, only the contribution arising from the electron density at the nuclei can be studied, since apart from the relativistic corrections, the Fermi contact parameter is the only property averaged over R that Kennedy has studied [66].

The results reported from this work seek reassurance from the Fermi contact parameters

published by Babb and Dalgarno for $v = 0 - 9$, $N = 1$ [67]. Electron densities at the nuclei derived from those results are consistent with the ones here reported to at least five significant figures; on the other hand they differ from those derived from Kennedy's at the fourth significant figure and they are consistently higher by 0.00025 a_0^{-3}. The results obtained in this work and Kennedy's derived from his unpublished Fermi contact parameters for the rotationless levels of H_2^+, are reported in table 8.5. Similarly, if a comparison is made on $\langle p^4 \rangle$, Kennedy's values, extracted from his relativistic corrections and his Fermi contact parameters, are consistently higher by 0.011 $a_0^{-4}\hbar^4$ than the ones reported in this work. The electron densities at the nuclei and $\langle p^4 \rangle$ differences can then explain the difference of 0.006-0.007 cm^{-1} in the results of the relativistic corrections.

In addition, in figure 8.7 the behaviour for the rotationless levels of the relativistic corrections obtained in this work is plotted against the expectation values of the non-adiabatic bond lengths; on the same scale, Kennedy's results averaged over R do not differ significantly. Also in figure 8.7 are reported Kennedy's results [63] as a function of R before averaging over R. When non-adiabatic calculations are performed on the dissociation energies and $\langle R \rangle$, the values of the former increase and as a consequence the values of the latter decrease (see chapters 4 and 5); in particular for (0,0) the bond length range of significance about $R = 2.0$ a_0 is slightly reduced. It may be seen from the figure that averaging over a smaller range of R will result in a slightly largest result in magnitude. Presumably this happens to a similar extent for higher levels.

The relativistic corrections reported here, which include non-adiabatic effects, should be more reliable than Kennedy's, except perhaps for $v = 19$.

v	$\langle H_{\rm rel}\rangle/cm^{-1}$ $N=0$	$\langle H_{\rm rel}\rangle/cm^{-1}$ $N=1$	$\langle H_{\rm rel}\rangle/cm^{-1}$ $N=5$	$\langle H_{\rm rel}\rangle/cm^{-1}$ $N=25$
0	-1.592 1	-1.590 0	-1.561 3	-1.237 7
1	-1.555 9	-1.553 9	-1.527 4	-1.233 8
2	-1.523 4	-1.521 6	-1.497 0	-1.233 0
3	-1.494 5	-1.492 8	-1.470 1	-1.235 5
4	-1.468 7	-1.467 4	-1.446 6	-1.241 5
5	-1.446 7	-1.445 3	-1.426 3	-1.251 6
6	-1.427 6	-1.426 3	-1.409 1	-1.266 3
7	-1.411 6	-1.410 4	-1.395 0	-1.286 8
8	-1.398 7	-1.397 6	-1.383 9	
9	-1.388 8	-1.387 9	-1.375 9	
10	-1.382 0	-1.381 2	-1.371 1	
11	-1.378 3	-1.377 7	-1.369 4	
12	-1.377 8	-1.377 3	-1.370 9	
13	-1.380 5	-1.380 2	-1.375 9	
14	-1.386 7	-1.386 5	-1.384 4	
15	-1.396 3	-1.396 3	-1.396 6	
16	-1.409 6	-1.409 7	-1.412 9	
17	-1.426 4	-1.426 8	-1.433 4	
18	-1.445 1	-1.445 6		
19	-1.454 0	-1.454 1		

Table 8.4: H_2^+: relativistic corrections for all the vibrational bound levels, for $N = 0, 1, 5, 25$.

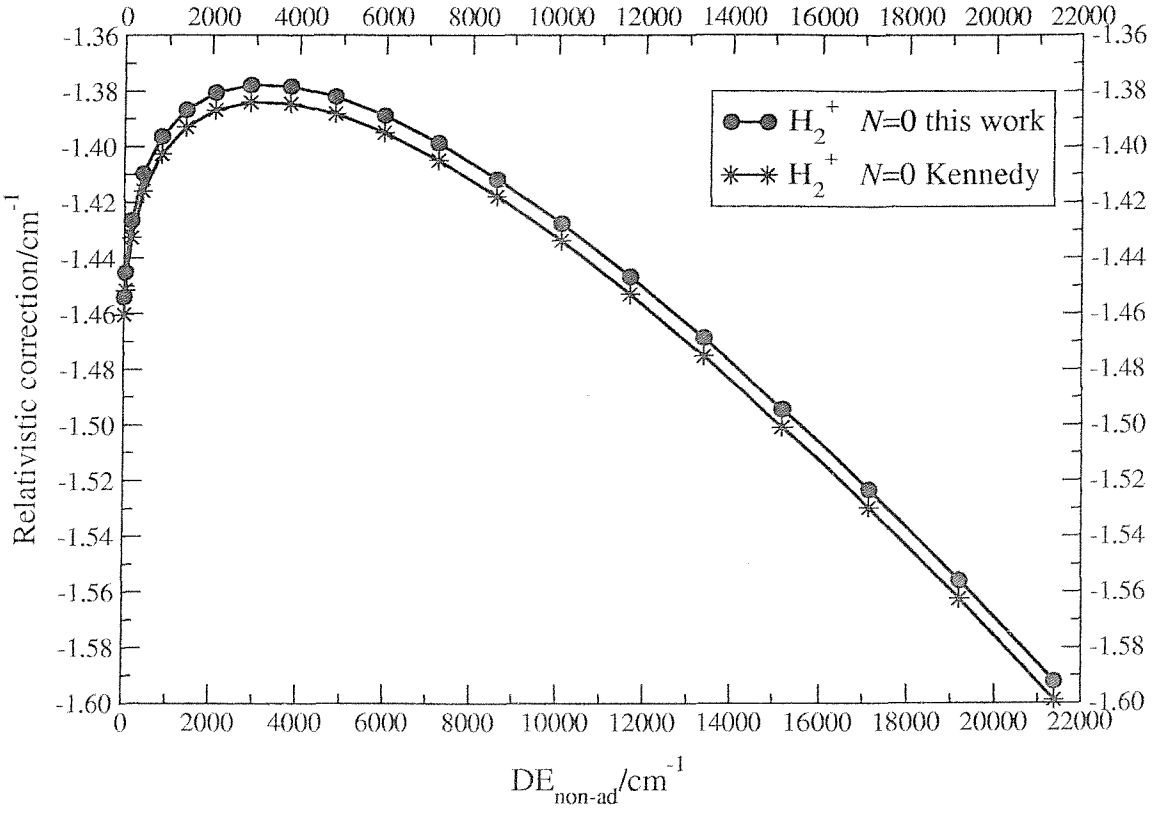

Figure 8.1: $H_2^+(v,0)$: comparison between the results reported in this work and Kennedy's [2, 63] for the relativistic corrections against dissociation energies.

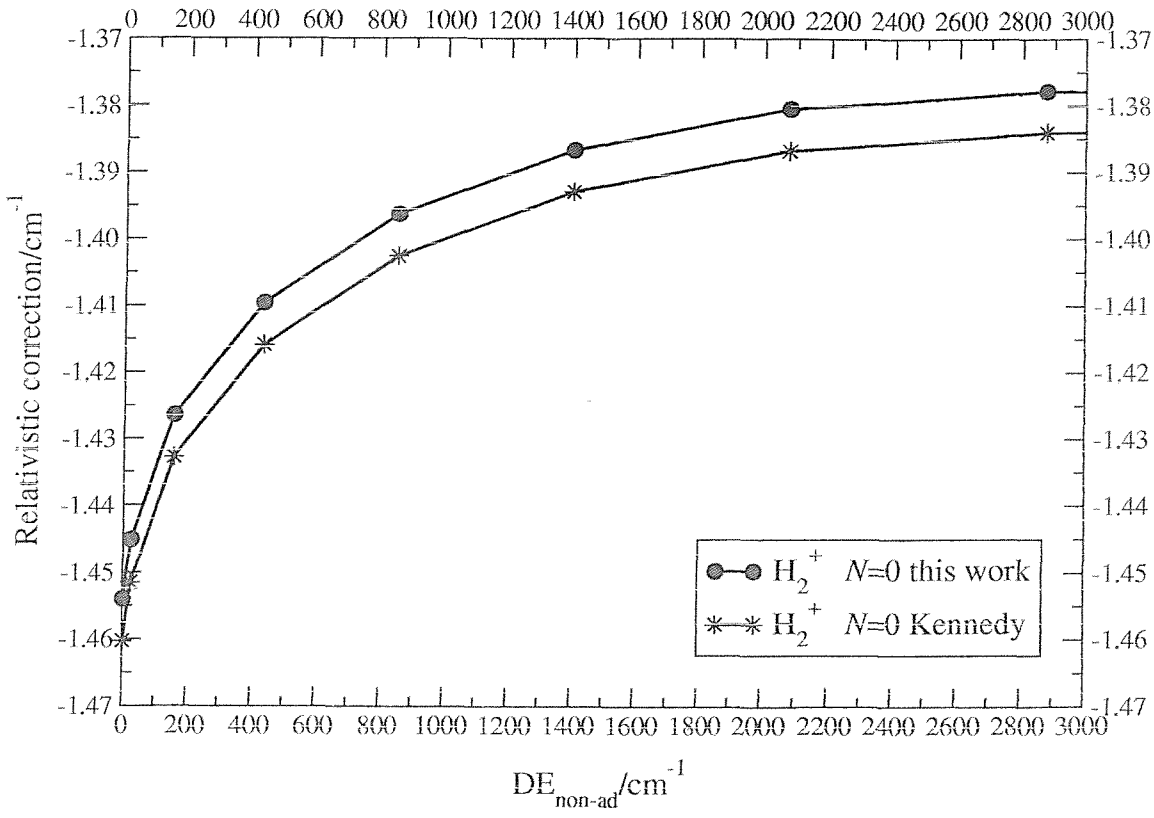

Figure 8.2: $H_2^+(v,0)$: comparison between the results reported in this work and Kennedy's [2, 63] for the relativistic corrections against dissociation energies in the range 0-3000 cm^{-1}.

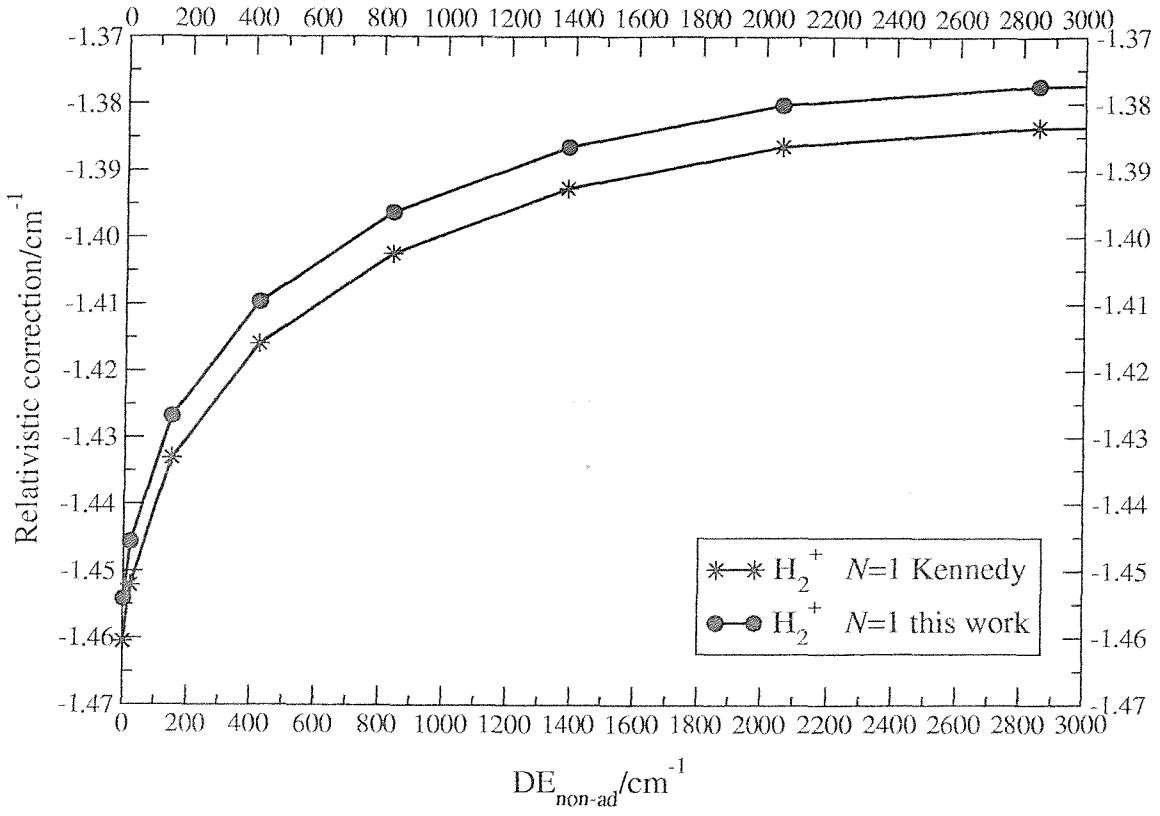

Figure 8.3: $H_2^+(v,1)$: comparison between the results reported in this work and Kennedy's [2, 63] for the relativistic corrections against dissociation energies in the range 0-3000 cm^{-1}.

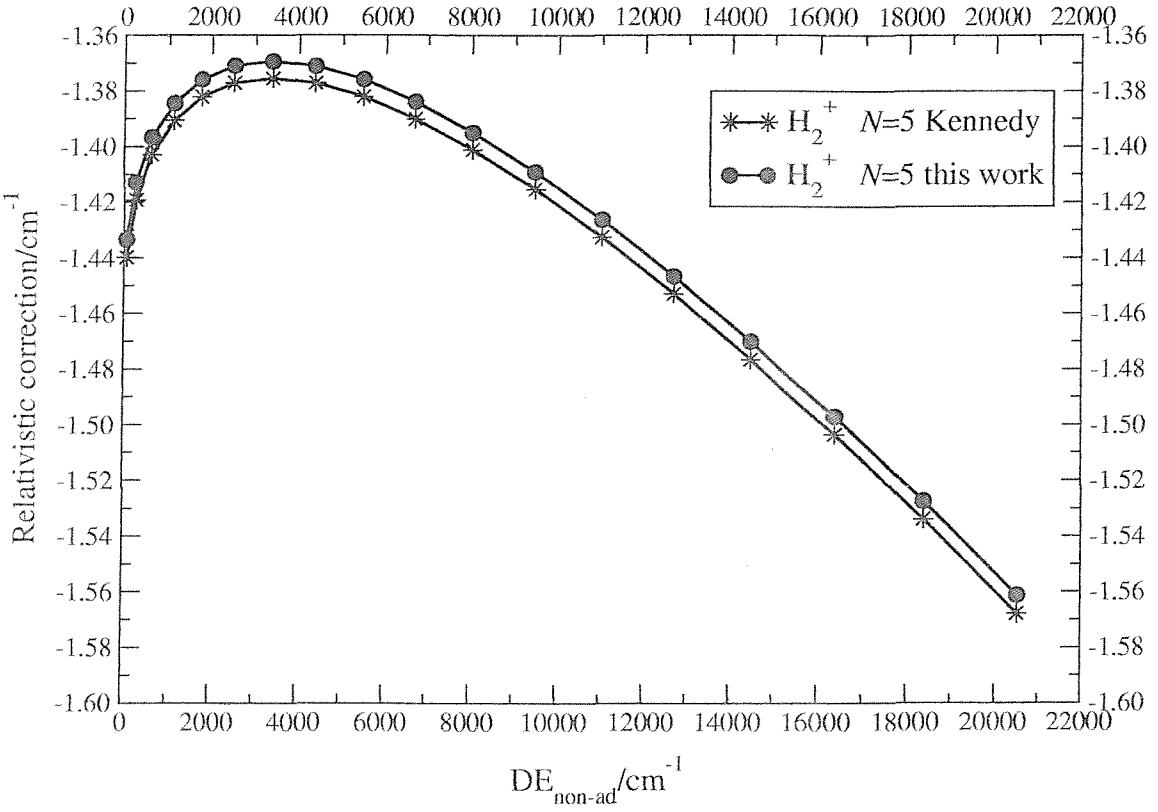

Figure 8.4: $H_2^+(v,5)$: comparison between the results reported in this work and Kennedy's [2, 63] for the relativistic corrections against dissociation energies.

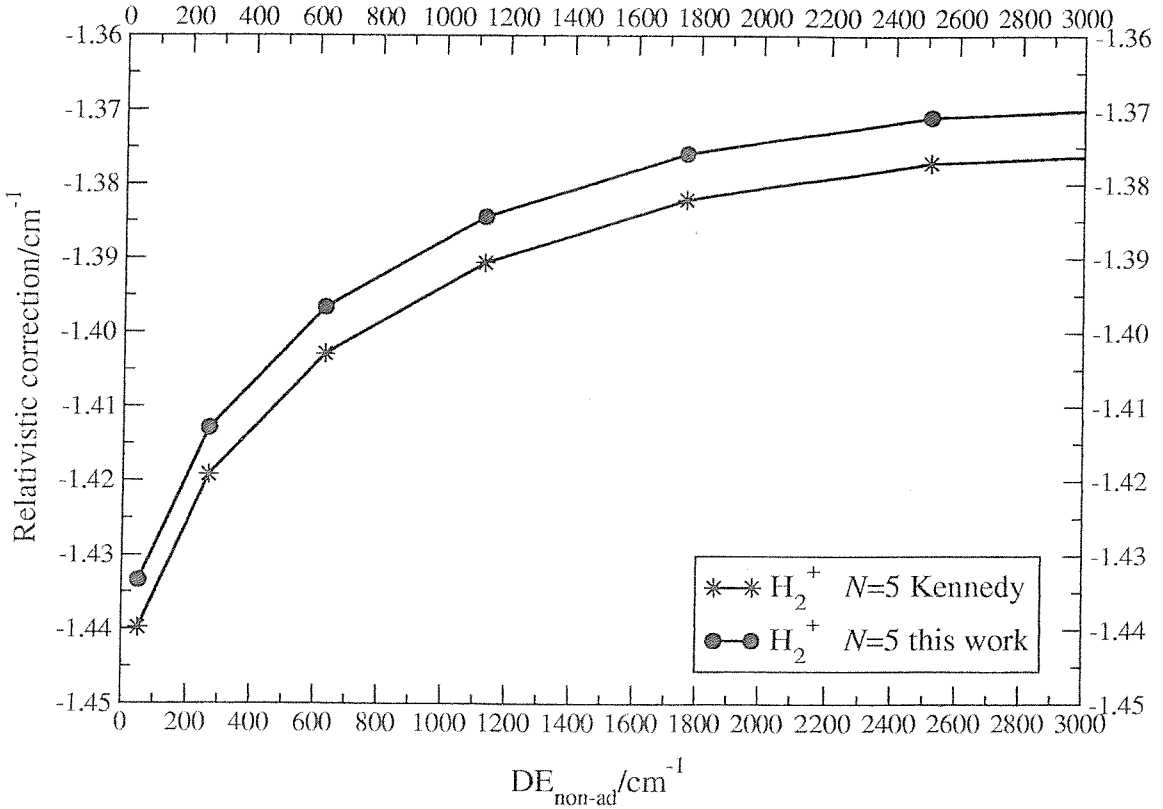

Figure 8.5: $H_2^+(v,5)$: comparison between the results reported in this work and Kennedy's [2, 63] for the relativistic corrections against dissociation energies in the range 0-3000 cm^{-1}.

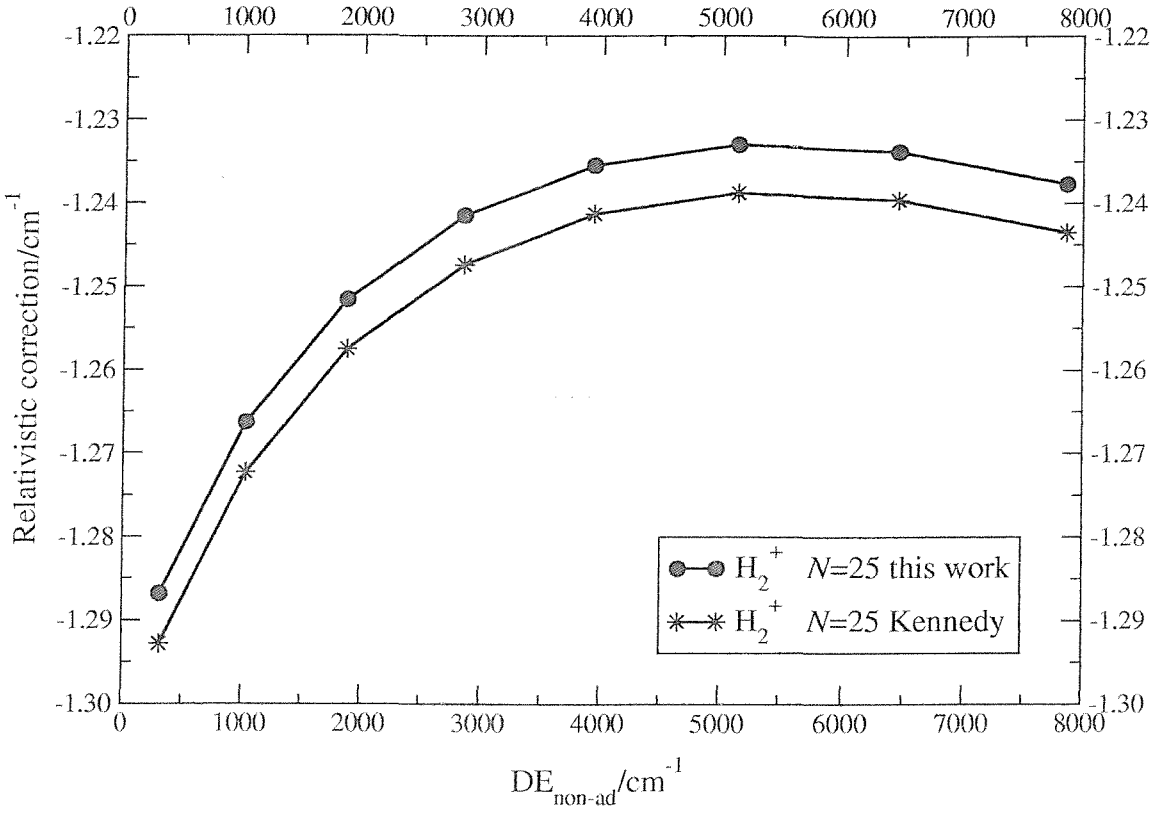

Figure 8.6: $H_2^+(v,25)$: comparison between the results reported in this work and Kennedy's [2,63] for the relativistic corrections against dissociation energies.

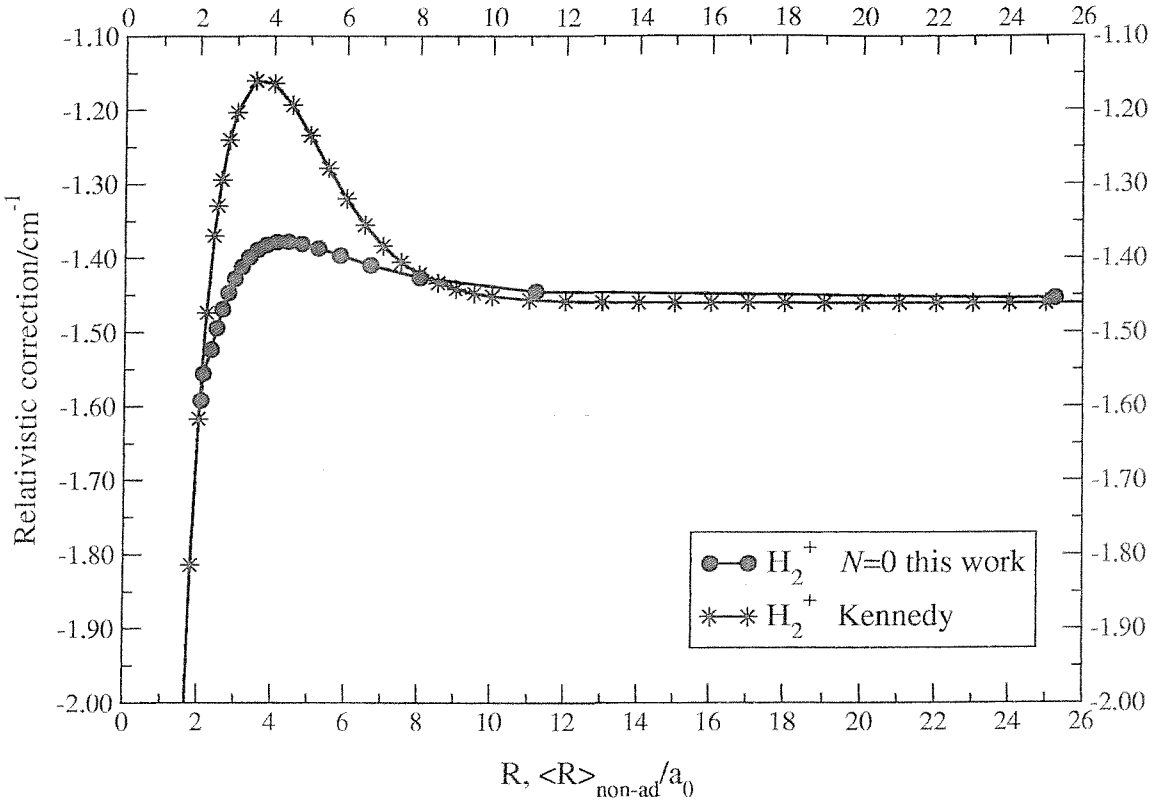

Figure 8.7: H_2^+: relativistic correction for the rotationless levels of H_2^+ obtained in this work plotted against the expectation values of the non-adiabatic bond lengths; the starred line represents Kennedy's results [2, 63] reported as a function of R before averaging over R.

v	$\langle\delta(\boldsymbol{r}_{1e})\rangle/a_0^{-3}$ [66]	$\langle\delta(\boldsymbol{r}_{1e})\rangle/a_0^{-3}$ this work	$\langle p^4\rangle/a_0^{-4}\hbar^4$ [66]	$\langle p^4\rangle/a_0^{-4}\hbar^4$ this work
0	0.206 988	0.206 737	6.296 589	6.285 656
1	0.201 560	0.201 311	6.135 310	6.124 512
2	0.196 543	0.196 295	5.986 916	5.976 216
3	0.191 910	0.191 663	5.850 617	5.839 992
4	0.187 638	0.187 399	5.725 741	5.715 176
5	0.183 710	0.183 463	5.611 712	5.601 184
6	0.180 106	0.179 857	5.508 034	5.497 496
7	0.176 813	0.176 564	5.414 305	5.403 768
8	0.173 818	0.173 567	5.330 175	5.319 632
9	0.171 112	0.170 860	5.255 389	5.244 824
10	0.168 685	0.168 433	5.189 752	5.179 152
11	0.166 533	0.166 279	5.133 135	5.122 496
12	0.164 651	0.164 395	5.085 488	5.074 808
13	0.163 038	0.162 782	5.046 831	5.036 104
14	0.161 694	0.161 434	5.017 257	5.006 488
15	0.160 623	0.160 363	4.996 953	4.986 136
16	0.159 831	0.159 569	4.986 156	4.975 296
17	0.159 329	0.159 069	4.985 105	4.974 216
18	0.159 132	0.158 874	4.993 014	4.982 112
19	0.159 148	0.158 887	4.999 430	4.988 536

Table 8.5: H_2^+, $N = 0$ levels: comparison between the results for the expectation values of p^4 and the electron density at the nuclei obtained in this work and Kennedy's [63] obtained from unpublished results.

8.5 Conclusions

In this chapter the relativistic corrections for some vibration-rotational levels of H_2^+ are reported; however many other levels can be studied. The results are obtained through a non-adiabatic approach.

After the introduction of the perturbation operator, a detailed exposition of the numerical methods developed and applied to achieve the results is given; the main difficulty is presented by the expectation values of p^4 to be studied with the scattering and transformed Hamiltonian method. Since the transformed form of this operator, p_t^4, introduces a significant contribution that depends on $\partial/\partial R$, an alternative method is developed to solve this problem, since the scattering method cannot deal with operators containing $\partial/\partial R$.

For this purpose, while the main contribution to the relativistic corrections arising from $\langle p^4 \rangle$ is studied with the scattering method, the LEVEL program is modified to account for the $\partial/\partial R$ part of the problem; this approach allows the study all the vibration-rotational levels of interest. Unfortunately this method does not include $\Sigma - \Pi$ coupling; for this reason for high rotational levels the results are not expected to be so accurate as for rotationless and low rotational levels.

An explanation of the constant difference with Kennedy's results [63] is found through the investigation of the expectation values of p^4 and the electron densities at the nuclei. Reassurance of the reliability of the results reported in this work is found in Babb and Dalgarno's Fermi contact parameters [67].

The results reported in this work should be of interest for a comparison with experimental results concerning transition frequencies.

Chapter 9

Conclusions and further work

After a short introduction about the overall aims of this work, in chapters 2 and 3 the different levels of approximation to solve the Schrödinger equation, the theoretical approaches and the calculation methods, that have been used in this work to obtain the reported results, are described in detail. Through two unitary transformations, a transformed Hamiltonian in which no nuclear motion terms involving cross-derivatives between nuclear and electronic coordinates appear, may be obtained. This form of the Hamiltonian allows the study of properties of the ground electronic states of the hydrogen molecular cation and its isotopomers to a high level of accuracy. The transformed Hamiltonian is used in a scattering method. Two different methods have been used; a variational and a scattering method, the former used mainly as a test for the latter which allows the study of all the vibration-rotational levels of interest for all the three cations H_2^+, D_2^+ and HD^+.

Chapter 4 is dedicated to the study of the non-adiabatic correction to the dissociation energies of the ground electronic states of H_2^+, D_2^+ and HD^+; attention is confined to the bound levels. It is shown how for v=0 or for N=0 it is possible to predict the adiabatic corrections to the dissociation energies for D_2^+ and HD^+ starting from those of H_2^+, through scaling factors based on the relative reduced masses. However, scaling becomes increasingly less successful as v (for constant N) or N (for constant v) increase. The same comments are true for the non-adiabatic corrections except for the few high lying levels of HD^+ that are found to be atypical.

In chapter 5 the non-adiabatic correction to the bond lengths for all the three cations

is reported. A previous work by Moss [37] showed that the non-adiabatic correction to the bond length of HD^+ v=20, N=0 was anomalous. In this work further levels are found for HD^+ where the non-adiabatic corrections are anomalous, in that they do not lie on smooth curve predicted from the corrections for H_2^+ [32]. While in general corrections to the bond length are negative and increase in magnitude with v for given N or with N for given v, for some levels the correction is positive.

The work contained in chapter 6 goes further than the original aim of this work. Since Frolov [39,40] has recently published dissociation energies and other properties for the (0,0) level of the ground electronic states of T_2^+, HT^+ and DT^+, a comparison with his results is desirable. For this reason, non-adiabatic dissociation energies and non-adiabatic bond lengths are computed and with the respective non-adiabatic corrections are presented in this work, for all the rotationless levels of the ground electronic states of HT^+ and DT^+. As expected from the results obtained for the heteronuclear molecule HD^+ and reported in chapters 4 and 5, HT^+ and DT^+ show similar anomalies for high vibrational levels. As realized for HD^+, the intermediate transformed Hamiltonian does not handle the g/u symmetry breaking as successfully as hoped in the region of rapid change; the g/u symmetry breaking might not be fully accounted for by the intermediate transformed Hamiltonian.

In chapter 7 new results for the dipole polarizability of the hydrogen molecular cation and its isotopomers are reported. Many levels have been studied, although levels close to dissociation will require more effort. Only levels with $N = 0$ and $N = 1$ are considered, since for a given N, the $(N+1)$ values of $|M|$ must be considered separately, but again other N could be studied if necessary. HD^+ is of particular interest here since only one previous calculation of its polarizability has been reported; the presence of an asymmetric charge distribution provides novelty. The result here reported for (0,0) is close to the only previous one. The opportunity is also taken to revisit H_2^+ (0,0), but including higher-order contributions than previous studies does not removed the difference between experiment and theory.

In chapter 8 the relativistic corrections for some rotational levels of H_2^+ are reported.

After the introduction of the appropriate perturbation operator, a detailed exposition of the numerical methods developed and applied to achieve the results is given; the main difficulty is presented by the expectation values of p^4 when they are to be studied with the scattering and transformed Hamiltonian method. Since the transformed form of this operator, p_t^4, presents a significant dependence on $\partial/\partial R$, an alternative method is developed to solve this problem, since the scattering method cannot deal with any dependence on R. For this purpose, while the main contribution to the relativistic corrections arising from $\langle p^4 \rangle$ is studied with the scattering method, a modified LEVEL program [7] is used to solve the $\partial/\partial R$ part of the problem. This approach allows the study of all the vibration-rotational levels of interest. Unfortunately this method does not allow the inclusion of $\Sigma - \Pi$ coupling; for this reason, for high rotational levels, the results are not expected to be so accurate as for rotationless and low rotational levels. However, the results reported in this work should be of interest for a comparison with experimental results.

This work may be of relevance for metrologists in improving the accuracy of the determination of the mass of the proton to the electron mass, but improvements in results concerning the radiative correction are needed. The hydrogen molecular cation H_2^+, is thought to be intimately involved in the initiation of astrochemistry in the interstellar medium and yet it has not been observed extraterrestrially, unlike H_3^+. Successful observation of interstellar H_2^+ will involve knowledge of accurate transition frequencies.

Further work could include the radiative correction, the study of properties for the first electronic excited state of the homonuclear species of the hydrogen cation and the quasi-bound levels of the isotopomers.

Bibliography

[1] A. Leach and R. E. Moss, *Annu. Rev. Phys. Chem.*, **46**, 55, (1995).

[2] R. E. Moss, *Molec. Phys.*, **80**, 1541, (1993).

[3] R. E. Moss, *J. Chem. Soc. Faraday Trans.*, **89**, 3851, (1993).

[4] R. E. Moss, *Molec. Phys.*, **78**, 371, (1993).

[5] B. Grémaud, D. Delande and N. Billy, *J. Phys. B*, **31**, 383, (1998).

[6] R. E. Moss and I. A. Sadler, *Molec. Phys.*, **68**, 1015, (1989).

[7] R. J. Le Roy, *A Computer Program Solving the Radial Schrödinger Equation for Bound and Quasibound Levels*, University of Waterloo Chem. Phys. Res. Rep. CP642, (2000).

[8] M. Shapiro and G. G. Balint-Kurti, *J. Chem. Phys.*, **71**, 1461, (1979).

[9] E. A. Hylleraas, *Z. Phys.*, **71**, 739, (1931).

[10] G. Hunter and H. O. Pritchard, *J. Chem. Phys.*, **46**, 2146, (1967a).

[11] J. W. Cooley, *Math. Comp.*, **15**, 363, (1961).

[12] A. Carrington and R. A. Kennedy, *Gas Phase Ion Chemistry. Ions and Light.*, volume 3, ed. M. T. Bower (Academic Press), (1984).

[13] M. Born and K. Huang, *Dynamical Theory of Crystal Lattices*, Oxford University Press, London and New York, (1954), appendix VIII.

[14] G. Hunter and H. O. Pritchard, *J. Chem. Phys.*, **46**, 2153, (1967b).

[15] D. M. Bishop, *Mol. Phys.*, **28**, 1397, (1974).

[16] D. M. Bishop and L. M. Cheung, *Phys. Rev. A*, **16**, 640, (1977).

[17] L. Wolniewicz and J. D. Poll, *Mol. Spectrosc.*, **72**, 264, (1978).

[18] L. Wolniewicz and J. D. Poll, *J. Chem. Phys.*, **73**, 6225, (1980).

[19] L. Wolniewicz and J. D. Poll, *Can. J. Phys.*, **63**, 1201, (1985).

[20] L. Wolniewicz and J. D. Poll, *Mol. Phys.*, **59**, 953, (1986).

[21] I. A. Sadler, *A Transformed Hamiltonian Theory for* HD^+, Ph.D. thesis, University of Southampton, Southampton, (1988).

[22] R. E. Moss and I. A. Sadler, *Molec. Phys.*, **64**, 165, (1988).

[23] R. E. Moss and I. A. Sadler, *Molec. Phys.*, **66**, 591, (1989).

[24] R. A. Kennedy, R. E. Moss and I. A. Sadler, *Molec. Phys.*, **64**, 177, (1988).

[25] J. M. Hutson, *Chem. Phys. Lett.*, **151**, 565, (1988).

[26] E. Fues, *Ann. Phys.*, **80**, 367, (1926).

[27] I. S. Gradshteyn and I. M. Ryzhik, *Table of Integrals, Series and Products*, (Academic Press), (1965).

[28] A. Erdelyi, *Bateman Manuscript Project: Higher Trascendental Functions*, volume 2, (MaGraw Hill), (1953).

[29] B. R. Johnson, *J. Chem. Phys.*, **13**, 445, (1973).

[30] G. G. Balint-Kurti, R. E. Moss, I. A. Sadler and M. Shapiro, *Phys. Rev. A*, **41**, 4913, (1990).

[31] A. Carrington and R. A. Kennedy, *Molec. Phys.*, **56**, 935, (1985).

[32] R. E. Moss, *Molec. Phys.*, **89**, 195, (1996).

[33] R. E. Moss and D. Joplin, *Chem. Phys. Lett.*, **260**, 377, (1996).

[34] R. E. Moss and L. Valenzano, *Molec. Phys.*, **100**, 649, (2002).

[35] E. R. Cohen and B. N. Taylor, *Rev. Mod. Phys.*, **59**, 1121, (1987).

[36] J. H. Van Vleck, *J. Chem. Phys.*, **4**, 327, (1936).

[37] R. E. Moss, *Molec. Phys.*, **97**, 3, (1999).

[38] R. E. Moss and I. A. Sadler, *Molec. Phys.*, **61**, 905, (1987).

[39] A. M. Frolov, *Phys. Rev. E*, **65**, 046705, (2002).

[40] A. M. Frolov, *J. Phys. B*, **35**, L331, (2002).

[41] E. R. Cohen and B. N. Taylor, *Phys. Today*, **53(8)**, 9, (2000).

[42] J. Shertzer and C. H. Greene, *Phys. Rev. A*, **58**, 1082, (1998).

[43] A. K. Bhatia and R. J. Drachman, *Phys. Rev. A*, **59**, 205, (1999).

[44] J. M. Taylor, A. Dalgarno and J. F. Babb, *Phys. Rev. A*, **60**, R2630, (1999).

[45] P. L. Jacobson, R. A. Komara, W. G. Sturrus and S. R. Lundeen, *Phys. Rev. A*, **62**, 012509, (2000).

[46] R. E. Moss and L. Valenzano, *Molec. Phys.*, **100**, 1527, (2002).

[47] W. G. Sturrus, E. A. Hessels, P. W. Arcuni and S. R. Lundeen, *Phys. Rev. A*, **44**, 3032, (1991).

[48] P. L. Jacobson, D. S. Fisher, C. W. Fehrenbach, W. G. Sturrus and S. R. Lundeen, *Phys. Rev. A*, **56**, R4361, (1997).

[49] P. L. Jacobson, D. S. Fisher, C. W. Fehrenbach, W. G. Sturrus and S. R. Lundeen, *Phys. Rev. A*, **57**, 4065(E), (1998).

[50] D. M. Bishop and B. Lam, *Molec. Phys.*, **65**, 679, (1988).

[51] R. E. Moss, *Phys. Rev. A*, **58**, 4447, (1998).

[52] R. E. Moss, *Chem. Phys. Lett.*, **311**, 231, (1999).

[53] L. Hilico, N. Billy, B. Grémaud and D. Delante, *J. Phys. B*, **34**, 491, (2001).

[54] V. I. Korobov, *Phys. Rev. A*, **63**, 044501, (2001).

[55] R. E. Moss, *Phys. Rev. A*, **61**, 040501, (2000).

[56] P. R. Bunker, *Chem. Phys. Lett.*, **27**, 322, (1974).

[57] A. K. Bhatia and R. J. Drachman, *Phys. Rev. A*, **61**, 032503, (2000).

[58] W. Kolos and L. Wolniewicz, *Rev. Mod. Phys.*, **35**, 473, (1963).

[59] D. M. Bishop, *J. Chem. Phys.*, **66**, 3842, (1977).

[60] A. Carrington, I. R. McNab and C. A. Montgomerie, *J. Phys. B*, **22**, 3551, (1989).

[61] A. Carrington, I. R. McNab, C. A. Montgomerie and R. A. Kennedy, *Mol. Phys.*, **67**, 711, (1989).

[62] A. Carrington, I. R. McNab and C. A. Montgomerie, *Chem. Phys. Lett.*, **160**, 237, (1989).

[63] M. H. Howells and R. A. Kennedy, *J. Chem. Soc. Faraday Trans.*, **86**, 3495, (1990).

[64] R. E. Moss, *Advanced Molecular Quantum Mechanics: an introduction to relativistic quantum mechanics and the quantum theory of radiation*, Chapman and Hall, London, (1973).

[65] J. W. Gonsalves and R. E. Moss, *Chem. Phys. Lett.*, **62**, 534, (1979).

[66] R. A. Kennedy, *unpublished results*.

[67] J. F. Babb and A. Dalgarno, *Phys. Rev. A*, **46**, R5317, (1992).